Mechanical properties of fly ash/slag based geopolymer concrete with the addition of macro fibres

by

Ryno Barnard

Thesis presented in partial fulfilment of the requirements for the degree Master of Engineering (Research) in the Faculty of Engineering at Stellenbosch University

Supervisor: Prof WP Boshoff
Department of Civil Engineering

December 2014

Declaration

By submitting this thesis electronically, I declare that the entirety of the work contained therein is my own, original work, that I am the sole author thereof (save to the extent explicitly otherwise stated), that reproduction and publication thereof by Stellenbosch University will not infringe any third party rights and that I have not previously in its entirety or in part submitted it for obtaining any qualification.

December 2014

Abstract

Geopolymer concrete is an alternative construction material that has comparable mechanical properties to that of ordinary Portland cement concrete, consisting of an aluminosilicate and an alkali solution. Fly ash based geopolymer concrete hardens through a process called geopolymerisation. This hardening process requires heat activation of temperatures above ambient. Thus, fly ash based geopolymer concrete will be an inadequate construction material for in-situ casting, as heat curing will be uneconomical.

The study investigated fly ash/slag based geopolymer concrete. When slag is added to the matrix, curing at ambient temperatures is possible due to calcium silicate hydrates that form in conjunction with the geopolymeric gel.

The main goal of the study is to obtain a better understanding of the mechanical properties of geopolymer concrete, cured at ambient temperatures. A significant number of mix variations were carried out to investigate the influence that the various parameters, present in the matrix, have on the compressive strength of fly ash/slag based geopolymer concrete. Promising results were found, as strengths as high as 72 MPa were obtained. The sodium hydroxide solution, the slag content and the amount of additional water in the matrix had the biggest influence on the compressive strength of the fly ash/slag based geopolymer concrete.

The modulus of the elasticity of fly ash/slag based geopolymer concrete did not yield promising results as the majority of the specimens, regardless of the compressive strength, yielded a stiffness of less than 20 GPa. This is problematic from a structural point of view as this will result in large deflections of elements. The sodium hydroxide solution had the most significant influence on the elastic modulus of the geopolymer concrete.

Steel and polypropylene fibres were added to a high- and low strength geopolymer concrete matrix to investigate the ductility improvement. The limit of proportionality mainly depended on the compressive strength of the geopolymer concrete, while the amount of fibres increased the energy absorption of the concrete. A similar strength OPC concrete mix was compared to the low strength geopolymer concrete and it was found that the OPC concrete specimen yielded slightly better flexural behaviour. Fibre pull-out tests were also conducted to investigate the fibre-matrix interface.

From the knowledge gained during this study, it can be concluded that the use of fly ash/slag based geopolymer concrete, as an alternative binder material, is still some time away as there are many complications that need to be dealt with, especially the low modulus of elasticity. However, fly ash/slag based geopolymer concrete does have potential if these complications can be addressed.

Opsomming

Geopolimeerbeton is ‘n alternatiewe konstruksiemateriaal wat vergelykbare meganiese eienskappe met beton waar OPC die binder is, en wat bestaan uit ‘n aluminosilikaat en ‘n alkaliese oplossing. Vliegas-gebaseerde geopolimeerbeton verhard tydens ‘n proses wat geopolimerisasie genoem word. Hierdie verhardingsproses benodig hitte-aktivering van temperature hoër as dié van die onmiddellike omgewing. Gevolglik sal vliegas-gebaseerde geopolimeerbeton ‘n ontoereikende konstruksiemateriaal vir *in situ* gietvorming wees, aangesien hitte-nabehandeling onekonomies sal wees.

Die studie het vliegas/slagmentgebaseerde geopolimeerbeton ondersoek. Wanneer slagment by die bindmiddel gevoeg word, is nabehandeling by omliggende temperature moontlik as gevolg van kalsiumsilikaathidroksiede wat in verbinding met die geopolimeriese jel vorm.

Die hoofdoel van die studie was om ‘n beter begrip te kry van die meganiese eienskappe van geopolimeerbeton, wat nabehandeling by omliggende temperature ontvang het. ‘n Aansienlike aantal meng variasies is uitgevoer om die invloed te ondersoek wat die verskeie parameters, aanwesig in die bindmiddel, op die druksterkte van die vliegas/slagmentgebaseerde geopolimeerbeton het. Belowende resultate is verkry en sterktes van tot so hoog as 72 MPa is opgelewer. Daar is gevind dat die sodiumhidroksiedoplossing, die slagmentinhoud en die hoeveelheid water in die bindmiddel die grootste invloed op die druksterkte van die vliegas/slagmentgebaseerde geopolimeerbeton gehad het.

Die styfheid van die vliegas/slagmentgebaseerde geopolimeerbeton het nie belowende resultate opgelewer nie. Die meeste van die monsters, ongeag die druksterkte, het ‘n styfheid van minder as 20 GPa opgelewer. Vanuit ‘n strukturele oogpunt is dit problematies, omdat groot defleksies in elemente sal voorkom. Die sodiumhidroksiedoplossing het die grootste invloed op die styfheid van die vliegas/slagmentgebaseerde geopolimeerbeton gehad.

Staal en polipropileenvesels is by ‘n hoë en lae sterke geopolimeer beton gevoeg om die buigbaarheid te ondersoek. Die die maksimum buigbaarheid het hoofsaaklik afgehang van die beton se druksterkte terwyl die hoeveelheid vesels die beton se energie-opname verhoog het. ‘n OPC beton mengsel van soortgelyke sterkte is vergelyk met die lae sterkte geopolimeerbeton en daar is gevind dat die OPC beton ietwat beter buigbaarheid opgelewer het. Veseluittrektoetse is uitgevoer om die vesel-bindmiddel se skeidingsvlak te ondersoek.

Daar kan tot die gevolgtrekking gekom word dat, alhoewel belowende resultate verkry is, daar steeds sommige aspekte is wat ondersoek en verbeter moet word, in besonder die styfheid, voordat geopolimeerbeton as ‘n alternatiewe bindmiddel kan optree.

Volgens die kennis opgedoen tydens hierdie studie, kan dit afgelei word dat die gebruik van vliegas/slagmentgebaseerde geopolimeerbeton, as 'n alternatiewe bindmiddel, nog 'n geruime tyd weg is, as gevolg van baie komplikasies wat gehandel moet word, veral die lae elastisiteitsmodulus. Tog het vliegas/slagmentgebaseerde geopolimeerbeton potensiaal as hierdie komplikasies verbeter kan word.

Acknowledgements

I would like to express my sincere thank you to the following people during the past two years for all the support and guidance:

- Professor Billy Boshoff, for being a great mentor and for all the advice, patience and support during my thesis.
- The lab assistants; Charlton Ramat, Peter Cupido and Hershen Adonis, for helping me during the long hours of mixing and testing in the lab.
- All the people who sponsored me the various materials required for my mix designs.
- Stellenbosch University and Element Consulting Engineers Namibia, for the financial assistance that made all of this possible.
- Family members, for all the prayers, love and words of encouragement over the past two years.
- My South African family, the Lloyd's and O'kennedy's for their love and support and always having an open door for me throughout the 11 years that I have spent in South Africa.
- Problem solving prayer group, for keeping me motivated and determined to finish.
- Jolandi Cilliers, for her love and support during the past two years.
- Friends, for keeping me sane and motivated and for making the past two years bearable and fun in the midst of all the hard work. I would like to thank the following friends personally in alphabetical order;
    - Dawie De Klerk
    - Diederick Dippenaar
    - Human Steenkamp
    - Koos Loubser
    - Llywelyn Lloyd
    - Louwrens Mostert
    - Petrus Theart
    - Philip Piek
    - Rudi van Wyk
    - Wessel Smalberger

And lastly, but most important I would like to thank God, my Saviour, for his unconditional love, abundance of grace and all the blessings that He gave me during the past two years. All the glory and honour goes to Him who gave me strength and perseverance.

Table of Contents

List of figures

List of Tables

Nomenclature

Symbol/Abbreviations	Description	Unit
SEM	Scanning electron microscope	
OPC	Ordinary Portland cement	
CSH	Calcium silicate hydrate	
GGBS	Ground granulated blast furnace slag	
GGCS	Ground granulated corex slag	
HPFRC	high performance fibre reinforced concrete	
FRC	fibre reinforced concrete	
GFRC	geopolymer fibre reinforced concrete	
OFRC	OPC fibre reinforced concrete	
GSFRC	Geopolymer steel fibre reinforced concrete	
OSFRC	OPC steel fibre reinforced concrete	
GPFRC	Geopolymer polypropylene fibre reinforced concrete	
OPFRC	OPC polypropylene fibre reinforced concrete	
LOP	Limit of proportionality	
M	Molar concentration	
δ	Deflection	mm
Re3	Equivalent flexural ratio	
E_c	Modulus of elasticity	GPa
ε	Strain	
ρ	Density	kg/m^3
σ	Compressive strength	MPa
F	Force	N
A	Area	mm^2
I	Moment of inertia	mm^4
ω	Distributed load	N/m
l	Span	m
F_{eq3}	Mean force for the equivalent flexural strength	F-m
$f_{e,3}$	Equivalent flexural strength	MPa
f_L	Limit of proportionality	MPa

Chapter 1
Introduction

Worldwide, the production of ordinary Portland cement (OPC) was approximately 4 Gt in the year 2013 (Statista 2014). At the current growth rate of the world's population, the levels of OPC production will only increase, providing enough cement to build infrastructure that will ensure adequate lifestyles. Approximately 7% of the world's greenhouse emissions into the atmosphere are due to the production of OPC (Hardjito et al. 2004). The carbon footprint of OPC is, on average, approximately 820 kg CO_2 per tonne manufactured (Motorwala et al. 2008).

Due to the excessive use of OPC, environmental concerns developed regarding the damage caused during the extraction of the raw materials and due to large amount of CO_2 emissions during the manufacturing process of OPC. It should be noted that the production of OPC is only an issue due to the large quantity that is produced each year. Compared to other materials, such as steel and aluminium, less energy is used to produce OPC (Sakulich 2011). In seeking for solutions to reduce global warming and the high amount of CO_2 emissions, researchers introduced a new kind of binder known as alkali activated cement or better known as geopolymers.

Geopolymer concrete is well known for its promising mechanical properties, acid resistance and fire resistance and therefore is a potential alternative construction material with comparable properties to OPC concrete. Geopolymers emit approximately 80% less CO_2 than OPC during production, making it a more environmental friendly building material (Sakulich 2011, Alzeer and MacKenzie 2013).

Traditional low calcium based geopolymer concrete requires heat curing and is already used in the precast industry as many precast factories have heat curing facilities available. The problem is that in-situ casting is still the conventional construction method and therefore it would be ideal for geopolymer concrete to be advanced to a point where in-situ casting is possible. To achieve this, geopolymer concrete must be able to cure at ambient temperatures. During this study the curing of geopolymer concrete at ambient temperatures was investigated. According to previous research done in this specific field, the addition of slag in the matrix accelerates the curing process and ensures ambient temperature curing. Therefore, a fly ash/slag based geopolymer concrete was investigated in this study.

Low calcium based geopolymer concrete hardens through a process called geopolymerisation. The binder, consisting mainly of silica and aluminium, is broken down by a dissolution process in which the silica and aluminium ions are released. A condensation process follows in which the aluminium and silica ions are interlocked with oxygen ions to form the hardened material. When slag is added to the geopolymer matrix, calcium silicate hydrates (CSH) are formed in conjunction with the geopolymeric gel. The CSH improves both the setting time and the compressive strength of fly ash/slag based geopolymer concrete when it is cured at ambient temperatures (Davidovits 2011, Yip et al. 2008).

An area that has not yet been advanced is the design of a geopolymer concrete mix that will yield desired target strength. In the case of designing OPC concrete, the water to binder ratio primarily determines the strength. However, the strength of geopolymer concrete is influenced by various constituents and ratios, making it more complex to design for a specific strength. This study investigated the influence of the various constituents on the mechanical properties of geopolymer concrete. This investigation forms the basis of this study.

Like OPC concrete, geopolymer concrete has a brittle failure which results in a low flexural strength. Brittleness of both concrete types is compensated by conventional steel reinforcement. Steel reinforcement adds ductility to concrete and increases its flexural resistance. Alternatively, fibres can be added to improve the ductility of concrete. The addition of macro steel and –polypropylene fibres was investigated in this study to determine whether it improves the brittle behaviour of fly ash/slag based geopolymer concrete.

The research methodology used includes physical experiments. The mechanical properties of geopolymer concrete were obtained by conducting tests on cube-, cylindrical-, beam- and panel specimens.

The study has three main objectives. The first and most important is to determine the mechanical properties of fly ash/slag based geopolymer concrete. The second objective is to improve the mechanical properties, mainly the flexural behaviour, when fibres are added to the matrix. The third and final objective is to compare the flexural properties of fly ash/slag based geopolymer concrete and OPC concrete.

A possible outcome of this study would be to conclude that fly ash/slag geopolymer concrete, cured at ambient temperatures, has the required properties to be utilised as an alternative binder material in the construction industry.

The layout of the report is as follows: Chapter 2 contains the literature review that was conducted to gain knowledge of geopolymers and to obtain information of previous work done. A literature review

of fibres in concrete is provided in Chapter 3. In Chapter 4 the test setups of all the various tests that have been carried out, are explained. Chapter 5 contains information of the materials used and explains the various mix designs that was used to cast the different specimens required for testing. The results of the tests that were carried out are given in Chapter 6 and are discussed in detail in Chapter 7. Chapter 7 also includes the various trends that were observed as well as all the problems that occurred during the experimental part of the study. Chapter 8 concludes the findings of this research and provides essential recommendations for further studies.

Chapter 2
Geopolymer concrete

2.1. Background of geopolymers

In 1978, Professor Joseph Davidovits introduced the development of a new family of mineral binders with an amorphous structure, named geopolymers. This was a class of solid materials, produced by the reaction of an aluminosilicate powder and an alkaline liquid. The initial goal for the research done on these geopolymers was to find a more fire resistant binder material due to the high amount of fires in Europe at that time. This research led to the material being used as coatings for the fire protection of cruise ships and thermal protection of wooden structures etc. (Provis et al. 2009). The main focus shifted to a use in the construction industry after an observation that it was possible to produce high performance and reliable concrete with cement-like properties when fly ash was alkaline activated (Provis et al. 2009).

2.1.1. Terminology

A "geopolymer", in general, is defined as a solid and stable material consisting of aluminosilicates formed by alkali hydroxide or/and alkali silicate activation (Provis et al. 2009).

The chemical designation of these polymers was based on silico-aluminates. The term poly(sialate) was chosen to be used, with "sialate" being the abbreviation for silicon-oxo-aluminate (Davidovits 1989, Davidovits 1991). The poly(sialate) network consists of Si_4^+ & Al_3^+ ions in forth-fold coordination, sharing oxygen ions and ranges from amorphous to semi-crystalline (Davidovits 1989, Sakulich 2011).

An empirical formula for the poly(sialate) is given as follow:

Mn (-(SiO2) z–AlO2)n, wH2O

Where "*z*" is a value between 1 and 3 depending on the chemistry of the reaction, "*M*" is the alkali element that is used; "*n*" is the degree of polymerisation and "*w*" is the hydration extent (Sakulich 2011, Davidovits 1989).

2.1.2. Chemistry

Three types of polysialates have been distinguished by Davidovits and are shown in Figure 2.1.

Poly (sialate)
(-Si-O-Al-O-)

Poly (sialate-siloxo)
(-Si-O-Al-O-Si-O-)

Poly (sialate-disiloxo)
(-Si-O-Al-O-Si-O-Si-O-)

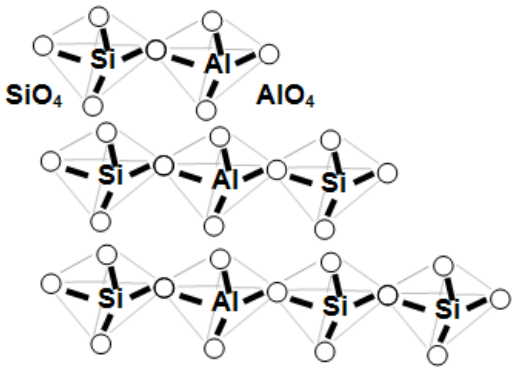

Figure 2.1: Chemical structure of polysialates (Wallah and Rangan 2006)

A chemical reaction known as geopolymerisation involves aluminosilicate oxides (Si_2O_5 and Al_2O_2) to react with polysilicates, yielding three dimensional polymeric bonds (Si-O-Al-O) under highly alkaline conditions. This reaction is also known as a geosynthesis, better described as a reaction that chemically integrates minerals (in this case polymeric bonds) which eventually forms the main building blocks of the final geopolymer material (Khale and Chaudhary 2007).

The polysilicates used are usually sodium or potassium silicate, produced by the chemical industry and these materials are either crystalline (glassy structure) or non-crystalline (amorphous) (Wallah and Rangan 2006, Davidovits 1991). The geopolymer process mainly depends on the parameters, including the chemical and mineralogical composition of the binder material, the concentration of the alkaline solution, the water content and curing temperature (Temuujin et al. 2009).

The silica to aluminium ratio has an influence on the strength of geopolymer concrete and this ratio mainly depends on the chemical composition of the starting material, concentration of the alkali solution, curing temperature and the curing time (Fernández-Jiménez et al. 2006). Fernández-Jiménez et al. (2006) concluded that not all the aluminium and silica ions are reactive in the binder. They also found, by experimenting with different fly ashes, that the percentage of silica reactive in the material was similar but the percentage of aluminum reactive in the mixture varied.

The geopolymerisation process is discussed, in more detail, in the following section to ensure a better understanding of the binding process of geopolymer concrete.

The geopolymerisation process consists of three stages:

1. The first stage in the geopolymerisation process is the dissolution of the silica and aluminium ions within the amorphous phase of the binder material. The process is activated by the alkaline solution during initial mixing. Thus, the hydroxides are necessary during this stage of the geopolymerisation process. The dissolution process starts immediately after the alkali solution comes in contact with the binder e.g. fly ash, slag, metakaolin (Fernández-Jiménez et al. 2006).

   The dissolution process results in the formation of a disordered gel phase known as the geopolymeric gel binder phase (Provis et al. 2009). The pore network of this gel contains the water that was added during the mixing of the alkaline materials, but unlike OPC, water does not form part of the chemical structure of the geopolymer. The framework of the geopolymeric gel is a highly connected three dimensional network, consisting of aluminate and silicate tetrahedral (Silva et al. 2012). This network has a negative charge, mainly due to Al^{3+} ions which is in forth-fold coordination. These Al^{3+} ions are localised on one or more of the oxygen ions that is bridging in each aluminate tetrahedron. The negative network is then balanced by the positively charged alkali metals such as sodium, calcium or potassium (Provis et al. 2009).

   The alkali solution with a high hydroxide concentration breaks the Si-O-Si, Al-O-Al, and Si-O-Al bonds that are present in the glasslike phase of the binder and releases silica and aluminium ions in the solution. The silicon and aluminium ions will then form Si-OH and Al-OH groups (Fernández-Jiménez et al. 2006). The rate of dissolution is mainly dependent on the composition of the binder and the PH of the alkali solution (Saeed et al. 2010).

2. A condensation reaction between the neighbouring silica and alumina molecules takes place in the solution. The alkali solution also acts as a catalyst during this stage. This reaction causes the neighbouring hydroxyl ions to form an oxygen bond which links the molecules and a water molecule.

3. The final stage is called poly-condense, which forms an interlocking network of oxygen bonded tetrahedral. The reaction is activated when mild heat is applied to the solution. (Van Chanh et al. 2008)

The following equations represent the polycondensation process which occurs the moment when the binder and the alkaline solution are mixed together (Equation 2.1), to final poly-condensing process (Equation 2.2). Equation 2.1 represents stage two in the geopolymerisation process and Equation 2.2 represents stage three.

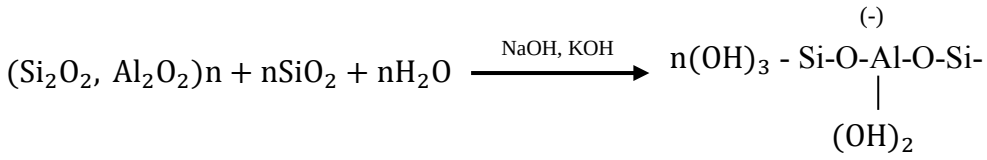

(2. 1)

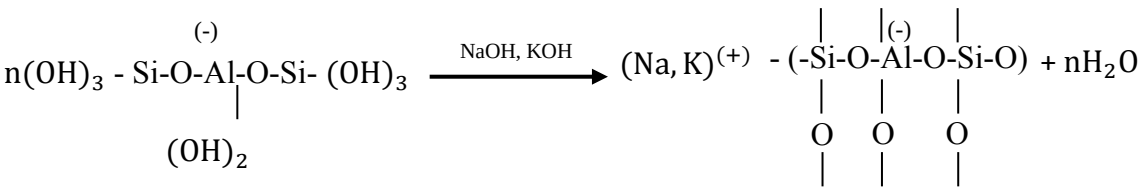

(2. 2)

As observed from Equation 2.2, water is extracted from the reaction. This result confirms that water does not participate in the geopolymerisation process. The water is expelled from the matrix during curing and evaporates through nano-pores in the matrix. The role of the water in the mixture is only to ensure workability of the fresh geopolymer concrete. This is why geopolymers are known as alkali activated cement (Davidovits 1994, Hardjito and Rangan 2005). It must be understood that the initial amount of water will have an effect on the properties of geopolymers as the concentration of the alkaline solution will be influenced when water is added.

2.1.3. Geopolymer terminology vs ordinary Portland cement terminology

Figure 2.2 illustrates the chemistry of OPC (Left) and geopolymers (Right). OPC hardens through a hydration process while geopolymers harden through a polycondensation process.

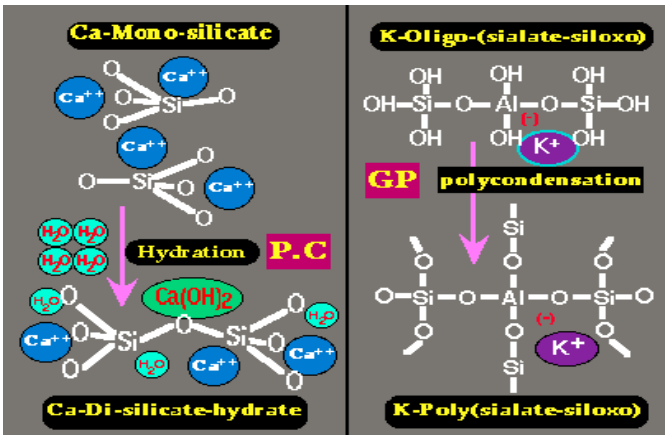

Figure 2.2: Chemistry of Portland cement and geopolymer cement (Davidovits 2013)

The fact that geopolymer concrete has better heat resistance compared to OPC concrete confirms that there is no hydrates present in the matrix. Hydrates tend to explode when exposed to extreme heat (Davidovits 2013). It must be noted that this property is only valid for geopolymer concrete that consists of a low calcium binder material. Hydrates tend to form in conjunction with geopolymeric gels when the binder has a high calcium content. This is explained in Section 2.2.3.

Figure 2.3 shows a mortar structure of OPC concrete (left) and geopolymer concrete (right). The mortar structure of OPC concrete has a coarser surface compared to that of geopolymer concrete. The coarse surface of the OPC concrete may lead to cracks, causing weak areas. The chances of cracking will be less on the smoother surface of geopolymer concrete (Davidovits 2013). The smoothness of the geopolymer concrete is mostly due to fly ash being used as binder.

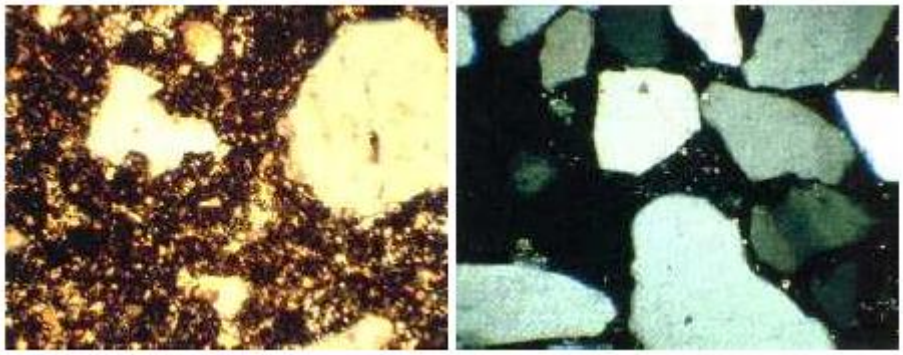

Figure 2.3: Comparison of surface roughness of OPC concrete and geopolymer concrete (Davidovits 2013)

2.1.4. Health and safety concerns

In a developing country such as South Africa, the use of labour is promoted in the construction industry and therefore it is essential to ensure that the materials that are worked with do not cause any health concerns.

Most of the researchers, investigating geopolymer concrete, have used a combination of sodium hydroxide and sodium silicate as the alkaline solution. This mixture shows promising mechanical properties. However, these constituents can be dangerous to work with in normal circumstances. This problem is a major concern for the construction industry as is it will be difficult to work with fresh geopolymer concrete by the use of labour. Working with these types of materials requires some safety precautions.

Sodium hydroxide is a substance which evolves in a strong exothermic reaction once added to water. The high rise in temperatures is due to the separation of the sodium hydroxide molecules into Na^+ (sodium) and the OH^- (hydroxide) ions (Evonik Industries 2010).

The rules of safety for these alkaline materials can be divided into two categories: Corrosive products which have some hostile properties and irritant products which are friendlier to work with (Davidovits 2013). The corrosive products must be handled with safety equipment such as glasses, gloves and masks. The two categories and their respective products are shown in Table 2.1.

Table 2.1: Hostile and friendly products (Davidovits 2013)

Hostile	Friendly
CaO (quick lime)	$Ca(OH)_2$
NaOH, KOH	Portland Cement, Iron Slag
Sodium metasilicate: SiO_2:Na_2O = 1.0	Slurry Soluble Silicate/Kaolin
	1.25 < SiO_2:Na_2O < 1.60
Any Soluble silicate: SiO_2:Na_2O < 1.60	Any Soluble silicate: SiO_2:Na_2O > 1.60

Sodium hydroxide is a very corrosive and hazardous substance that will cause severe burns and irreversible damage when it comes in contact with eyes or open skin. Consuming a certain amount of sodium hydroxide can be fatal. Sodium hydroxide is, however, neither genotoxic nor carcinogenic which means that no damage will be done to any parts of the body when sodium hydroxide is separated into its constituent ions (Evonik Industries 2010).

If a sodium hydroxide solution is above 0.5 M it is hazardous. A safe concentration is 0.05 M to 0.5 M and will only cause an irritation to the eyes and skin. A sodium hydroxide concentration of less than 0.05 M typically holds no danger or irritation to the skin or eyes (Evonik Industries 2010).

Most of the geopolymer concrete mix designs, found in literature, especially those based on fly ash geopolymer concrete, comprises SiO_2:M_2O molar ratios below 1.2 (M being Na or K) when using additional silicate solution in its alkaline mixture. This geopolymer concrete mixes are user-hostile and cannot be handled by ordinary labour force (Davidovits 2013, Geopolymer Institute 2006).

Geopolymer concrete mix designs, based on user friendliness, which can be handled by ordinary labour forces, generally contain alkaline soluble silicates with a SiO_2:MO_2 ratio more than 1.6 (Davidovits 2013). Note that a ratio of more than 1.6 was used in all the mix designs in this study.

2.2. Geopolymer categories

As mentioned, geopolymers are formed by alkali-activating a variety of materials including fly ash, blast furnace slag, thermally activated clays etc. to produce a cement-like material.

The three most common raw binders used in geopolymerisation are slag, calcined clays (metakaolin) and coal fly ash. The binder materials should contain high levels of aluminium (Al) and silicon (Si) in amorphous form.

Many different materials have already been investigated and used as the binder in geopolymer concrete mixes, including:

- Class F fly-ash (low amount of calcium)
- Class C fly-ash (high amount of calcium)
- Calcined kaolin or metakaolin
- Natural minerals containing Al and Si
- Silica fume
- Slag
- Red mud
- Albite

(Motorwala et al. 2008, Swanepoel and Strydom 2002, Davidovits 1999, Palomo et al. 1999)

Metakaolin was widely used as the binder in the early stages, but due to its flat shape it tends to have an unviable high water demand (Provis et al. 2009). Fly ash particles have a rounder shape, ensuring more promising workability and a low water demand.

There are currently four different geopolymer categories (Davidovits 2013), including:

- Slag based geopolymer
- Rock based geopolymer
- Fly ash based geopolymer
- Ferro-sialate based geopolymer

2.2.1. Slag based geopolymer

The first geopolymer developed was a slag based geopolymer in the 1980s. It was a type (K, Na, Ca)-poly(sialate) which resulted from the research of Davidovits and J.L. Sawyer at Lone Industries in the USA. This research resulted in an invention well known today as Pyrament® cement (Davidovits 2013).

Pyrament® cement is ideal for the repairing of airline runways made of OPC concrete, industrial pavements and highways. The reason for using this type of cement is due to its the rapid strength gain as it can reach strengths of up to 20 MPa after just 4 hours (Geopolymer Institute 2013).

Slag is a partially transparent material and a by-product in the process of melting iron ore. It usually consists of a mixture of metal oxides and silicon dioxide. Slag has many purposes for which it can be used, including assisting temperature control during smelting and minimizing the final liquid product before the molten metal is removed from the furnace (Slag Cement Association 2002). It is also used in the cement and concrete industry.

For over a century slag has been used in concrete. The substitution of OPC with slag is one of the many benefits that it provides to OPC concrete, reducing life cycle costs and improving the workability of the fresh concrete (Slag Cement Association 2002).

Other benefits for the use in OPC concrete include:

- Easier finishability
- Higher compressive and flexural strength
- Improved resistance to acid materials

(Slag Cement Association 2002)

The reactions of slag in alkali activating systems and in cement blends are dominated by the small particles. The particles that are above 20 μm usually react slowly, while particles under 2 μm react completely within 24 hours. Thus, when slag is used in geopolymerisation, careful control of the particle size distribution must be ensured to control the strength of the binder (Provis et al. 2009)

The chemical composition of slag has a significant influence on the geopolymer matrix. Figure 2.4 shows a scanning electron microscope (SEM) image of ground granulated blast furnace slag (GGBS). As depicted in the figure it is clear that the slag particles have sharp edges which may lead to lower workability of fresh geopolymer concrete when added.

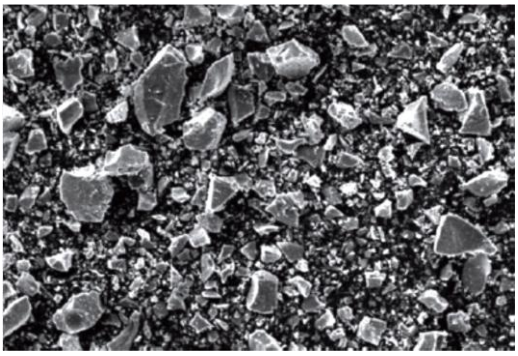

Figure 2.4: SEM image of typical GGBS (Wan et al. 2004)

Three types of slag are discussed in this study, including:

- Iron blast-furnace slag
- Corex slag
- Steel slag

2.2.1.1. Iron blast-furnace slag

Blast-furnace slag is a non-metallic product, consisting mostly of silicates and alumino-silicates of calcium and other bases which develop in a molten condition simultaneously with iron oxides

(Lewis 1992). This process takes place in a blast furnace. The primary role of the blast furnace is to reduce the iron oxides to molten, metallic iron. Molten iron is collected at the bottom of the furnace with the liquid slag floating on top (Lewis 1992) .

As mentioned, the primary constituents of slag are impurities from the iron ore, mainly consisting of silica and aluminium combined with calcium and magnesium oxides from the flux stone. The composition of the slag depends on the composition of the iron ore (Lewis 1992).

2.2.1.2. Corex slag

The Saldanha steel plant, in South Africa, is currently using a more environmental friendly process to produce iron. This process is called the Corex process. The coke ovens and the blast-furnace in the conventional process are replaced by a direct reduction shaft and melter-gasifier. A quenched slag, called corex slag, is a by-product of this process (Alexander et al. 2003).

Corex slag was used in this study. During a study done on fly ash/slag based geopolymer concrete, Nath and Kumar (2013) concluded that ground granulated corex slag (GGCS) yielded almost similar results than ground granulated blast-furnace slag (GGBS). He also concluded that GGCS is a safe and suitable replacement for GGBS and that there is no significant difference in the microstructure of the two materials (Nath and Kumar 2013). The corex slag, in fact, yielded slightly higher compressive strengths compared to blast-furnace slag.

2.2.1.3. Steel making slag

Steel slags are by-products formed during the process in which molten iron is converted to a specific type or grade of steel. The production of steel is a batch process in which the furnace is filled with the necessary metal. The alloying materials are adjusted to produce the desired composition of the steel. The molten steel in conjunction with the slag is extracted from the furnace and the process is repeated. Practically all steel slags are air cooled. Steel making slag is produced in small quantities compared to blast-furnace slag and is not as widely used (Lewis 1992).

The composition of steel making slag consists mainly of calcium silicates, calcium alumino-ferrites and fused oxides of calcium, iron, magnesium and manganese. The compositions vary depending on the furnace, grade of steel and the compositions of the materials added.

Steel making slag usually contains a higher amount of iron and magnesium compared to blast-furnace slag and is lower in silica. It is heavier and denser than blast-furnace slag particles and the particles usually have more resistance against polishing and wear (Lewis 1992).

2.2.2. Rock based geopolymer

To compose this type of geopolymer, a fraction of the MK-750 in the slag based geopolymer is replaced by natural rock forming materials such as feldspar and quarts. This mixture yields a

geopolymer with better properties and less CO_2 emissions than that of the ordinary slag based geopolymer (Davidovits 2013). However, not much research has been done on the reaction kinetics of these natural rock forming materials under alkaline conditions.

The "MK" is an abbreviation for metakaolin and the "750" represents the temperature at which it was produced. The components of rock based geopolymer cement is metakaolin MK-750, blast-furnace slag, natural rock forming materials (calcined or non-calcined) and a user friendly alkali silicate.

2.2.3. Fly ash based geopolymer

2.2.3.1. History of fly ash

The most sufficient way to generate heat is to ignite a material that will generate heat continuously in the presence of oxygen until the material is combusted. Coal is a perfect example of such a material and it is mined worldwide and mostly used to produce energy. The heat that is generated from the burning coal is used to produce this energy (Provis et al. 2009).

Coal-burning power stations produce various by-products of which fly ash contributes the highest amount. About 70% to 80% of the total mass of ash produced is fly ash and consists mainly of fine, spherical aluminosilicate particles (Sakulich 2011). In countries such as South Africa, Brazil, India and Russia, the amount of coal available for power stations is relatively high, making fly ash a feasible binder for geopolymer concrete.

Fly ash is commonly used as a substitute for OPC in concrete and the addition of it provides the following:

- Fly ash consists of spherical particles which improve the workability of the fresh OPC concrete. This enables one to reduce the amount of water in the mix which reduces the amount of bleeding of OPC concrete.
- Improves mechanical properties such as compressive strength, due to the water reduction and ensures a higher reactiveness and better "packing" of particles.
- Reduce the cost of the OPC concrete.
- Reduces the CO_2 emissions.
- Reduces drying shrinkage.
- Smoother surface.

(Provis et al. 2009)

Figure 2.5 and Figure 2.6 show the spherical shape of fly ash (Motorwala et al. 2008).

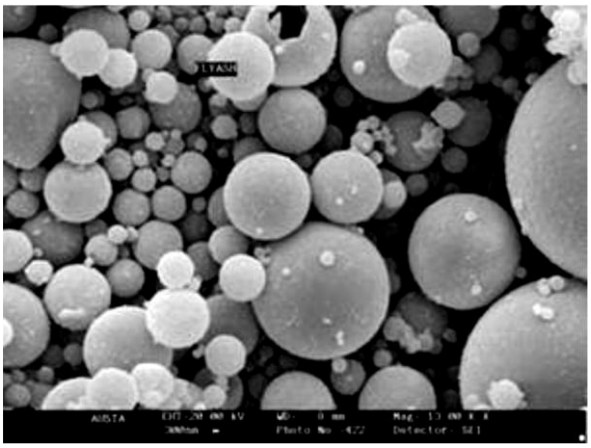

Figure 2.5: Ungraded fly ash

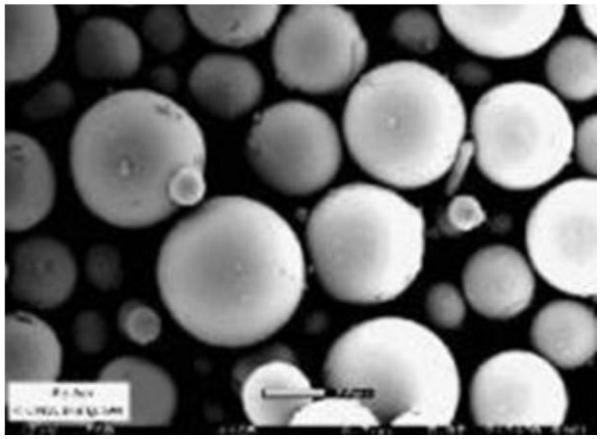

Figure 2.6: Graded fly ash

Fly ash has various characteristics that must be considered, including:

- Loss in ignition (LOI) - measurement of the un-burnt carbon that remains in the ash.
- Fineness - Depends mainly on how the coal is crushed and its grinding process.
- Uniformity

A finer gradation usually results in a more reactive fly ash due to a larger surface area that is exposed to the alkaline solution (Motorwala et al. 2008).

Fly ash can be divided into two groups, namely: type F fly ash and type C Fly ash. Geologically older coals typically produce type F fly ash which is low in calcium and is a pozzolan (Sakulich 2011). Low calcium fly ash consists mainly of aluminium and silicon with a CaO content of less than 10% (Hardjito and Rangan 2005). Low calcium fly ash is mainly chosen over high calcium fly ash due to the high amount of calcium that may interfere with the geopolymerisation process as it tends to produce calcium silicate hydrates (Hardjito and Rangan 2005).

Geologically younger coal produces type C fly ash which is rich in calcium and does not always require an activator. Type C fly ash usually contains 20% or more CaO. In South Africa only low calcium fly ash is produced.

The chemical composition of fly ash depends on the mineral composition of the burned coal. The silica can vary between 40% and 60% and the aluminium between 20% and 30% (Khale and Chaudhary 2007).

The use of fly ash is environmental friendly in three ways. It reduces the amount of virgin material that needs to be extracted when producing OPC, less greenhouse emissions are emitted into the earth's atmosphere and less energy is used during the production process of the geopolymer constituents (Sakulich 2011).

Fly ash does not have a calcination step and therefore fly ash based geopolymer concrete has extremely low embodied energies, consuming approximately 70% less energy compared to OPC concrete with the same strength (Sakulich 2011).

2.2.3.2. Types of fly ash based geopolymers

Currently there are two types of geopolymers based on class F fly ashes:

- **Alkali-activated fly ash geopolymer:**

This kind of geopolymer usually requires heat curing at 60 ℃ to 80 ℃. It is also known as the alkali activation method. A high concentration of sodium hydroxide solution is required to ensure an adequate geopolymerisation process. The mixture consists of fly ash and a user-hostile sodium hydroxide solution. The fly ash particles are embedded into an aluminosilicate gel with a Si:Al ratio of 1 to 2 (Davidovits 2013). This is a zeolite type material.

- **Fly ash/slag based geopolymer:**

This kind of geopolymer is more user-friendly and it hardens at room temperature. The mixture consists of a user-friendly silicate, blast furnace slag and fly ash. The fly ash particles are embedded into a geopolymer matrix with and Si:Al ratio of 2. This is a (Ca,K)-poly(siliate-siloxo) geopolymer (Davidovits 2013). This type of geopolymer was investigated in this study and it is discussed in more detail in the following section.

2.2.3.3. Fly ash/slag based Geopolymer concrete

As stated in Section 2.1.2, the dissolution of the silica and aluminium, present in the binder, governs the geopolymerisation process. The formulation of the fly ash/slag based geopolymer concrete structure depends mainly on the availability of the silicate $SiO_n(OH)_{4-n}^{n-}$ and aluminate $Al(OH)^{4-}$ monomers, present in the alkaline medium (Yip et al. 2008). The formulation is further dependent on

the degree of dissolution of these monomers from the original aluminosilicate binder. A monomer is a single molecule that binds with other single molecules to form a polymer.

When a calcium silicate material is added to the matrix, the governing reactions become more complex. The reaction can take place under two circumstances (Yip et al. 2008):

1. The calcium can precipitate as $Ca(OH)_2$,which will lower the alkalinity of the medium and, as a result, it will be the driving force for the dissolution of the monomers. During the mixing of the geopolymer cement, Ca^{++} will react with OH^- to form $Ca(OH)_2$. It will further react with CO_2 available in the atmosphere. This reaction will form calcite which is the main hardening mechanism. The process will take place in conjunction with the dissolution of the aluminosilicate material (Astutiningsih and Liu 2005).

Davidovits (2011), however, stated that, according to their lab experience, the reaction as discussed above does not occur in the reaction medium and would only occur after the geopolymer concrete has hardened and comes in contact with the atmosphere. According to Davidovits (2011), the second circumstance is the correct reaction and will be discussed in in the following section.

2. The formation of the geopolymeric gel will be changed as calcium will interact with the dissolved silicate and aluminate species. The formulation of the structure will consist of Si, Al and Ca ions. Yip (2008) concluded that the dissolution of manufactured calcium silicates, at low alkalinity, forms a combination of cementitious calcium silicate hydrate (CSH) - and geopolymeric gels.

The improved compressive strength and setting times can be explained by the formation of the CSH gel. The gel increases the compressive strength of the fly ash/slag based geopolymer concrete and accelerates the setting time (Davidovits 2011).

The CSH gels precipitate due to the alkali activation of the slag in the matrix and the process is as follow:

The mineral composition, available in the slag's glassy phase, consists mainly of melilite, indicated in Figure 2.7. Melilite is a solid solution which mainly consists of gehlenite $Ca_2Al_2SiO_7$, akermanite $Ca_2Mg(Si_2O_7)$ and merwinte $Ca_3Mg(SiO_4)_2$. As depicted in the Figure 2.7, aluminium is found in gehlenite and magnesium in akermanite and also in merwinte (not shown in the figure). For the purpose of geopolymer chemistry, gehlenite is the molecule that can react during the geopolymerisation process.

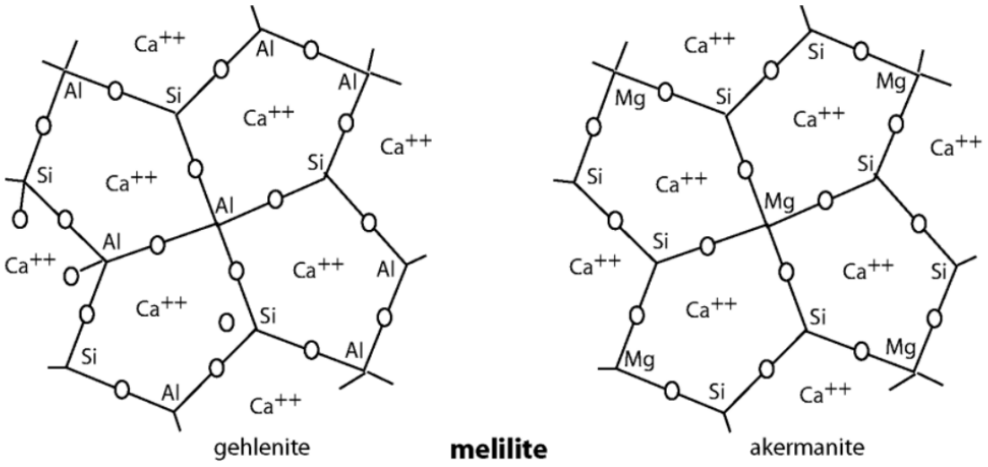

Figure 2.7: Mineral formulation of gehlenite and akermanite in melilite glass (Davidovits 2011)

The melilite undergoes a severe alkaline cleavage (Figures 2.8 and 2.9). The gehlenite yields ortho-sialate hydrate molecules and releases aluminium hydroxide ($Al(OH)_3$). The akermanite yields Ca-di-siloxonate (CSH) molecules and releases $Mg(OH)_3$. The merwinte undergoes the exact same cleavage as akermanite but it releases $Ca(OH)_2$

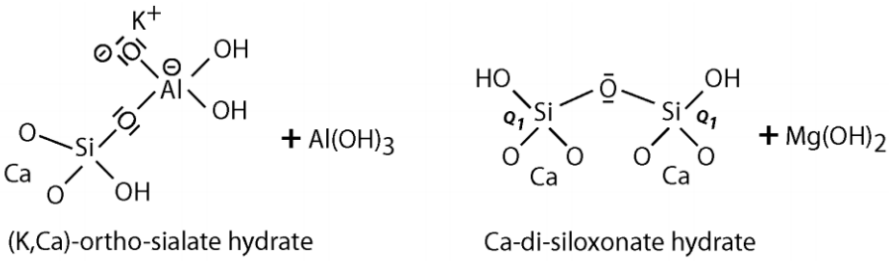

Figure 2.8: The first step of the melilite alkalinisation (Davidovits 2011)

Secondly, the ortho-sialate hydrate molecules condense with the CSH molecules and form a quadratic ortho-(sialate-di-siloxo) molecule [Si-O-Al-Si-O-Si-O]. The CSH molecules remains isolated in the matrix and the free $Al(OH)_3$, $Mg(OH)_3$, $Ca(OH)_2$ reacts with CO_2 to form carbonates.

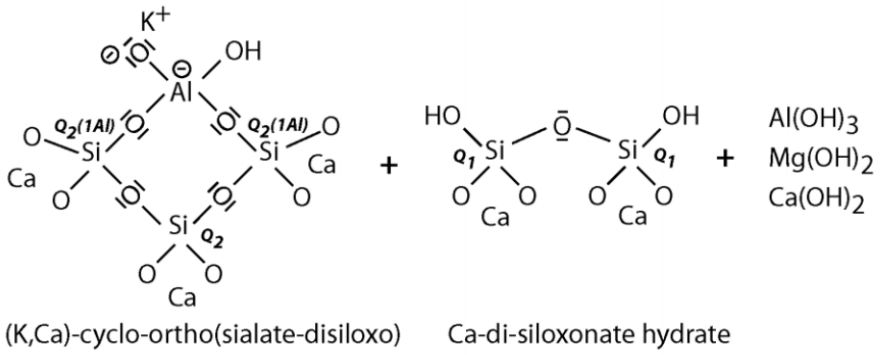

Figure 2.9: The second step of the melilite alkalinisation (Davidovits 2011)

2.2.4. Ferro-sialate based geopolymer

This type of geopolymer has the same properties as rock based geopolymers but contains geological elements with high iron oxide content, giving the geopolymer a red colour (Davidovits 2013). Some of the aluminium atoms in the matrix are substituted with iron ions to yield a poly(ferro-sialate) type geopolymer with the following formation: (Ca,K)-(-Fe-O)-(-Si-O-Al-O-). The user-friendly geopolymer is a result of the geopolymerisation of a calcium type geopolymer with geological elements that is rich in iron oxides and ferro-kaolinite. These materials usually originate from the weathering of acid rocks such as granite (Davidovits et al. 2012).

2.3. Alkali activator

Silica is a material that dissolves in strong alkaline conditions (high-pH). The alkaline solution is active during the dissolution of the silica and aluminum and it plays an important role in the condensation process (Lindgård et al. 2012).

The common activators used for geopolymers are sodium hydroxide, potassium hydroxide, sodium silicate and potassium silicate. Sodium hydroxide was the main activator used in this study, with the addition of sodium silicate to increase the silica content in the matrix.

In a study done by Palomo et al. (1999), they found that the type of alkaline solution plays a significant role in the properties of the of the geopolymer concrete matrix.

The choice of alkaline solution depends on the reactivity required and the cost of the solution. Previous investigations have found that sodium hydroxide, in conjunction with sodium silicate, proved to be an effective alkaline activator, yielding promising mechanical properties as it improves the reaction between the binder and alkali solution (Memon et al. 2013, Xu and Van Deventer 2000).

Xu and Van Deventer (2000) also found that sodium hydroxide caused a higher rate of dissolution compared to that of potassium hydroxide.

The dissolution process of silica and aluminium, available in fly ash, is shown in Figure 2.10. The alkaline solution attacks the surface of the particle. The particle breaks open, exposing smaller particles which are either hollow or partially filled with smaller ashes. The alkali attacks the partially open particle from the inside out as well as from the outside in and the process will go on until the ash particle is completely consumed (Al Bakri et al. 2011).

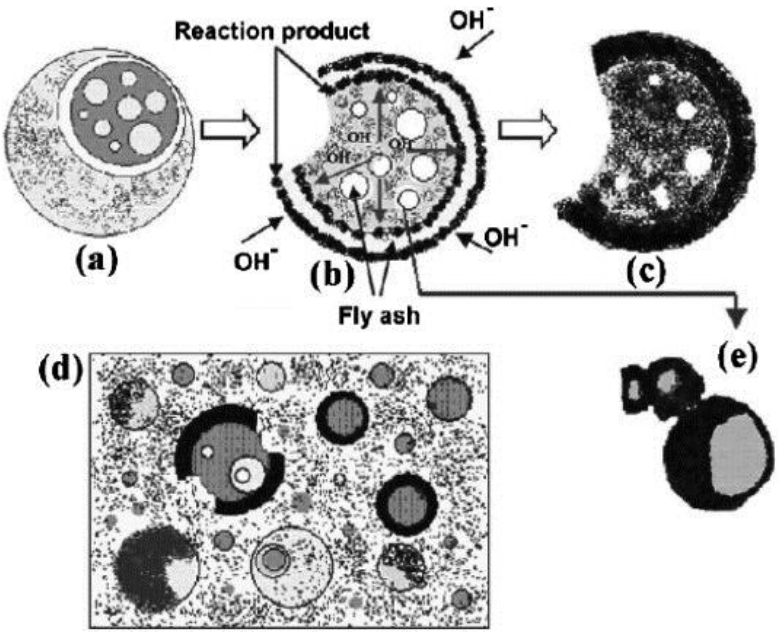

Figure 2.10: Descriptive model of the alkali activation of fly ash (Pacheco-Torgal et al. 2008)

2.3.1. Sodium hydroxide solution

Sodium hydroxide, also known as caustic soda, is produced by the electrolysis of sodium chloride brine in a membrane or diaphragm electrolytic cell (Occidental Chemical Corporation 2000). The largest users of caustic soda are the paper industry and manufacturers that need an alkaline based material. Sodium hydroxide is available in four forms: beads, flakes, compounders and solid castings. These forms have the same chemical composition (Occidental Chemical Corporation 2000).

2.3.2. Sodium silicate solution

Solutions of alkali silicates, also known as "waterglass", can be produced by either dissolving alkali silicate pellets in hot water or by hydrothermally dissolving a reactive silica source, mainly silica sand, into the respective alkali hydroxide solution (PQ Europe 2004). The hydrothermal dissolving process is described by:

$$2MOH + x\ SiO_2 \rightarrow M_2O.\ x\ SiO_2 + H_2O \qquad \textbf{(2. 3)}$$

As shown in Equation 2.3, the chemical composition of soluble silicates can be identified by the following formula: $(SiO_2)x(M_2O)$ where "M" is either sodium (Na) or potassium (K). Silicate solutions are mainly identified by the $SiO_2{:}M_2O$ ratio (PQ Europe 2004). This ratio plays a major role in the geopolymerisation process.

Potassium silicate solutions are similar to sodium silicate solutions with the most significant difference being that potassium silicate is somewhat more viscous than a sodium silicate solution (PQ Europe 2004).

Studies showed that the reaction in the geopolymerisation process occur at a higher rate when a soluble silicate is present in the solution, compared to only using an alkaline hydroxide (Palomo et al. 1999).

2.4. Mechanical properties of geopolymer concrete

Geopolymer concrete is known for its promising and comparable mechanical properties to that of OPC concrete. The compressive strength is known to be the key characteristic as it determines the overall strength of any type of concrete. A significant amount of research has been done to investigate the properties of geopolymer concrete and some of the important properties are listed below:

- Heat resistance
- Low creep and drying shrinkage
- Young's modulus and Poisson's ratio
- Resistance to chemical attack
- Ambient curing
- Compressive strength
- Tensile strength
- Ductility
- Durability
- Workability
- Setting times

Some of these properties are discussed in more detail in the following sections.

2.4.1. Typical mechanical properties

- **Heat resistance**

As mentioned, the investigation of geopolymeric materials started after the many catastrophic fires in France that occurred in a short passage of time in the 1970s. The investigation of the heat resistance of various alternative materials has been conducted since 1972, which later led to the introduction of geopolymers in 1978. Heat resistance tests that were conducted on geopolymer concrete yielded good results as it tends to have better heat resistance compared to that of OPC concrete (Davidovits 1989).

The primary reason for better heat resistance is that geopolymer concrete yields from a poly-condensation process and not from a hydration process as OPC concrete. Hydrate tends to explode when exposed to extreme heat (Davidovits 2013). Note that this mechanical property is only valid if a low-calcium binder is used.

- **Creep and drying shrinkage**

In a study done by Wallah et al. (2006), their results showed that the geopolymer concrete specimens undergoes low creep and low drying shrinkage. The test was carried out over a period of 1 year and most of the results showed that geopolymer concrete experience less creep than OPC concrete. However, Wallah et al. (2006) did not carry out exhaustive number of tests and therefore more research is required to draw an adequate comparison between the creep and drying shrinkage of geopolymer concrete and OPC concrete.

The results were compared to the values predicted by the draft Australian Standard for OPC concrete structures, as discussed in Section 4.3.3 (AS3600 2005). It was clear that the OPC concrete creep is higher than that of geopolymer concrete for the specific specimens that were tested (Wallah and Rangan 2006).

It must be noted that the drying shrinkage of geopolymer concrete, cured at ambient temperatures, shows shrinkage significantly higher than that of heat cured geopolymer concrete (Wallah and Rangan 2006). The excess water in the geopolymer concrete evaporates during the heat curing process, eliminating almost any chance of drying shrinkage. Wallah and Rangan (2006) concluded that the drying shrinkage for geopolymer concrete cured at ambient temperatures is similar compared to that of OPC concrete.

The results found by Wallah and Rangan are shown in Figure 2.11.

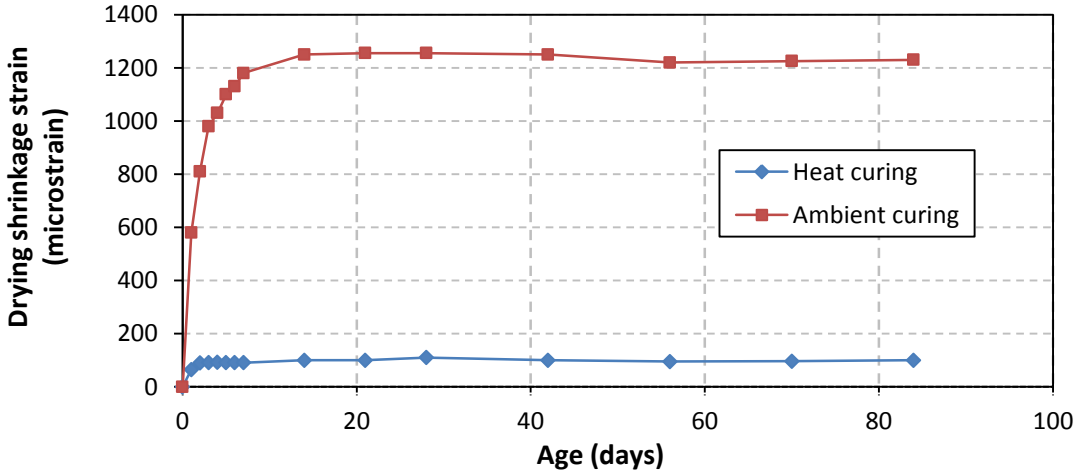

Figure 2.11: Drying shrinkage of heat cured and ambient cured specimens (Wallah and Rangan 2006)

- **Modulus of elasticity and Poisson's ratio**

Tests have been conducted on the stress-strain relationship of low calcium fly ash based geopolymer concrete and it showed similar results to that of OPC concrete. The results were similar for both the

ascending and descending parts of the stress-strain curve (Hardjito et al. 2005). The stress-strain curve of geopolymer concrete agrees well with the predictions that were originally developed for OPC concrete. As for OPC concrete, the modulus of elasticity increased with the increase of compressive strength. The results of Hardjito et al. (2005) showed that the Poisson's ratio of the geopolymer concrete specimens, with compressive strengths ranging between 40 MPa and 90 MPa, was similar to that of OPC concrete. The Poisson's ratio was determined in accordance with the Australian Standard AS 1012.17 (1997).

The modulus of elasticity and Poisson's ratio results obtained by Hardjito et al (2005) is shown in Table 2.2. The curing of the fly ash based geopolymer concrete took place at elevated temperatures.

Table 2.2: Young's Modulus and Poisson's Ratio (Hardjito et al. 2005)

Mean compressive strength (MPa)	Age of concrete (Days)	Modulus of elasticity (GPa)	Poisson's ratio
89	90	30.8	0.16
68	90	27.3	0.12
55	90	26.1	0.14
44	90	23	0.13

According to the results found by Hardjito et al. (2005), they suggested that the same provisions of current codes and standards for OPC concrete structures can be used to design geopolymer concrete based structures, particular focusing on low calcium fly ash based geopolymer.

Joseph and Mathew (2012) found similar and even better results compared to Hardjito et al. (2005). According to Joseph and Mathew (2012) the modulus of elasticity can be brought equal to that of OPC concrete by selecting the appropriate aggregate content as well as the optimum fine aggregate to total aggregate ratio. The results obtained by Joseph and Mathew (2012) are shown in Table 2.3. It must be noted that the results found by both were also obtained by using fly ash based geopolymer concrete cured at elevated temperatures.

Table 2.3: Young's Modulus and Poisson's Ratio (Joseph and Mathew 2012)

Mean compressive strength (MPa)	Age of concrete (Days)	Modulus of elasticity (GPa)	Poisson's ratio
45	28	42.4	0.19
47	28	45.1	0.2
56	28	59.1	0.24
49	28	47.5	0.2

Fernandez-Jimenez et al. (2006) obtained modulus of elasticity values of less than 20 GPa for geopolymer concrete with strengths above 30 MPa. Lee and Lee (2013) investigated fly ash/slag based geopolymer concrete at ambient temperatures. The results that they found were not as promising as that of only fly ash based geopolymer concrete cured at elevated temperatures, with modulus of elasticity values between 10 GPa and 21 GPa. They compared the modulus of elasticity values with the CEB-FIP model code and the ACI Building Code 318-08 and it was found that the obtained values were 20% to 40% lower than the predicted values (Lee and Lee 2013).

According to previous research it is suggested that fly ash based geopolymer concrete, cured at elevated temperatures, yields higher modulus of elasticity values compared to fly ash/slag based geopolymer concrete that cures at ambient temperatures. The modulus of elasticity of fly ash/slag based geopolymer concrete will be investigated in this study.

- **Chemical attack**

According to previous research, geopolymers showed excellent resistance against chemical attack such as sulphate and acid (Wallah and Rangan 2006). The sulphate did not cause any damage to the surface of the heat-cured fly ash based geopolymer concrete and there was also no significant decrease in compressive strength after exposure to a sulphate solution up to one year (Wallah and Rangan 2006).

Exposure to sulphuric acid did damage to the fly ash based geopolymer concrete specimens and caused mass loss. It also lowered the compressive strength, but when compared to the OPC concrete specimens, it showed better resistance to sulphuric acid (Wallah and Rangan 2006).

The use of OPC concrete in aggressive environments such as marine applications are always a concern, but geopolymer concrete has shown promising resistance to this kind of exposure (Hardjito et al. 2005, Wallah and Rangan 2006).

According to the results found by Bakharev (2005), the ordering of the aluminosilicate gel plays a role when considering the resistance against chemical attack. They found that the crystalline geopolymer materials that were prepared with sodium hydroxide were more stable to sulphuric and acetic acid than amorphous geopolymers that were prepared with a sodium silicate activator. Thus, the material composition must be chosen wisely for aggressive environments (Bakharev 2005).

Another study showed that geopolymer concrete, soaked in a 5% sodium sulphate solution, did not show any significant change in compressive strength or geometry after 12 months (Hardjito et al. 2004).

- **Compressive strength**

It has been confirmed that geopolymer concrete can reach significantly high compressive strengths when cured either by heat activation or at ambient temperatures (Nath and Sarker 2012, Hardjito et al. 2004).

Heat activation is necessary to accelerate the geopolymerisation process and therefore higher compressive strengths will be achieved when heat activated, compared to ambient curing. However, Nath and Sarker (2012) concluded that it is possible to achieve adequate strengths when curing at ambient temperatures. The addition of slag in the matrix improves the compressive strength of the geopolymer concrete significantly when cured at ambient temperatures (Nath and Sarker 2012).

Factors that influence the compressive strength of the geopolymer concrete are discussed in more detail in the following section.

2.4.2. Factors influencing the mechanical properties

There are significantly more factors that can influence the compressive strength of geopolymer concrete, compared to the water to binder ratio which is the major factor for OPC concrete. A significant amount of research has already been done to investigate the mechanical properties of geopolymer concrete and some of the factors that may influence the strength are discussed in the following section.

- **Curing temperature**

The geopolymerisation process is accelerated when the curing temperature is increased, yielding a more efficient dissolution process. Temperature plays an important role in the curing process as the geopolymerisation process will not be as efficient at lower temperatures (Hardjito et al. 2004). However, with the addition of slag in the matrix, curing can take place at ambient temperatures (Nath and Sarker 2012).

Khale et al. (2007) found that there was no significant increase in strength when the curing temperature reached temperatures of more than 75 ℃. In other experimental results, the compressive strength did not change significantly when temperatures were more than 60°C (Hardjito and Rangan 2005). The results found by Hardjito and Rangan (2005) are shown in Figure 2.12.

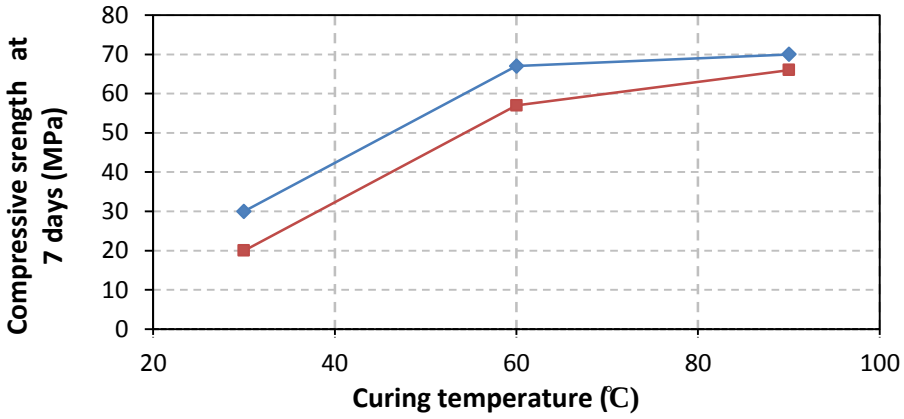

Figure 2.12: Effect of curing temperature on compressive strength (Hardjito and Rangan 2005)

The creep and drying shrinkage is also significantly less when curing takes place at high temperatures (Bondar et al. 2011). Most of the water will evaporate during the curing process.

- **Heat curing time**

Longer curing time leads to a more efficient geopolymerisation process, yielding higher compressive strengths. According to the results found by Hardjito et al. (2004), there was no significant change in compressive strength after 24 hours. The results for the curing time of Hardjito et al. (2004) are shown in Figure 2.13. The fly ash based geopolymer concrete was cured at 60 ℃. Some results show that geopolymer concrete may reach strengths of up to 70% of its final strength within the first three to four days (Bondar et al. 2011).

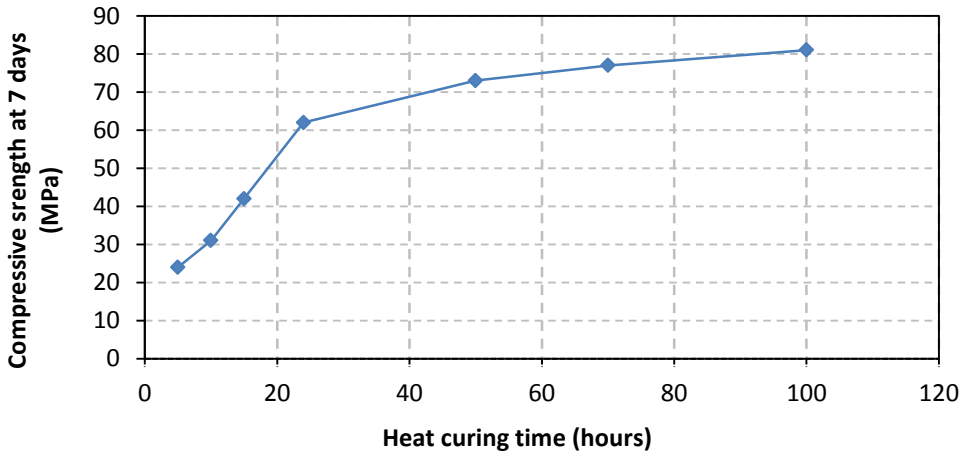

Figure 2.13: Influence of heat curing time on compressive strength (Hardjito et al. 2004)

- **Mixing Time**

A longer mixing period yields higher compressive strengths and a lower fresh concrete workability. Hardjito et al. (2005) suggested that the geopolymerisation process is enhanced when the mixing time

is increased, yielding higher compressive strengths. The results obtained by Hardjito et al. (2005) are shown in Figure 2.14.

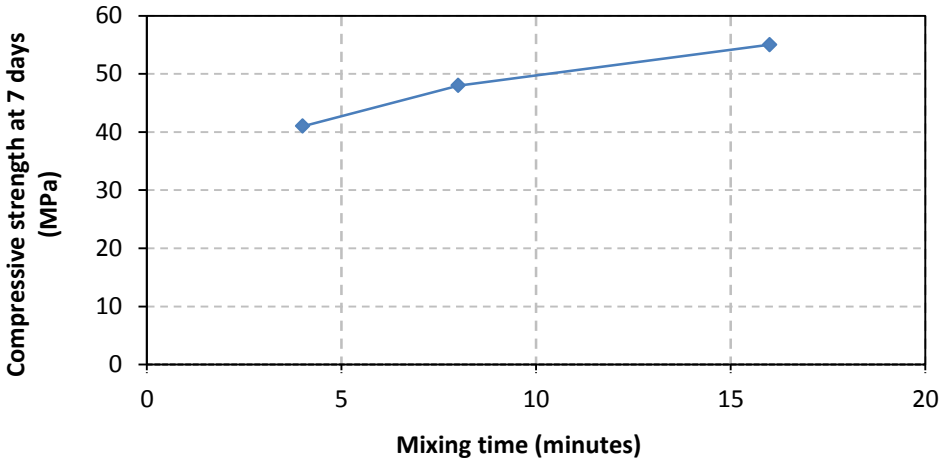

Figure 2.14: Effect of mixing time on compressive strength (Hardjito and Rangan 2005)

- **Sodium hydroxide concentration**

An increase of the sodium hydroxide concentration yields a higher compressive strength (Hardjito et al. 2004, Lloyd and Rangan 2010, Arioz et al. 2012). The reason for the increase in strength is that more aluminosilicates can be dissolved, forming stronger bonds. This is probably one of the most influential aspects regarding the compressive strength of geopolymer concrete (Van Jaarsveld et al. 2003). The influence of the molarity of the sodium hydroxide solution is shown in Figure 2.15.

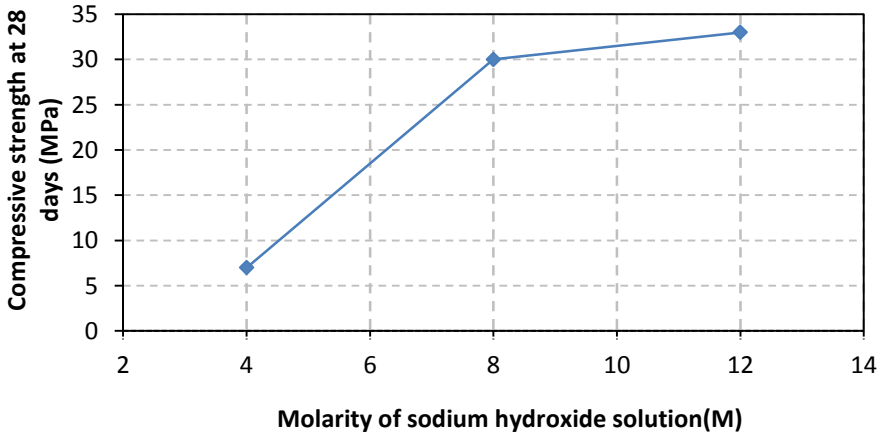

Figure 2.15: Influence of the sodium hydroxide concentration on the compressive strength (Arioz et al. 2012)

- **Sodium silicate to sodium hydroxide ratio**

An increase of the silicate solution in the matrix will yield higher compressive strengths (Lloyd and Rangan 2010, Hardjito and Rangan 2005, Joseph and Mathew 2012). The results found by Joseph et al. (2012) are shown in Figure 2.16. According to laboratory tests done by Hardjito (2005) a ratio of

2.5 is suggested to yield the best results. This is also more cost efficient as sodium silicate is typically cheaper than sodium hydroxide (Davidovits 2011).

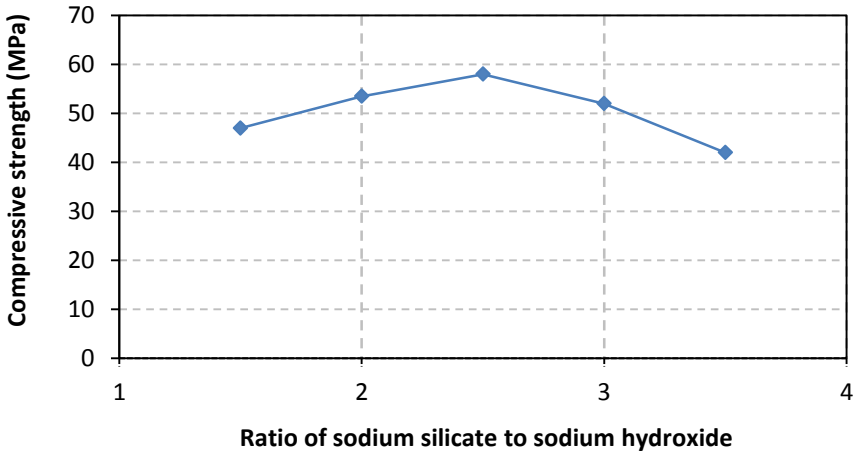

Figure 2.16: Influence of the SS/SH ratio on the compressive strength (Joseph and Mathew 2012)

- **Silicate to aluminum ratio**

Silica is a material that dissolves easily in alkaline conditions. The amount of silica influences the formation of particle interaction and an increase of silica in the matrix will yield better aluminosilicate bonds, resulting in better mechanical properties. Thus, the higher amount of silica available in the matrix, the stronger the geopolymer (Yip et al. 2008).

- **Availability of aluminium**

The availability of aluminium contributes significantly to the properties of geopolymer concrete (Fernández-Jiménez et al. 2006). The amount of aluminium available and the rate of release throughout the reaction, affects the geopolymer strength, setting characteristics, microstructure, acid resistance and control the strength development (Provis et al. 2009). The fact that geopolymerisation is a strongly kinetically controlled process, factors such as the rate of release of aluminium as well as the availability of it must be understood (Provis et al. 2009). The amount of silica available is also important but not that critical as it can be added via the addition of a soluble silicate in the case of deficiency.

By understanding the rate of release of aluminium in the binder from a precursor, it becomes possible to predict and control the properties of the geopolymer that will be generated (Provis et al. 2009).

A study showed that the release rate of aluminium in metakaolin (binder) is similar when different alkali metals are used for the activation process, compared to the varying release of aluminium when fly ash is used as the binder. This concludes that aluminium is more freely available in metakaolin.

Thus, the rate of release of aluminium in fly ash is in general slower and highly dependent on the alkali concentration and type (Fernández-Jiménez et al. 2003, Lee et al. 2002, Provis et al. 2009).

- **Water content in the mixture**

Although water does not take part in the geopolymerisation process, the initial amount of water in the mixture does have an effect on the properties of geopolymer concrete.

Lloyd et al (2010) investigated the water content to the geopolymer solids in various mixes. The water content was taken as the mass of water added to the hydroxide solution, the mass of water in the silicate solution as well as additional water added to the mix. The geopolymer solids were taken as the mass of fly ash, the mass of sodium hydroxide flakes and the mass of sodium silicate solids.

It was found that the compressive strength of geopolymer concrete decreases as the water-to-geopolymer solid ratio increases (Lloyd and Rangan 2010).

The water content will also influence the workability of the fresh geopolymer concrete and the following guidelines, as shown in Table 2.4, can be used to determine the workability of a fly ash based geopolymer concrete:

Table 2.4: Example for the design of fly ash based geopolymer concrete (Lloyd and Rangan 2010)

Water-Geopolymer solids mass ratio	Workability	Design Compressive strength (MPa)
0.16	Very Stiff	60
0.18	Stiff	50
0.2	Moderate	40
0.22	High	35
0.24	High	30

- **Addition of slag in the matrix (calcium silicate source)**

The compressive strength of geopolymer concrete will increase with the addition of slag in the matrix. However, the geopolymerisation process is significantly dependent on the crystallinity of the calcium silicate source, the alkalinity of the alkaline solution and the metakaolin/fly ash to slag ratio (Yip et al. 2008). The addition of slag accelerates the setting time of the geopolymer concrete cured at ambient temperature (Davidovits 2011).

2.5. Applications of geopolymer concrete

Geopolymer materials have a wide range of applications in different industry fields, which include the automobile, aerospace, metallurgy, civil engineering as well as in the paper industry. The type of

application depends on the chemical structure of the geopolymer in terms of the silicate to aluminium ratio.

Some of the applications are shown in Table 2.5. A low Si:Al ratio (1 to 3) initiates a 3D structure that is very rigid, while a higher ratio (more than 15) results in a more polymeric structure. In the field of civil engineering, the lower ratio is more suitable.

Table 2.5: Applications of geopolymeric materials (Davidovits 1999)

Si:Al ratio	Applications
1	Bricks, Ceramics, Fire protection
2	Low CO_2 cements and concretes
	Radioactive and toxic waste, Encapsulation
3	Fire protection fibre glass composite
	Foundry equipment, heat resistance composite, 200° C - 1000° C
>3	Tooling for aeronautics titanium process
	Sealants for industry, 200° C - 600° C
20-35	Fire resistant and heat resistant composites

Geopolymer concrete has been successfully used in the precast industry to produce sewer pipes, railway sleepers and other prestressed building components (Lloyd and Rangan 2010). This is mainly due to the early strength gain that geopolymer concrete provides and the fact that heat curing processes are already in use at precast factories.

Geopolymers have similar bonding properties to that of OPC and the shear and bondage strength of fly ash based geopolymer concrete structures can be calculated with the same design provisions currently available in design codes and standards for OPC concrete (Lloyd and Rangan 2010).

During a study done by Gourley et al. (2005), they confirmed that geopolymer precast concrete sewer pipes have outperformed OPC concrete pipes in aggressive sewer conditions. This may improve the durability of the networks, ensuring less maintenance.

2.6. Concluding summary

Geopolymer concrete has great potential as an alternative, due to the growing demand for a construction material with a lower carbon footprint. It proves to have promising mechanical properties compared to OPC concrete and geopolymer concrete structures can be designed according to similar codes and standards. It must be noted that the majority of the research was conducted on fly ash based geopolymer concrete, i.e. low calcium based geopolymer concrete.

However, this is only possible by a full understanding of the chemistry of geopolymer concrete. The mechanical properties and the factors influencing it must also be understood to ensure that consistent and adequate mixes can be designed.

For geopolymer concrete to be an adequate alternative to OPC concrete, it must be advanced to a point where the material make up of a geopolymer matrix, with certain strength, can be determined prior to mixing.

Geopolymer concrete is still a relatively new binder material and therefore it is important that a great amount of knowledge, regarding the material, is gathered to ensure that the geopolymer technology grows to fulfil these expectations.

The material parameters of the fly ash/slag based geopolymer concrete and their influence on the compressive strength are investigated in this study. The goal of this investigation is to provide information that can be used when designing a fly ash/slag based geopolymer concrete mix. The influence of the various parameters can used to control the compressive strength of the designed mix.

Chapter 3
Fibres in concrete

3.1. Background

The most significant property of OPC concrete is its compressive strength. The tensile resistance is significantly less due to the brittleness of the material. An unreinforced OPC concrete structure has a limited elastic response and once this elastic limit has been reached, micro cracks followed by macro cracks occur and finally rupture (Clarke et al. 2007).

However, this problem has been dealt with and conventional steel reinforcement is currently the most common solution for the problem. The reinforcing steel increases the ductility of OPC concrete, causing the tensile resistance to increase. However, conventional steel reinforcement does not compensate for small cracks in areas less critical in the OPC concrete structure. The small cracks can have a major influence on the durability of the structure as water and other deleterious substances can enter through the cracks, causing the steel to corrode.

The most common reason for cracks to occur is due to shrinkage and loading of members. The addition of fibres in a concrete matrix can be a solution for this problem.

The first usage of fibre reinforcing in OPC concrete stretches as far back as the ancient era when straw and horse hair were mixed into the building materials for extra strength (Owens 2009). Asbestos fibres were also used more widely in recent times before it was banned due to severe health issues related to asbestos. In 1874, steel fibres were one of the first alternatives to conventional reinforcing but it was only in the 1970's that fibre reinforcing was used on a larger scale in Japan, USA and Europe (Labib and Eden 2006).

As for OPC concrete, geopolymer concrete shows similar properties regarding the brittleness and tensile resistance. The ratio of tensile strength to compressive strength is significantly low. Therefore, the addition of fibres has already been introduced in geopolymer concrete to improve the ductility of the matrix.

Fibres do not necessarily improve the elastic response or the stress at which cracking occurs, but rather improves the post-elastic properties after the concrete has cracked (Clarke et al. 2007). The

bondage of the fibres plays a major role in the energy absorption and therefore it is essential to understand the properties of the different fibres available.

Figure 3.1 illustrates the role of fibres in reinforced concrete. The brittle graph indicates the behaviour of plain concrete. When a load is applied, the concrete reaches its maximum capacity and loses all of its strength after rupture occurred. Strain softening occurs due to the opening of a single failure crack. As the crack opens, the fibres inside the matrix tends to pull out, providing additional energy to the matrix. In the case of strain hardening concrete, an inelastic strain region exists due to multiple micro cracking. In this region the strain capacity of the concrete will increase, resulting in an increase of stress resistance. A post stress peak will be reached and strain softening will occur. Strain hardening will usually occur when high performance fibre reinforced concrete (HPFRC) is used and strain softening will occur when normal strength fibre reinforced concrete is used (FRC). As mentioned, the main difference between the two fibre reinforced concrete types is the multiple micro-cracking stage (Tjiptobroto and Hansen 1991, Brandt 2008). The type of cracks that will form when the first peak load is reached is shown in Figure 3.2.

The area under the curves depends on the amount and type of fibres in the matrix. In the case of low volume fibres, the area under the curve will be smaller than when more fibres are added. Thus, the larger the area, the more energy is provided by the fibres. The important properties of the fibres relate to the material type (elastic modulus and tensile strength), the geometry of the fibre (length and diameter) and the fibre shape.

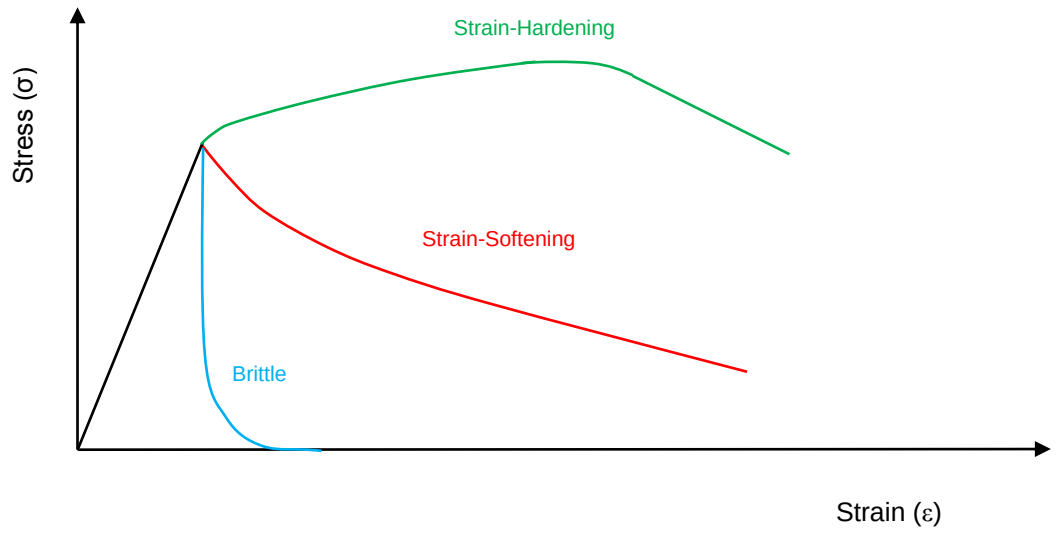

Figure 3.1: Typical stress-strain curves for fibre-reinforced

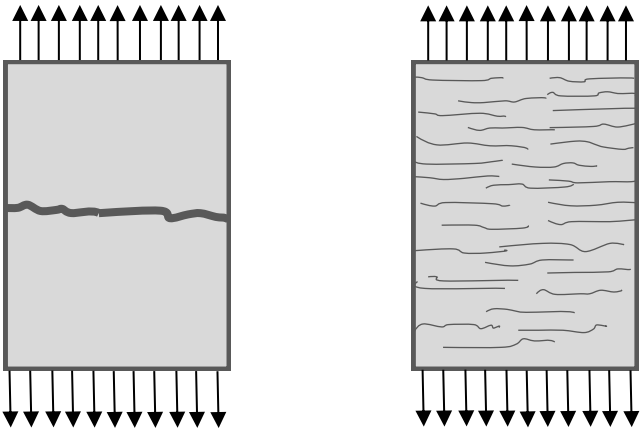

a) Fibre reinforced concrete **b) High performance fibre reinforced concrete**

Figure 3.2: Cracks in FRC and HPFRC

There are typically three orientation levels of reinforcement generally used in concrete:

1. **Randomly distributed in three dimensions:** This orientation level makes use of either micro- or macro fibres. The fibres are distributed evenly in the matrix during mixing, pointing in random directions. This is a familiar fibre reinforcement orientation level. A small amount of fibres will effectively be situated in the correct position in which the force is acting, resulting that on average only 15% of the fibres are orientated correctly (Girard 2008).

2. **Randomly distributed in two dimensions:** A typical example is spray-up fibre reinforced concrete. The reinforcement is orientated randomly within a thin plane. Typically 30% to 50% of the reinforcement is optimally orientated when distributed in two dimensions (Girard 2008). Although 2D reinforcing is more efficient than 3D reinforcing, it is still not efficient enough as most of the reinforcement lies within the horizontal plane, situated outside the critical zone. The tension zone in a concrete element is considered as the critical zone. Other examples include thin cast plates and steel mesh reinforcement.

3. **One dimensional reinforcing** is the conventional steel bar reinforcing method, used to design structures. It is also the most efficient method of reinforcing. The majority of reinforcement is placed in the tension zone, maximizing the effectiveness of the reinforcement (Girard 2008).

The fibre pull-out behaviour is a critical aspect when considering FRC. To ensure maximum energy absorption the fibre must pull out properly, i.e. without rupturing. In the case of FRC, fibre rupture is not ideal as the amount of energy provided to the matrix will be less than that provided during proper fibre pull out. As depicted in Figure 3.3, fibre rupture generates a significantly higher resisting force

compared to when the fibre is pulled out. However, the area under the fibre pull-out curve is significantly larger than the area under the fibre rupture curve. Thus, the energy provided will be significantly higher in the case of fibre pull-out and the post crack behaviour of a concrete element will increase when the ratio of fibre pull-out to fibre rupture increase.

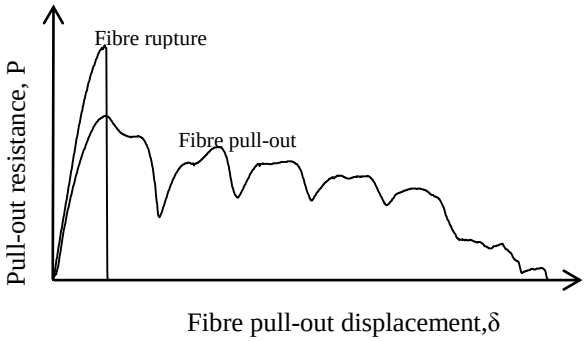

Figure 3.3: Fibre rupture vs. fibre pull-out.

Fibres can be divided into two categories: micro fibres and macro fibres.

3.2. Micro fibres

The role of micro fibres is, traditionally, to reduce plastic shrinkage cracks during the curing period of concrete (Li et al. 2011). However, a significant amount of research over the past years saw the use of micro fibres being shifted to structural applications, for example the development of strain hardening cement-based composites (SHCC). The addition of micro fibres in concrete results in a material that can exhibit high toughness and can tolerate a significant amount of damage in tension (Pereira 2012). This result is achieved when the fibres are bridging the cracks that form. The multiple-cracking behaviour ensures very small crack widths which increases its durability. The strain hardening behaviour and the small crack widths ensure a low water and chloride permeability, retarding the corrosion process (Ahmed and Mihashi 2007).

The length of the fibres vary from 5 mm to 30 mm and have a diameter of less than 0.1 mm. Due to the fineness of these fibres, a limited amount can be added. The workability of the fresh concrete will decrease significantly if an excessive amount of micro fibres are added. Typically 0.1% fibres, by volume of the concrete, are added to a matrix (Jiabiao et al. 2004).

Other benefits that micro fibres provide when they are added (Cement and concrete association of New Zealand 2009):

- Fire resistance
- Reduced permeability
- Increased shatter resistance
- Reduction of plastic shrinkage cracking

3.3. Macro fibres

The development of macro fibres is still relatively new to the industry and was only introduced in the 1990s. However, there was a great increase in utilisation over the last decade. The main purpose of the fibres is to bridge the cracks and to provide structural support to the hardened concrete. The primary use of these fibres in the construction industry is to reduce the conventional tension reinforcement or slab thickness.

The lengths of these fibres vary form 20 mm to 64 mm and the diameter ranges between 0.5 mm to 2 mm. The tensile strength of the fibres ranges from 120 MPa to strengths higher than 3000 MPa and it has a modulus of elasticity ranging from 5 GPa to 200 GPa (Owens 2009, Zollo 1997).

The workability is also influenced when macro fibres are added to fresh concrete, although not as significantly as in the case of micro fibres.

The addition of macro fibres provides the following benefits to hardened concrete:

- Impact resistance
- Increased tensile strength
- Increased ductility
- Increased post crack resistance

The addition of macro synthetic fibres and -steel fibres are investigated in this study.

3.4. Types of fibres

As stated above, fibres can be divided into micro fibres and macro fibres. These categories can further be divided in the different materials for fibres. The different materials have different properties and it depends on the properties required before choosing the fibre material.

The different types of fibres available are the following (ACI Committee 544 1973):

- Glass
- Steel
- Synthetic
- Natural fibres

Table 3.1 shows fibres from the different categories as stated above. The fibres are produced in different shapes and sizes (Figure 3.4), which influences the bonding characteristics between the fibre and the concrete matrix. The maximum bond length of a fibre is half of the full length of the fibre. Various mechanical properties are given in the table which will be useful when choosing a fibre.

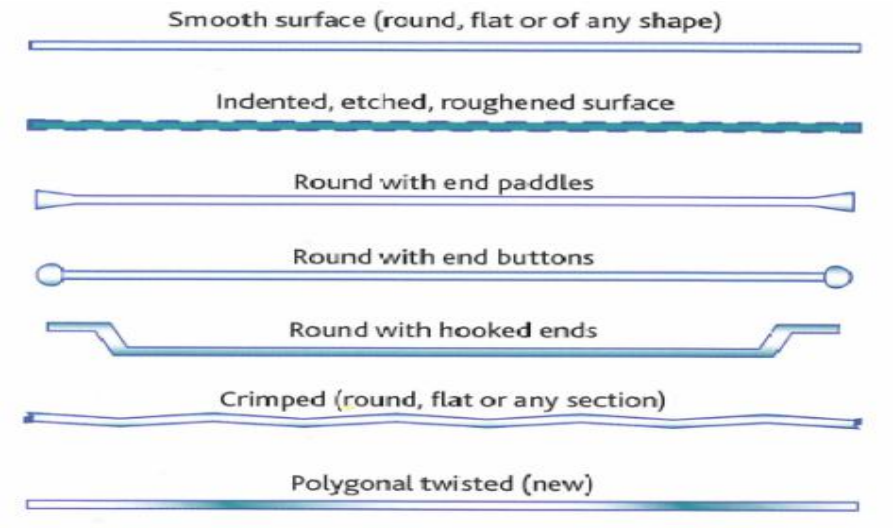

Figure 3.4: Type of fibres (Cement & Concrete Association of New Zealand 2009)

Table 3.1: Different fibre types (Owens 2009, Zollo 1997)

Type of fibre	Specific gravity	Tensile strength (MPa)	Elastic Modulus (GPa)
Glass	2.6	2000-4000	80
Steel	7.8	1000-3000	200
Synthetic			
Acrylic	1.16-1.18	296-1000	14-19
Aramid I	1.44	2930	62
Aramid II	1.44	2344	117
Carbon I	1.9	1724	380
Carbon II	1.9	2620	230
Nylon	1.14	965	5
Polyester	1.34-1.39	228-1103	17
Polyethylene	0.92-0.96	76-586	5- 117
Polypropylene	0.9-0.91	138-690	3-5
Alkali-resistant	2.7-2.74	2448-2482	79-80
Non Alkali-resistant	2.46-2.54	3103-3447	65-72
Natural			
Coconut	1.12-1.15	120-200	19-26
Sisal	-	276-568	13-26
Bagasse	1.2-1.3	184-290	15-19

3.4.1. Glass fibres

The use of glass fibre reinforced concrete was first introduced in the early 1960's, consisting of soda-lime silica glass and borosilicate glass. However, it was found that these types of fibres were alkali active and weakened when added to concrete. Alkali resistant fibres were successfully developed in the 1960's and were first implemented in 1971 (Owens 2009). Alkali resistant glass fibres are primary used in concrete to act as tensile-load carrying members. The polymer and the concrete matrix will bind together. This bondage causes tensile forces to be carried over via shear stresses throughout the structure (Girard 2008).

The amount of glass fibres in the matrix must be enough to provide adequate strength. The orientation of the fibres also plays a major role in the strength efficiency, therefore a higher quantity then needed is usually added to ensure adequate resistance. Glass fibres have promising physical properties and are relatively low in cost, which made them the most favourable fibres for a long period of time. The quantity glass fibres are usually 5% of the total volume of the matrix, but the more random the orientation of the fibres, the higher quantity is required (Girard 2008).

During a study done on the addition of glass fibres in OPC concrete, a conclusion was made that the addition of glass fibres reduces bleeding of the OPC concrete. Due to the decrease of bleeding, the surface integrity of the concrete improved and the probability of cracks reduced. The compressive strength after 28 days of the concrete was improved by 20% to 25% and the flexural and tensile splitting strength was improved by 15% to 20% (Chandramouli et al. 2006).

3.4.2. Steel fibres

Steel fibres are normally used to increase the toughness of concrete by improving the load bearing capacity and the impact resistance. The steel fibres are produced in different shapes and sizes, depending of the properties required (Cement & Concrete Association of New Zealand 2009).

These fibres were initially used as secondary reinforcement or for crack control in less critical areas of the concrete elements, but nowadays it is widely used as main reinforcement in industrial floor slabs, shot-crete and precast elements.

The tensile resistance, provided by the fibres bridging a crack, will depend on the quantity of fibres embedded over a crack plain. Therefore, it is essential to have an adequate amount of fibres in the design mix. Another important aspect that has to be taken into consideration is the tensile strength of the fibres, as rupture must be avoided. The rupturing of the fibres will lead to a rapid loss of load carrying capacity (Cement & Concrete Association of New Zealand 2009).

Steel fibres typically have no influence on the compressive strength of concrete and will only increase the tensile strength.

A study by Bernal et al. (2010) was conducted on alkali-activated slag concrete with the addition of steel fibres. The results showed that geopolymer concrete had a lower reduction in compressive strength compared to that of OPC concrete when steel fibres were added. The flexural toughness was increased when higher volume fibres were added. The durability performance, such as permeable porous quantity and water absorption, improved significantly with the addition of fibres. The mechanical performance of the reinforced geopolymer concrete even showed similar results to that of OPC reinforced concrete (Bernal et al. 2010).

3.4.3. Synthetic fibres

Synthetic fibres are man-made fibres which resulted from research and development in the textile and petrochemical industries (Owens 2009). The fibres are produced from organic polymers which come in various formulations. These fibres can provide effective reinforcement for concrete and are relatively low in price (Zheng and Feldman 1995).

Various fibres have been incorporated into concrete mixes and the properties of these fibres are shown in Table 3.1. The fibre volume in the mix can be divided into high volume percentage (0.4% to 0.8%) and low volume percentage (0.05% to 0.3%) (Owens 2009).

It is usually assumed that synthetic fibres do not improve the tensile strength of the concrete and only participate after cracking has occurred. However, some results show that the tensile strength can be improved when higher volume fibres are added (Zheng and Feldman 1995).

Polypropylene Fibres

Polypropylene fibres have been used to reinforce concrete from the 1960's. Polypropylene fibres are usually produced by an extrusion process in which the polymer is hot drawn through a die until desired diameter is reached and chopped in various lengths as required (Owens 2009).

The polypropylene fibre is a synthetic hydrocarbon polymer and it is a hydrophobic material. This leads to disadvantages such as weak bond characteristics with a cement matrix. It has a low melting point and a relatively low modulus of elasticity (Owens 2009).

The specific gravity of polypropylene fibres ranges from 0.9 to 0.91. The tensile strength is between 138 MPa and 690 MPa. The elastic modulus ranges from 3 GPa to 5 GPa.

3.5. Concluding summary

The use of fibres in concrete is certainly beneficial and a significant amount of research has been done on fibre reinforced OPC concrete (FROC). The addition of fibres in a concrete matrix not only improves the toughness and in some cases the tensile strength of the concrete but it also improves the durability by improving plastic shrinkage cracking etc.

The research done on fibre reinforced geopolymer concrete (FRGC) is not as advanced as FROC and therefore the addition of fibres in fly ash/slag based geopolymer concrete is investigated in this study, determining whether it has similar properties and advantages to that of FROC. Macro steel fibres and -synthetic (polypropylene) fibres are added to fly ash/slag based geopolymer concrete in different volumes and the results are compared to FROC.

Chapter 4
Test Setup

Due to the major negative impact that OPC concrete has on the environment, different studies have been conducted to advance potential alternatives that can partially replace OPC concrete as building material. In this study, fly ash/slag based geopolymer concrete is investigated to conclude whether it can serve as an adequate building material for construction purposes.

The fly ash/slag geopolymer concrete mainly consists of a combination of fly ash and slag as the binder and an alkaline solution consisting of a combination of sodium hydroxide and sodium silicate together with fine- and coarse aggregates. In most of the research done till thus far, heat activation was used as the curing process. During this study, ambient curing is investigated to conclude whether adequate mechanical properties for the geopolymer concrete can be obtained. Ambient curing is necessary for in-situ casting.

The first goal of the study is to obtain mix designs that have adequate compressive strengths. Other properties such as the density, modulus of elasticity, flexural strength, setting time and temperature development tests of the fly ash/slag based geopolymer concrete are investigated to obtain a better understanding of its mechanical properties.

The workability of the fly ash/slag based geopolymer concrete is not investigated in significant detail, however, diameter slump tests have been carried out to gather some information regarding the workability.

The second goal of the study is to investigate whether the ductility and the flexural toughness of the geopolymer concrete can be improved by adding fibres to the matrix. The flexural behaviour of the fibre reinforced geopolymer concrete (FRGC) is compared to fibre reinforced OPC concrete (FROC). Various tests, including three point bending tests, round panel tests and fibre pull-out tests were carried out to gather information.

The tests procedures and -setups are discussed in the following sections.

4.1. Mixing procedure

4.1.1. Geopolymer concrete mixing procedures

Various concrete mixers have been used, depending on the size and purpose of the mix. All the mixes, except those containing fibres, were carried out in a 25 l pan mixer. The fibre reinforced geopolymer concrete mixes required a larger volume mixer and it was decided to rent a 400 l drum mixer from a local tool hiring company.

The mixing time and procedure of all the mixes were constant, as far as possible, throughout the mixing period to ensure consistency.

All the dry materials were first mixed together before any liquid was added. The sand was added first followed by the binder (fly ash and/or slag) and then the stone. The alkaline solutions and additional water were added separately to the mix. A mixing procedure of Hardjito et al. (2005) was used as a reference in this study. The exact mixing procedures are given in the following sections.

4.1.1.1. Mixes without fibres

The mixing procedure for the 25 l pan mixer was as follow:

1. The dry materials were mixed for 30 seconds before the alkaline solution and the water were added.
2. After the addition of the liquids, mixing was continued for another 3 minutes.

4.1.1.2. Mixes with fibres

The mixing procedure of the FRGC was different compared to the unreinforced geopolymer concrete mixes. The mixing procedure for the FRGC is as follow:

1. The dry materials were mixed for 30 seconds.
2. After 30 seconds only the additional water was added.
3. The fibres were added directly after the water and further mixed for two minutes.
4. Finally the alkaline solution was added and mixing was continued for another three minutes.

The reason for the different procedure is that the fibres had to be added before the alkaline liquid to provide enough time for casting, as fly ash/slag based geopolymer concrete tends to set rapidly. As stated in Chapter 2, water does not participate in the geopolymerisation process. Thus, the geopolymerisation process only starts after the alkaline liquid is added. The mixing process was closely monitored to ensure that no materials stuck to the sides of the drum.

4.1.2. OPC concrete mixing procedures

4.1.2.1. Mixes without fibres

Same as the geopolymer mixes described in Section 4.1.1.1.

4.1.2.2. Mixes with fibres

The fibre reinforced OPC concrete mixes were not mixed in the drum mixer as some of the mix designs were relatively sticky, i.e. some of the materials got stuck to the sides of the drum, especially when fibres were added to the matrix. The mixes were carried out in a 120 l pan mixer. It was possible to add all the water before adding the fibres and therefore the pan mixer could work efficiently without having rotating problems.

The mixing procedure of the FROC was as follow:

1. The dry materials were mixed for 30 seconds.
2. The water were added and mixed for two minutes.
3. The fibres were added and mixed for three minutes.

The curing procedure is discussed in the following sections.

4.2. Curing procedure

The curing of fly ash/slag based geopolymer concrete differs from that of OPC concrete as water curing is not necessary.

4.2.1. Geopolymer concrete curing

The curing procedure of geopolymer concrete depends on the binder material in the mix. Heat curing is usually necessary when only fly ash is used as the binder material, i.e. a low calcium based binder. The majority of the mixes in this study included slag in the matrix and therefore ambient curing was possible.

After casting, the cubes were left to harden in the mixing laboratory. The samples were demoulded approximately one day after casting. After the demoulding process the samples were stored in a room with a controlled environment. The room had a constant temperature of 24 ± 2℃ and 65 ± 5% relative humidity.

The samples were stored in the room for the duration of 7 or 28 days before they were tested.

4.2.2. OPC concrete curing

The OPC concrete specimens were also demoulded one day after casting of the moulds. Due to the size of the panels and the beams, they were stored on the floor in the mixing laboratory and covered

with permanently soaked blankets to ensure that proper curing was possible. The cubes were however placed in curing baths at 25℃.

4.3. Workability

The workability of the geopolymer concrete was not an essential part of the study. However, diameter slump flow tests were carried out in order to obtain some information regarding the flow ability of the fly ash/slag based geopolymer concrete. As already mentioned, all the geopolymer concrete mixes had self-compacting characteristics. The binder material consisted of at least 60% fly ash which contributes to its self-compacting characteristics. The fly ash particles have a spherical shape which improves the workability. The OPC concrete on the other hand did not have self-compacting characteristics as it was challenging to design low strength self-compacting OPC concrete mix.

4.3.1. OPC concrete slump test

The OPC concrete slump test was carried out in accordance with the SANS Method 862-1:2006. The cone was filled in three layers. Each layer was compacted 25 times by means of a steel rod. The difference in vertical displacement was measured after the cone was removed.

4.3.2. Geopolymer concrete slump test

Due to its self-compacting characteristics, compaction with a rod was not necessary when the cone was filled with geopolymer concrete. After filling, the cone was lifted from the plate in such a way that the geopolymer concrete was able to flow without any obstruction. The test was finished when the geopolymer concrete flow ceased.

The largest diameter of the flow spread was measured, together with one measurement perpendicular to the largest diameter. The average of the two measurements was taken as the diameter slump.

4.4. Compression tests

The compressive tests were carried out in accordance with the SANS 5863:2006. In Total, six 100x100x100 mm cubes were tested 7 days (three cubes) and 28 days (three cubes) after casting. The cubes were tested on the 200t Contest compression testing machine (Figure 4.1) which was used to determine the maximum load of each cube. A constant load rate of 180 kN/min was applied to the non-casting sides of the cube until failure.

The maximum forces were used to calculate the compressive strength of each cube. The compressive strength is calculated using:

$$\boldsymbol{\sigma = \frac{F}{A}} \tag{4.1}$$

where

σ – Compressive strength (MPa)

F - Maximum force obtained from the contest (N)

A - Surface area on which force is applied (mm^2)

The average compressive strength of the three cubes was taken as the compressive strength of a certain mix.

Figure 4.1: Contest compression testing machine

4.5. Density of the geopolymer concrete

The density of the various geopolymer concrete specimens was determined before the cubes were crushed. As stated in Section 4.4, three specimens were tested on 7 days and three specimens were tested on 28 days for each mix design. Thus, the densities of the three cubes were obtained and the average was taken as the density of the specific mix design. The density was determined using:

$$\boldsymbol{\rho = \frac{m}{V}} \quad \textbf{(4. 2)}$$

where ρ is the density (kg/m^3), m the mass of the geopolymer concrete cube in kg and V is the volume of the cube in m^3. The volume of the cubes was measured with a vernier caliper to the nearest mm.

4.6. Modulus of elasticity test

The modulus of elasticity represents the stiffness of the geopolymer concrete. Modulus of elasticity can be defined as the ratio of uniaxial force to the resultant strain (Haranki 2009). From a structural point of view, the modulus of elasticity is an important aspect as the deflection of an element is directly dependent on it.

Cylindrical specimens with an aspect ratio of 2 (200mm depth, 100mm diameter) were used to conduct the modulus of elasticity test. The modulus of elasticity was determined in accordance with the ASTM C469/C469M–10. The specimens were tested on the 200t Contest compression testing

machine (Figure 4.2). A constant loading rate of 140 kN/min was applied to the specimen as required by the code.

Three 10 mm linear variable differential transducers (LVDT) were used to measure the deformation of the specimen at mid height. The LVDT's were spaced 120̊ apart and the average of the three was used as the final deformation. The load was measured by a 2MN HBM load cell to obtain more accurate results. A HBM spider8 data acquisition system was used to connect the load cell and the LVDT's to a computer.

The ASTM C469/C469M code required at least two cycled loadings, 30% to 40% of the compression strength. After the cycles, the constant load rate was applied until the maximum withstanding force was reached. The modulus of elasticity was calculated using:

$$E_c = \frac{S_2 - S_1}{\varepsilon_2 - \varepsilon_1} \quad (4.4)$$

where

E_c = Cord Modulus of elasticity (MPa)

S_2 = Stress corresponding to 50% of the ultimate load (MPa)

S_1 = Stress corresponding to 33% of the ultimate load (MPa)

ε_2 = Longitudinal strain produced by S_2

ε_1 = Longitudinal strain produced by S_1

The stresses (S_1 and S_2) were calculated by dividing the force by the cross sectional area of the specimen. The strain was calculated by dividing the vertical deflection with the gauge length. The gauge length is the original length over which the deflection was measured, in this case 70 mm.

The modulus of elasticity test setup is shown in Figure 4.2.

Figure 4.2: Illustration of the modulus of elasticity test

4.7. Three point bending test

The three point bending test determines the indirect tensile behaviour of fibre reinforced concrete. The test was carried out in accordance with BS EN 14651 (2007). A total of six 150x150x700 mm beam specimens were cast per mix design and were tested on 28 days. The test setup is shown in Figure 4.3. Each beam was notched 25 mm deep at the bottom centre of the beam prior to testing. The notch provides a known crack position which ensures that all the beams have the similar cracking behaviour.

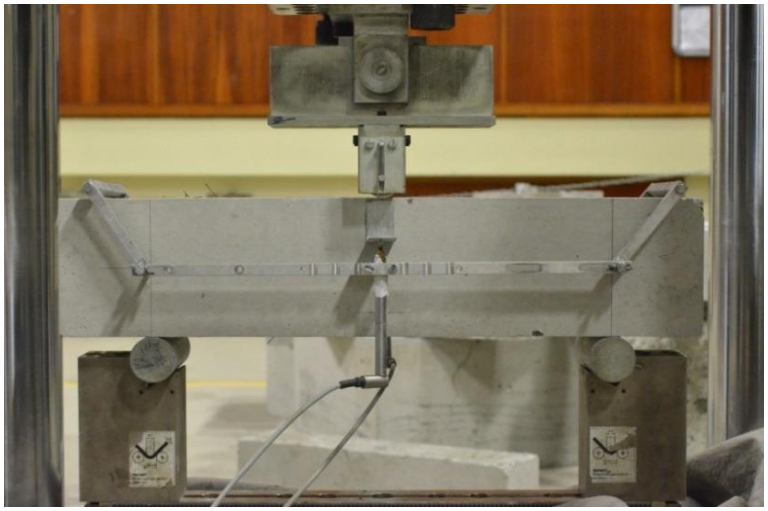

Figure 4.3: Three point bending test setup

The beam was tested on the non-casting sides and was simply supported on both edges, spanning a total length of 500 mm. A central load was applied using a 2MN Instron Materials Testing Machine at a constant crosshead displacement rate of 0.2 mm/min until an average central deflection (δ_L) of 3 mm was reached, as recorded by the two LVDT's.

The test was carried out to obtain various properties of the fibre reinforced geopolymer concrete. The main goal of the test was to obtain the equivalent flexural ratio (R_{e3} value). The R_{e3} value was calculated in accordance with RILEM TC 162 (2002) as follow:

The first step was to determine the area under the load-deflection curve. The area under the curve represents the energy absorption of the geopolymer concrete. The area is divided into two sections as illustrated in Figure 4.4. The clear area under the graph illustrates the energy absorption of unreinforced concrete and the shaded area illustrates the post crack energy absorption, provided by the fibres.

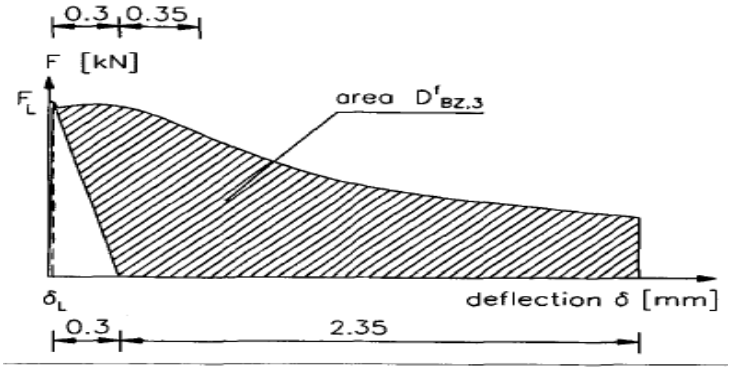

Figure 4.4: Post crack curve of fibre reinforced concrete (RILEM TC 162, 2002)

Only the shaded area under the curve must be calculated and therefore the clear part is subtracted from the graph. The clear area is taken as a right-angled triangle with the longer leg equal to the ultimate force and the shorter leg equal to 0.3. The unit of the area is presented in kNmm, i.e. Joule (J).

The energy absorption, provided by the fibres, was used to calculate the mean force for the equivalent flexural strength. The shaded are in Figure 4.4 is converted into a rectangle by using:

$$\boldsymbol{F_{eq3} = \frac{D^f_{BZ,3}}{\delta - 0.15}} \quad \textbf{(4.5)}$$

where F_{eq3} is the mean force, $D^f_{BZ,3}$ energy absorption capacity and δ is the deflection.

The mean force is equal to the value representing the top line of the rectangle and is used to determine the equivalent flexural strength.

The equivalent flexural strength was calculated by using:

$$\boldsymbol{f_{e,3} = \frac{3F_{eq3}l}{2bh^2_{sp}}} \quad \textbf{(4.6)}$$

The next step was to calculate the limit of proportionality (LOP) . The LOP is the ultimate stress that can be applied to an elastic object before permanent deformation occur (first crack). The LOP was calculated by using:

$$\boldsymbol{f_L = \frac{3F_L l}{2bh^2_{sp}}} \quad \textbf{(4.7)}$$

where f_L is the LOP (MPa), F_L is the ultimate load (N), l is the span of the beam (mm), b is the width (mm) and h_{sp} is the height (mm) between the tip of the notch and the top of the beam.

The R_{e3} value is the ratio between the equivalent flexural strength and the LOP and is determined by using:

$$R_{e3} = \frac{F_{eq3}}{f_L} \quad (4.8)$$

Figure 4.5 illustrates the difference between the LOP (f_L) and the equivalent flexural stress ($f_{e,3}$). The R_{e3} value will increase when the two points are closer to each other.

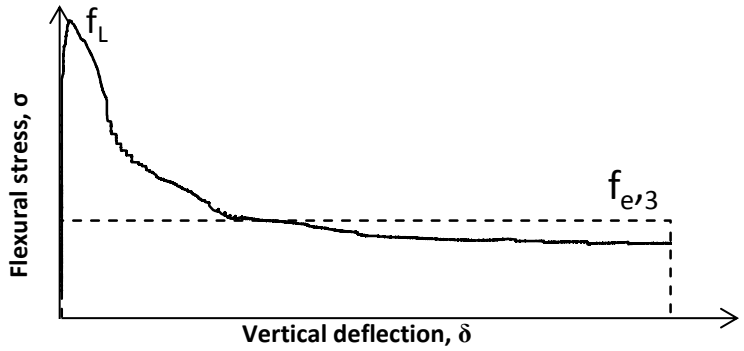

Figure 4.5: Illustration of the LOP and the equivalent flexural stress

4.8. Round panel test

The flexural toughness of fibre reinforced concrete (FRC) is determined by means of a round panel test. The toughness is expressed as energy absorption, after the panel has cracked, which represents the ability of the fibre reinforced concrete to distribute forces after cracking has occurred. The test is carried out in accordance with the ASTM C1550-12 code.

The code states that a diameter of 800 ± 10 mm and a thickness of 75 -5/+15 mm is required and if any of the specimens fall outside of this range, it must be discarded. Three round panels were tested per mix design. Section 7.5, of the ASTM C1550 code, states that only two successful tests are required for adequate results. A test is considered successful if failure occurs that include at least three radial cracks. Specimens were discarded if the failure mode was different.

When centrally loaded, the round panel experiences bi-axial bending in response to the load. This causes the panel to fail in a similar mode related to in-situ behaviour of structures. The panel is supported at three symmetrical arranged pivot points on a pitch circle diameter of 750mm. The supports are of such nature that free rotation is possible about both the vertical and horizontal axis.

The test procedure was consistent for all the specimens. The panels were rested on the supports and centred with respect to both the supports and the loading piston. The test was carried out using a 2MN Instron Materials Testing Machine. A constant displacement rate of 4mm/min was applied up to a central vertical deflection of minimum 40 mm.

A 100 mm LVDT was positioned in the centre of the supporting frame in order to obtain the deflection at the centre of the panel. Using the LVDT ensured that only the deflection of the panel was taken into account, neglecting any deflection due to crushing of concrete or deflection caused by the

test setup itself. A small steel plate was placed between the tip of the LVDT and the panel to ensure that the LVDT did not slip into a large crack. Figure 4.6 illustrates the steel plate between the LVDT and the panel.

Figure 4.6: Illustration of the steel plate between the LVDT and the panel

The energy absorption was determined by calculating the area under the load-deflection curve. The area was calculated between the origin and a central displacement of 40 mm. Servere deformation in-situ is determined when the area is calcultated up to a central displacement if 40 mm. The round panel test setup is shown in Figure 4.7 (ASTM C1550 2012).

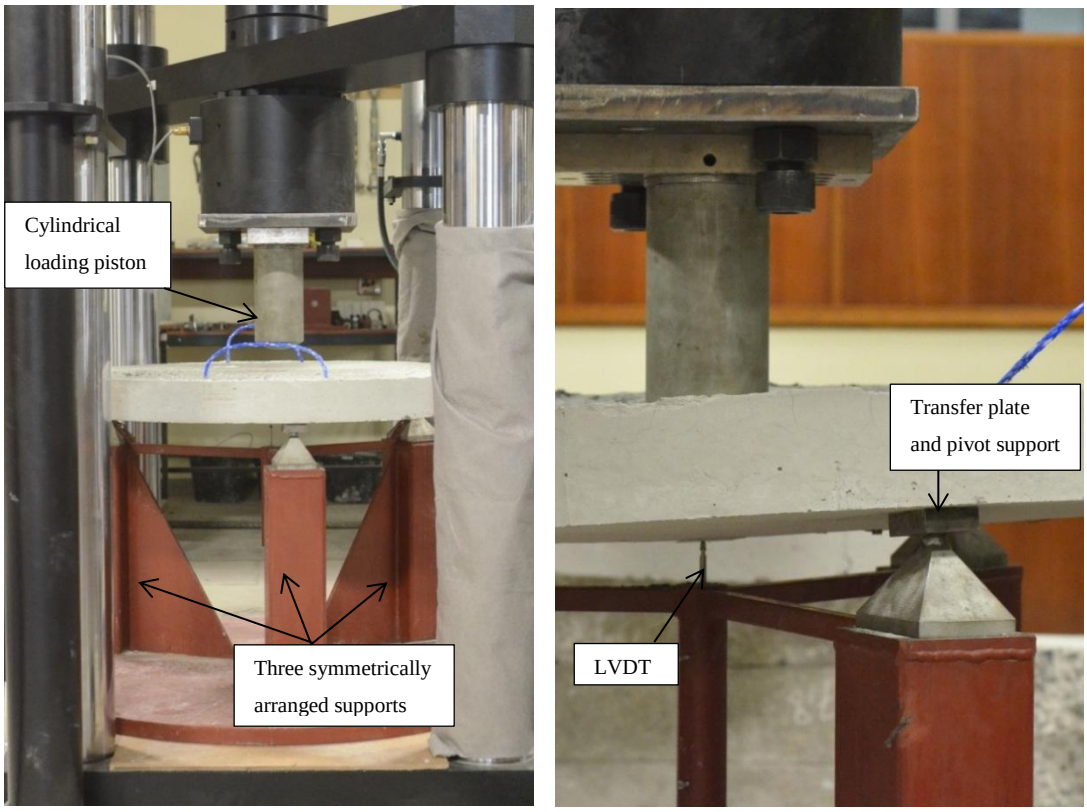

Figure 4.7: Schematically representation of the round panel test setup

4.9. Fibre pull-out test

When fibres are added to the matrix, the ductility of concrete is improved. This result is due to the energy provided by the fibres. Boshoff (2007) stated that for any fibre reinforced concrete (FRC), three structural components exist. The three components include the matrix, the fibre and the matrix-fibre interface. It is important to understand the single pull-out behaviour in a certain matrix and therefore tests were carried out to investigate this behaviour.

Two fibre types, steel and polypropylene, were used in this study and the pull-out behaviour of both was investigated.

The fibre pull-out test was carried out to obtain information regarding the bond strength between the fibre and the respective matrix. The critical length of the fibres was not determined in this study. The critical length according to Boshoff (2007) is the maximum embedment length that will ensure successful fibre pull-out. A length beyond the critical embedment length will lead to fibre rupture. The bond strength of a full embedded fibre was investigated in this study. The full embedment length of a fibre is half of its full length, in this case 25 mm.

The bond strength is determined by using:

$$\tau = \frac{P_{max}}{\pi L d} \quad (4.1)$$

where τ is the bond strength in (MPa), P_{max} is the maximum pull-out resisting force, L is the embedment length and d is the diameter of the fibre.

4.9.1. Test setup

The test setup for the fibre pull-out tests was a challenging task. The embedment of the fibres had to be carefully managed to ensure that the embedment length is as close to 25 mm as possible.

The mould is shown in Figure 4.8. A double 100x100x100 mm cube mould was divided by a 100x100x20 mm piece of wood. One mould will typically contain two rectangular concrete blocks, each containing a 25 mm embedded fibre (steel or polypropylene). The splitting of the cube mould was done to reduce the use of concrete and to ease the testing process as the blocks must fit into a hydraulic clamp as shown in Figure 4.10. The size of each concrete block was approximately 100x100x40 mm. Each fibre was marked at a length of 25 mm before it was embedded in the concrete. A total of eight specimens were cast per mix design.

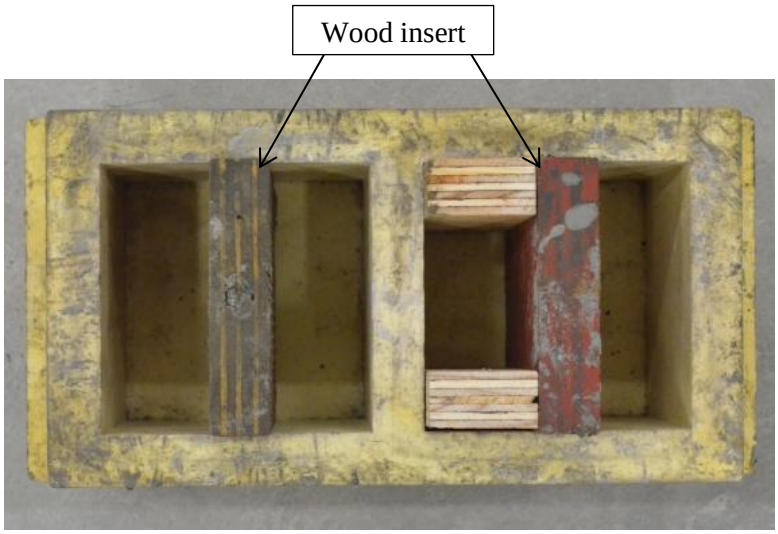

Figure 4.8: Fibre pull-out casting mould

The casting of the blocks was as follow:

1. The two sides of the mould were filled with fresh concrete.
2. The OPC concrete moulds were vibrate compacted to ensure that any trapped air can escape. The surface of both the geopolymer concrete and the OPC concrete were smoothed by using a flush tool.
3. The last step was to embed the fibres in the concrete specimens. This was very challenging and special care had to be taken to ensure that the embedment length is as close to 25 mm as possible. The cubes were left to harden for 24 hours without lifting or moving any of the moulds. This was to ensure that the fibres do not move.

The blocks were demoulded after 24 hours and the OPC concrete blocks were cured in water at 25℃ while the geopolymer concrete blocks were cured in the PPC laboratory at 24 ± 2℃.

The fibre pull-out test was carried out 28 days after casting. A constant pull-out rate of 0.2 mm/s applied out in a Zwick Z250 Materials Testing Machine. This ensured that each fibre was pulled out in approximately 120 seconds.

Before testing, the fibre was fastened by a gripping device. It was important that no slipping occurred while the fibre was pulled out. The fibre pull-out test setup is schematically shown in Figure 4.9. The top platen is fixed while the bottom platen moves down during the test, causing the fibre to pull out. A HBM 250 kg load cell was used to record the resisting force and two 50 mm LVDT's were used to ensure that only the displacement of the fibre was measured.

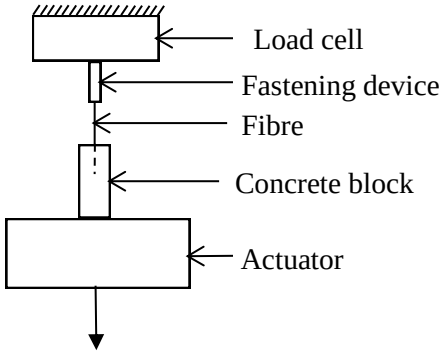

Figure 4.9: Schematically representation of the fibre pull-out test

Two fastening devices were used, one for the polypropylene fibre and the other for the steel fibre. An illustration of the two different fibre pull-out setups is shown in Figure 4.10. The only difference between the two setups is the gripping devices which are shown in Figure 4.11. The gripping device used for the steel fibre (Figure 4.11a) is an 8mm bolt with a 1.1 mm drilled hole. A smaller bolt is situated on the side of the gripping bold and is screwed in to press the fibre against the inside wall of the bigger bolt. This ensures adequate gripping. The steel fibre has a diameter of 1.05mm and therefore the possible eccentricity is negligible.

The polypropylene fibre is fastened the same way as a drill bit is fastened in a drill chuck. The fastening device used for the polypropylene fibre is shown in Figure 4.11b. The part of the fibre that is not embedded in the concrete is inserted in the drill chuck.

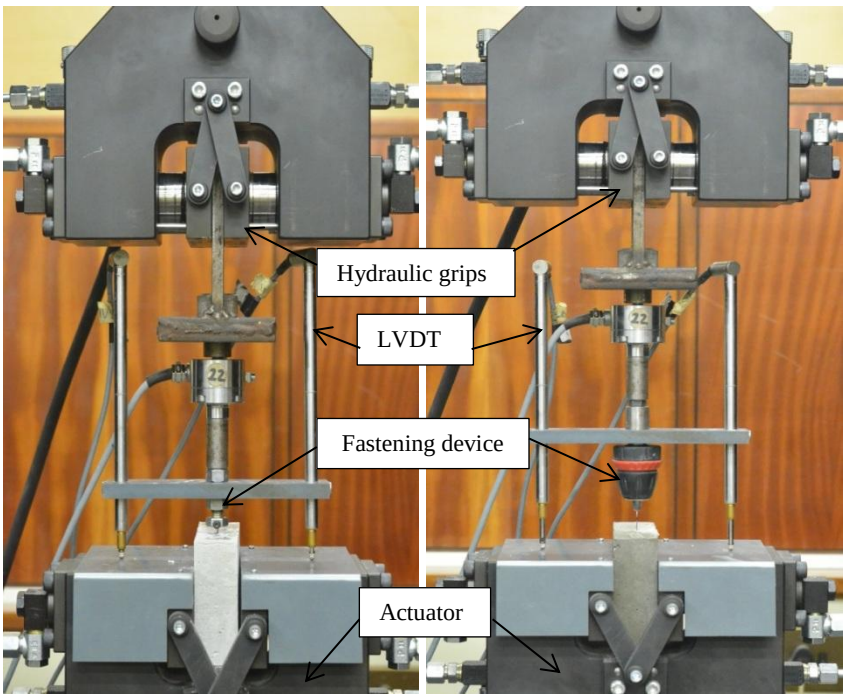

a) Steel fibre pull-out test setup **b) Polypropylene fibre pull-out test setup**

Figure 4.10: The steel fibre pull-out- and polypropylene fibre pull-out test setup

The fastening devices for both the steel fibres and the polypropylene fibres are shown in Figure 4.11. Hydraulic grips were used to clamp the concrete specimens.

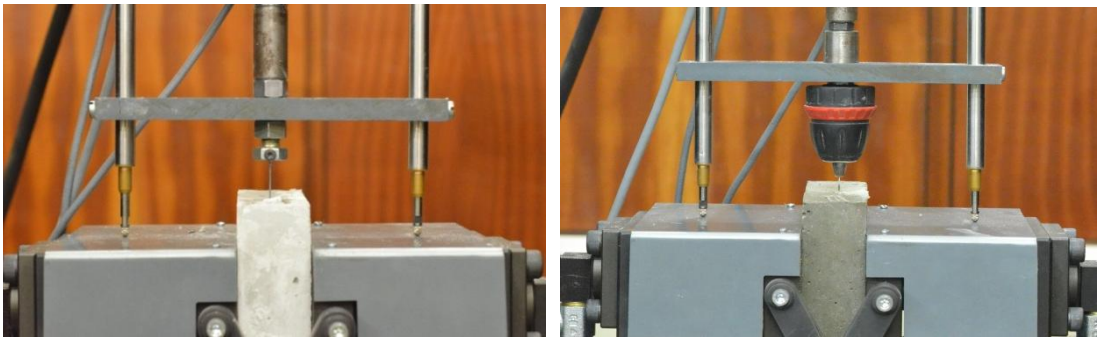

a) Steel fibre griping device **b) Polypropylene gripping device**

Figure 4.11: Gripping device for the steel- and polypropylene fibre

4.10. Setting time test

The setting time test was carried out in accordance with the SANS 50196-3 2006. It is acknowledged that the test is for testing the setting time of cement. This test will however still give a good indication of the setting time of a concrete. The setting time was determined by means of a Vicat test apparatus, penetration needles and a conic mould as shown in Figure 4.12. Initial setting of geopolymer concrete is reached when the 1.1 mm diameter initial setting time penetration needle (Figure 4.12b) measures a distance of 6 ± 3 m from the base plate. Final setting of the geopolymer concrete is reached when the ring, attached to the final setting time penetration needle (Figure 4.12c), shows no mark on the surface of the specimen. The needle will penetrate under the self-weight of the Vicat apparatus. The mass of the needle and falling cylinder is approximately 300g.

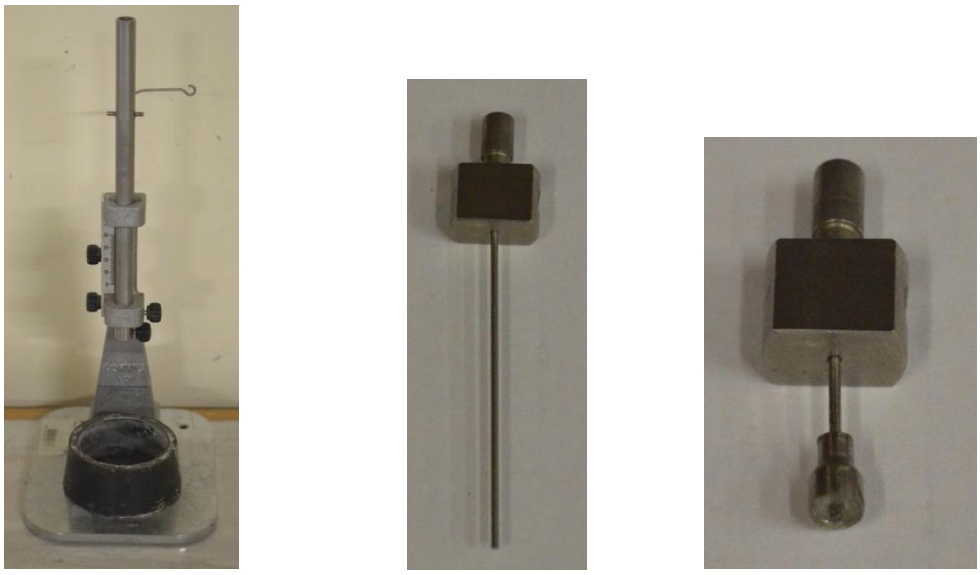

a) Vicat test apparatus **b) Initial setting penetration needle** **c) Final setting penetration needle**

Figure 4.12: Vicat test apparatus and penetration needles

After mixing, the fresh geopolymer mortar was sieved through a 4.75 mm sieve. The reason for the sieving was to obtain a mortar that can be tested. The stone particles would influence the test. Ahmadi (2000) concluded that the sieved mortar will have adequate consistency to perform the Vicat setting time test.

4.11. Temperature development test

The temperature development of some of the geopolymer concrete specimens was measured with temperature sensors, known as PT 100. The objective of the test was to obtain the temperature change during the curing process. The test setup is shown in Figure 4.13.

The geopolymer concrete was cast into a 5 L polystyrene “box” to ensure some isolation form the atmosphere. A copper pipe, with an inside diameter of 5 mm, were embedded in the geopolymer concrete and the temperature sensor were placed inside the tube. This was done to prevent the sensor of coming into direct contact with the geopolymer concrete, but it will still be able to measure the temperature accurately. The duration of the test was 3 days (72 hours). An OPC concrete mix with a corresponding strength to Mix 3b (50 MPa) was also tested to compare the curing temperature development of OPC concrete and geopolymer concrete.

Figure 4.13: Temperature test setup

Chapter 5
Test Program

The mix design procedure of geopolymer concrete varies from that of OPC concrete. When an OPC concrete mix is designed, the water and cement are calculated followed by the amount of aggregate. The OPC concrete mix is designed per m^3. Thus, for a typical OPC concrete mix design, the volume, in m^3, of the water, binder and stone is added together and subtracted from $1m^3$ to obtain the volume of sand in the matrix. The geopolymer concrete mix design, however, has more constituents making it more complex to design.

Another difference between OPC concrete and geopolymer concrete is the strength determination of the matrix. When an OPC concrete mix is designed, the strength mainly depends on the water to binder ratio. However, the compressive strength of geopolymer concrete depends on various parameters, making it difficult to accurately design a mix with a desired strength.

In this study, two mix design methods are used to design a geopolymer concrete mix. These methods are discussed in detail later in the chapter.

As mentioned, a geopolymer concrete matrix consists of various constituents including aggregates (stone and sand), a binder (fly ash and/or slag), an alkaline solution (combination of sodium hydroxide and sodium silicate) and additional water. Different mixes are designed to investigate the influence of the various parameters on the compressive strength. The mixes are explained, in more detail, later in this chapter.

5.1. Materials

The strength of geopolymer concrete not only depends on the various materials in the matrix but also on the chemical composition of the binder materials. The geopolymerisation process depends mainly on the amount of silica and aluminium available in these materials and therefore it was important to ensure that the origin of the fly ash was from the same power station and the slag from the same steel factory for all the mixes.

X-Ray Fluorescence (XRF) analyses were conducted to obtain the chemical compositions of the aggregates and binder materials.

5.1.1. Aggregates

The same aggregates used in OPC concrete were used for the geopolymer concrete. The aggregates were obtained from a local company in Stellenbosch. The aggregate types and origin were constant for all the mixes in this study.

5.1.1.1. Coarse aggregates

The course aggregates used in this study are 13.2 mm Greywacke stone.

5.1.1.2. Fine aggregates

A natural sand, marked as Malmesbury sand, was used for all the mixes in this study. A sieve analysis was carried out and is illustrated in Figure 5.1.

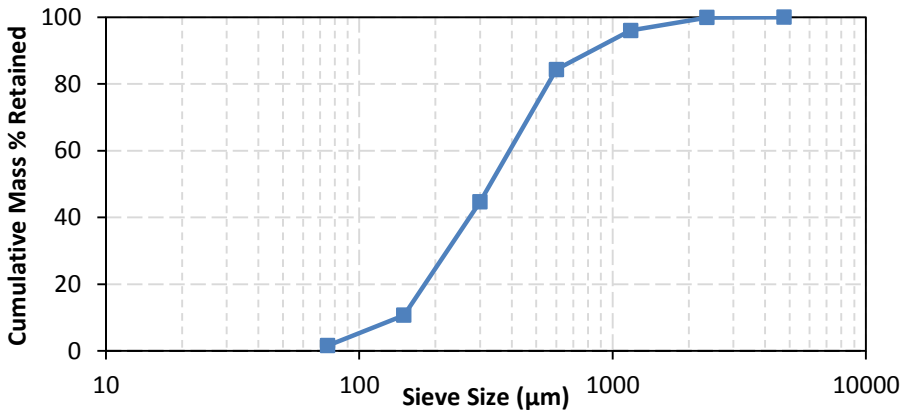

Figure 5.1: Sieve analysis of the fine Malmesbury sand

5.12. Binder materials

5.1.2.1. Fly ash

The fly ash used in this study was obtained from the silos of Lethabo power station, Northern Free State. The fly ash is categorised as ASTM type F fly ash, due to its low calcium content. The chemical composition of the fly ash is shown in Table 5.3. The Si:Al ratio for the fly ash is 1.7.

Table 5.3: XRF analysis of the fly ash

Al_2O_3 (%)	CaO (%)	Cr_2O_3 (%)	Fe_2O_3 (%)	K_2O (%)	MgO (%)	MnO (%)	Na_2O (%)	P_2O5 (%)	SiO_2 (%)	TiO_2 (%)	L.O.I. (%)
31.83	4.86	0.03	3.22	0.77	1.23	0.03	0.24	0.41	54.10	1.66	0.65

5.1.2.2. Slag

Ground Granulated Corex slag was used in this study. The slag was obtained from the iron production process at Saldanha Steel, Western Cape. The chemical composition of the corex slag is shown in Table 5.4. The Si:Al ratio for the slag is 2.05.The typical chemical composition of South African

ground granulated blast furnace slag is also shown in Table 5.4 in order to draw a comparison between the two different slag types.

Table 5.4: XRF analysis of the GGCS and GGBS

Al_2O_3 (%)	CaO (%)	Cr_2O_3 (%)	Fe_2O_3 (%)	K_2O (%)	MgO (%)	MnO (%)	Na_2O (%)	P_2O5 (%)	SiO_2 (%)	TiO_2 (%)	L.O.I. (%)
14.50	36.50	0.00	1.25	0.64	11.73	0.03	0.10	0.02	31.78	0.51	-1.08
11-16	32-37	0.00	0.3-0.6	0.8-1.3	10-13	0.7-1.2	-	-	34-40	0.7-1.4	-

5.1.3. Alkaline solutions

A combination of sodium hydroxide and sodium silicate was used as the alkaline solution.

5.1.3.1. Sodium hydroxide

The sodium hydroxide (NaOH) was obtained from Kimix Chemicals, South Africa in the form of flakes, with a specific gravity of 2.13 and a purity of 98%. The flakes were dissolved in normal tap water. Due to the exothermic reaction of sodium hydroxide when dissolved in water, it was left to cool down for approximately an hour prior to mixing. The mass of the sodium hydroxide flakes, per litre of solution, depended on the concentration of the solution required. The concentration is expressed in Molar, M.

The sodium hydroxide concentration was calculated as follows:

The molecular weight of sodium hydroxide is 40 g/mol. Thus, an 8 M concentration solution contains 8x40 = 320 g/l sodium hydroxide. This value is divided by the purity of the sodium hydroxide flakes to obtain a final concentration of 326.5 g/l sodium hydroxide flakes per litre of solution. The specific gravity of sodium hydroxide was used to convert the mass per solution to volume per solution. Due to the known volume of the sodium hydroxide, it is possible to calculate the amount of water per litre of solution.

Various sodium hydroxide concentrations were used in this study and the calculation for each is shown in Table 5.5. The mass percentages of sodium hydroxide flakes and water, per litre solution, are shown in the last two columns of the table.

Table 5.5: Properties of the sodium hydroxide solution

NaOH concentration (M)	Mass of NaOH per litre (kg)	NaOH volume per litre	Mass Water per litre (kg)	Relative density	Mass % NaOH	Mass % Water
6	0.24	0.11	0.89	1.13	21.67	78.33
8	0.33	0.15	0.85	1.17	27.83	72.17
12	0.49	0.23	0.77	1.26	38.88	61.12
16	0.65	0.31	0.69	1.35	48.50	51.50

5.1.3.2. Sodium silicate

The sodium silicate solution of Phase A was obtained from Kimix chemicals, Western Cape. The chemical composition of the silicate was Na_2O = 8.93%, SiO_2 = 29.8% (SiO_2: Na_2O = 3.34) and water = 61.78% by mass. The density of the sodium silicate solution was 1400 kg/m^3.

The sodium silicate solution of Phase B was obtained from PQ Corporations, Gauteng. The chemical composition of the silicate was Na_2O = 14.92%, SiO_2 = 29.8% (SiO_2: Na_2O = 2) and water = 55.28% by mass. The density of the sodium silicate solution was 1540 kg/m^3.

5.2. Mix design method

A design method has not yet been developed or published in which the volume of the materials can be calculated to yield specific properties. Therefore, mixes were designed by allocating certain percentages to all the respective materials. Mix designs found in literature were used as guidelines and new mixes were designed according to results and observations from the previous mix.

Two different approaches were used in this study. The first design method was based on assuming a certain density for the mix. Each material present in the matrix was allocated a percentage of the mass.

However, it was noticed that for the purpose of comparing various mixes with each other, this method was not adequate. The volume of the mixes varied for each mix design, making it impossible to have a consistent comparison. This result is due to the different relative densities of the various materials.

The second design method was similar to the first method, except that the mass assumption was replaced by designing a mix with a volume of 1 m^3. The mass of the materials were calculated taking into account the relative densities of the respective materials.

5.2.1. Design method 1: Mass assumption (Phase A)

The initial mix design method was done according to the methodology used by Lloyd and Rangan (2010). It was assumed that the unit-weight of the geopolymer concrete is 2400 kg/m^3. The aggregates, binder and alkaline liquids, were allocated a certain percentage of the total mass. The total mass of all the materials would then add up to 2400 kg. Although the relative densities of all the materials are available, this specific method was found in literature and according to Lloyd and Rangan (2010) it is an adequate method to design a geopolymer concrete mix. However, Phase B makes use of the relative densities.

The aggregates were allocated between 60% and 70% of the total mass of the geopolymer concrete. The aggregates were mainly stone and were allocated 55% to 70% of total mass of the aggregates.

The remaining mass consisted of alkaline liquid and binder material with the alkaline liquid to binder ratio varying between 0.35 and 0.55. The binder material consisted of 60% to 100% fly ash and remaining percentage was slag. The sodium silicate to sodium hydroxide ratio was taken as 1.5 to 2.5. No additional water was added to any of the mixes.

The mixes are categorised as Phase A

5.2.2. Design method 2: Volume assumption (Phase B)

The second design method ensured a more adequate comparison between the various mixes. The initial design of assuming a mass of 2400 kg/m^3 for the geopolymer concrete was replaced by designing a mix per volume of 1 m^3. The materials in the mix were each allocated a percentage of the 1 m^3. The volume of the materials was converted to mass by multiplying each volume with a relative density.

The aggregates took up between 59% and 65% of the total mass of the geopolymer concrete. The stone took up 44% to 68% of the total mass of the aggregates.

The remaining mass consisted of alkali liquids, binder material and additional water. The alkaline to binder mass ratio was between 0.15 and 0.34. The fly ash took up 60% to 80% of the binder material and the remaining binder mass consisted of slag. The sodium silicate to sodium hydroxide ratio was 0.5 to 2.

A total of 90 l of additional water was added to all the mixes. A further substitution of alkaline liquid, with water, was also done to investigate the effect of water in the matrix. A total 0% to 50% of alkaline liquid were substituted with additional water.

These mixes are categorised as Phase B.

The relative densities of all the materials are shown in Table 5.6.

Table 5.6: Relative densities

Material	Relative Density
Water	1
Stone	2.79
Sand	2.62
Slag	2.89
Fly ash	2.37
Sodium silicate solution	1.54
Sodium hydroxide solution (6 Molar)	1.13
Sodium hydroxide solution (8 Molar)	1.17
Sodium hydroxide solution (12 Molar)	1.26
Sodium hydroxide solution (16 Molar)	1.35

5.3. Mix designs for compressive tests

The mixes consisted of two batches (Phases A and B). The main difference between the two batches was the sodium silicate concentration. The mixes of Phase A contained a sodium silicate solution with a SiO_2:Na_2O ratio of 3.34 and the mixes of Phase B contained a sodium silicate solution with a SiO_2:Na_2O ratio of 2. Additional water was added to all the mixes of Phase B while no additional water was added to the mixes of Phase A. Design method 1 was used in Phase A and design method 2 was used to design the mixes of Phase B. The material make up of all the mixes (Phase A and Phase B) consisted of aggregates, slag, fly ash, sodium hydroxide, sodium silicate and water.

An initial mix design was developed that served as the reference mix design for each phase. One of the parameters in this matrix was changed to investigate how this specific parameter influences the compressive strength of the geopolymer concrete. All the other materials and ratios were kept constant. The different parameters that were investigated are discussed in sub sections under each Phase. Each subsection will contain the mixes that were designed to investigate the certain parameter.

Six cubes per mix design were cast, three for the 7 day test and three for the 28 day test.

5.3.1. Mix design Phase A

Six parameters were investigated in Phase A and a total of 14 mixes were carried out. The different sub phases are listed in the following section. The sub phases will contain the material makeup information of each mix design. The material make up is listed as kg/2400kg.

The reference mix had the following properties:

- 70% Aggregates (49 % Coarse aggregates, 21% Fine aggregates)
- Alkaline to fly ash ratio: 0.55
- 60% fly ash/40% slag of the binder mass
- Sodium silicate to sodium hydroxide ratio: 2.5
- Sodium hydroxide concentration: 6 M

The reference mix design is shown in Table 5.7.

Table 5.7: Reference mix design for Phase A (kg/2400kg)

Materials	(kg/2400kg)
Coarse aggregates	1176
Fine aggregates	504
Slag	186
Fly ash	279
Sodium silicate solution	182
Sodium hydroxide solution (6 Molar)	73

5.4.1.1. Phase A1: Sodium silicate to sodium hydroxide ratio

Phase A1 investigated the influence of the sodium silicate to sodium hydroxide ratio on the compressive strength of the fly ash/slag based geopolymer concrete.

The mixes for Phase A1 include the following:

- Mix 1a – Sodium hydroxide to sodium silicate ratio: 2.5
- Mix 2a – Sodium hydroxide to sodium silicate ratio: 2
- Mix 3a – Sodium hydroxide to sodium silicate ratio: 1.5

The mix design for Phase A1 is shown in Table 5.8.

Table 5.8: Phase A1 mix design (kg/2400kg)

Material (kg/2400kg)	Mix 1a	Mix 2a	Mix 3a
Coarse aggregates	1176	1176	1176
Fine aggregates	504	504	504
Slag	186	186	186
Fly ash	279	279	279
Sodium silicate solution	182	170	153
Sodium hydroxide solution (6 Molar)	73	85	102

5.4.1.2. Phase A2: Fly ash/slag content

Phase A2 investigated the influence of slag in the matrix. The total mass of the binder remained constant for all the mixes but the percentage of fly ash and slag in the binder varied.

The mixes for Phase A2 include the following:

- Mix 4a – Fly ash/slag: 100%/0% of the binder mass
- Mix 5a – Fly ash/slag: 80%/20% of the binder mass
- Mix 1a – Fly ash/slag: 60%/40% of the binder mass

The mix design for Phase A2 is shown in Table 5.9.

Table 5.9: Phase A2 mix design (kg/2400kg)

Material (kg/2400kg)	Mix 4a	Mix 5a	Mix 1a
Coarse aggregates	1176	1176	1176
Fine aggregates	504	504	504
Slag	0	93	186
Fly ash	465	372	279
Sodium silicate solution	182	182	182
Sodium hydroxide solution (6 Molar)	73	73	73

5.4.1.3. Phase A3: Aggregate content

Phase A3 investigated the aggregate content in the matrix. The alkaline to binder ratio remained the same. Thus, the amount of binder material and alkaline liquid decreased when the aggregate content increased. However, the alkaline to binder ratio remained the same.

The mixes for Phase A3 include the following:

- Mix 6a – 60% of the total concrete mass consist of aggregates
- Mix 7a – 65% of the total concrete mass consist of aggregates
- Mix 1a – 70% of the total concrete mass consist of aggregates

The mix design for Phase A4 is shown in Table 5.10.

Table 5.10: Phase A3 mix design (kg/2400kg)

Material (kg/2400kg)	Mix 6a	Mix 7a	Mix 1a
Coarse aggregates	1008	1092	1176
Fine aggregates	432	468	504
Slag	248	217	186
Fly ash	372	325	279
Sodium silicate solution	243	213	182
Sodium hydroxide solution (6 Molar)	97	85	73

5.4.1.4. Phase A4: Influence of fine aggregates in the aggregate content

Phase A4 investigated the influence of the fine aggregate in the matrix. The aggregate content remained the same while the fine aggregate to total aggregate changed. The influence on the compressive strength was investigated to obtain the optimum amount of fine aggregates in a matrix.

The mixes for Phase A4 include the following:

- Mix 1a – Fine aggregate to total aggregate: 0.3
- Mix 8a – Fine aggregate to total aggregate: 0.4
- Mix 14a – Fine aggregate to total aggregate: 0.45
- Mix 13a – Fine aggregate to total aggregate: 0.5

The mix design for Phase A4 is shown in Table 5.11.

Table 5.11: Phase A4 mix design (kg/2400kg)

Material (kg/2400kg)	Mix 1a	Mix 8a	Mix 14a	Mix 13a
Coarse aggregates	1176	1008	924	840
Fine aggregates	504	672	756	840
Slag	186	186	186	186
Fly ash	279	279	279	279
Sodium silicate solution	182	182	182	182
Sodium hydroxide solution (6 Molar)	73	73	73	73

5.4.1.5. Phase A5: Alkaline to binder ratio

Phase A5 investigated the influence on the compressive strength when the alkaline to binder ratio is changed. Note that the aggregate content was 60% of the total mass for the mixes in this phase. The aggregate content remained the same while the binder and the alkaline liquid content changed.

The mixes for Phase A5 include the following:

- Mix 9a – Alkaline to binder ratio: 0.35
- Mix 10a – Alkaline to binder ratio: 0.45
- Mix 6a – Alkaline to binder ratio: 0.55

The mix design for Phase A4 is shown in Table 5.12.

Table 5.12: Phase A5 mix design (kg/2400kg)

Material (kg/2400kg)	Mix 9a	Mix 10a	Mix 6a
Coarse aggregates	1008	1008	1008
Fine aggregates	432	432	432
Slag	284	265	248
Fly ash	427	397	372
Sodium silicate solution	178	213	243
Sodium hydroxide solution (6 Molar)	71	85	97

5.4.1.6. Phase A6: Sodium hydroxide concentration

Phase A6 investigated the influence of the sodium hydroxide concentration on the compressive strength of the geopolymer concrete. The mass of sodium hydroxide remained the same regardless of the concentration

The mixes for Phase A3 include the following:

- Mix 11a – Sodium hydroxide concentration: 3M
- Mix 1a – Sodium hydroxide concentration: 6M
- Mix 12a – Sodium hydroxide concentration: 8M

The mix design for Phase A4 is shown in Table 5.13.

Table 5.13: Phase A6 mix design (kg/2400kg)

Material (kg/2400kg)	Mix 11a	Mix 1a	Mix 12a
Coarse aggregates	1176	1176	1176
Fine aggregates	504	504	504
Slag	186	186	186
Fly ash	279	279	279
Sodium silicate solution	182	182	182
Sodium hydroxide solution	73	73	73

5.3.2. Mix design Phase B

Due to occurring problems in Phase A, a different approach was followed in Phase B. The problems included low workability of the fresh fly ash/slag based geopolymer concrete and a large amount of alkaline liquid in the matrix. The alkaline solution was reduced by replacing a fraction of it with tap water. The effect of additional water in the matrix was investigated to conclude whether the amount of alkaline solution can be reduced and still yield adequate compressive strengths. As mentioned, a different approach was used for the mix design of Phase B (design method 2: volume assumption) which ensured adequate comparisons.

A total of 30 mixes were carried out in Phase B and six parameters were investigated. The material make up, in kg/m^3, are illustrated in each sub phase.

The reference mix for Phase B had the following properties:

- 60% Aggregates by mass (37 % Coarse aggregates, 23% Fine aggregates)
- Alkaline to binder ratio: 0.31
- 60% fly ash/40% slag by binder mass
- Sodium silicate to sodium hydroxide ratio: 1.18
- Sodium hydroxide concentration: 8 M
- 90 l additional water
- 0% alkaline solution substituted with water

The reference mix design is shown in Table 5.14.

Table 5.14: Reference mix design for Phase B (kg/m^3)

Material	(kg/m^3)
Coarse aggregates	858
Fine aggregates	520
Slag	259
Fly ash	394
Sodium silicate solution	108
Sodium hydroxide solution (8 Molar)	92
Water	90

5.3.2.1. Phase B1: Water replacement

Phase B1 investigated the influence on the compressive strength when a percentage of the alkaline liquid was replaced by water. The amount of alkaline solution that was replaced by additional water ranged from 0% to 50% of the alkaline solution mass. The concentration of the alkaline liquid decreased when the amount of water increased in the matrix. Three slag contents were investigated.

The Phase consists of three categories:

1. 40% slag of the binder mass
2. 23% slag of the binder mass
3. 20% slag of the binder mass

The mixes for Phase B1 include the following:

Phase B1.1: 40 % slag of the binder mass

- Mix 1b – 0% alkaline liquid replaced by water
- Mix 2b – 10% alkaline liquid replaced by water
- Mix 3b – 25% alkaline liquid replaced by water
- Mix 4b – 50% alkaline liquid replaced by water

Phase B1.2: 23 % slag of the binder mass

- Mix 5b – 0% alkaline liquid replaced by water
- Mix 6b – 10% alkaline liquid replaced by water
- Mix 7b – 25% alkaline liquid replaced by water

Phase B1.3: 20 % slag of the binder mass

- Mix 8b – 0% alkaline liquid replaced by water
- Mix 9b – 10% alkaline liquid replaced by water
- Mix 10b – 25% alkaline liquid replaced by water

Note that Mix 4b did not harden properly and therefore it was concluded that a substitution of 50% of alkaline liquid decreased the concentration by such an extent that it caused inadequate hardening. It must be taken into account that this conclusion is for an 8 Molar sodium hydroxide concentration.

The mix design for Phase B1 is shown in Tables 5.15 and 5.16.

Table 5.15: Mix design for Phase B1.1 (kg/m^3)

	Phase B1.1			
Material (kg/m^3)	Mix 1b	Mix 2b	Mix 3b	Mix 4b
Coarse aggregates	858	858	858	858
Fine aggregates	520	520	520	520
Slag	259	259	259	259
Fly ash	394	394	394	394
Sodium silicate solution	108	98	81	54
Sodium hydroxide solution (8 Molar)	92	82	69	46
Water	90	104	125	162

Table 5.16: Mix design for Phases B1.2 and B1.3 (kg/m^3)

	Phase B1.2			Phase B1.3		
Material (kg/m^3)	Mix 5b	Mix 6b	Mix 7b	Mix 8b	Mix9b	Mix 10b
Coarse aggregates	858	858	858	858	858	858
Fine aggregates	520	520	520	520	520	520
Slag	148	148	148	126	126	126
Fly ash	485	485	485	504	504	504
Sodium silicate solution	108	98	81	108	98	81
Sodium hydroxide solution (8 Molar)	92	82	69	92	82	69
Water	90	104	125	90	104	125

5.3.2.2. Phase B2: Slag content

Phase B2 investigated how the slag content influence the compressive strength of the geopolymer concrete. The mixes used for this phase is exactly the same as that of Phase B1, therefore, no additional mixes were done and all conclusions in this phase is based on the results of Phase B1. Three different slag contents were used including 20% slag of the binder mass, 23% slag of the binder mass and 40% slag of the binder mass.

The Phase consists of 3 categories:

- 0% alkaline liquid replaced by water
- 10% alkaline liquid replaced by water
- 25% alkaline liquid replaced by water

The influence of the amount of water in the matrix was also investigated during this phase.

5.3.2.3. Phase B3: Fine aggregate content

The goal of Phase B3 was to conclude whether the ratio of fine aggregates to total aggregates has an influence on the compressive strength of the geopolymer concrete. As the fine aggregate content increased, the coarse aggregates decreased but the initial mass of aggregates remained the same. The other constituents and ratios remained the same. The mix design consists of three categories. Each category has a different water content.

The mixes for Phase B3 include the following:

Phase B3.1: 0% alkaline solution substituted with water:

- Mix 22b – Fine aggregates to total aggregates ratio: 0.32
- Mix 1b – Fine aggregates to total aggregates ratio: 0.38
- Mix 11b – Fine aggregates to total aggregates ratio: 0.43
- Mix 19b – Fine aggregates to total aggregates ratio: 0.55

Phase B3.2: 10% alkaline solution substituted with water:

- Mix 23b – Fine aggregates to total aggregates ratio: 0.32
- Mix 2b – Fine aggregates to total aggregates ratio: 0.38
- Mix 12b – Fine aggregates to total aggregates ratio: 0.43
- Mix 20b – Fine aggregates to total aggregates ratio: 0.55

Phase B3.3: 25% alkaline solution substituted with water:

- Mix 24b – Fine aggregates to total aggregates ratio: 0.32
- Mix 3b – Fine aggregates to total aggregates ratio: 0.38
- Mix 13b – Fine aggregates to total aggregates ratio: 0.43
- Mix 21b – Fine aggregates to total aggregates ratio: 0.55

The mix design for Phase B3 is shown in Tables 5.17, 5.18 and 5.19.

Table 5.17: Mix design for Phase B3.1 (kg/m^3)

	Phase B3.1			
Material (kg/m^3)	Mix 22b	Mix 1b	Mix 11b	Mix 19b
Coarse aggregates	941	858	776	609
Fine aggregates	442	520	597	754
Slag	259	259	259	259
Fly ash	394	394	394	394
Sodium silicate solution	108	108	108	108
Sodium hydroxide solution (8 Molar)	92	92	92	92
Water	90	90	90	90

Table 5.18: Mix design for Phase B3.2 (kg/m^3)

	Phase B3.2			
Material (kg/m^3)	Mix 23b	Mix 2b	Mix 12b	Mix 20b
Coarse aggregates	941	858	776	609
Fine aggregates	442	520	597	754
Slag	259	259	259	259
Fly ash	394	394	394	394
Sodium silicate solution	98	98	98	98
Sodium hydroxide solution (8 Molar)	82	82	82	82
Water	104	104	104	104

Table 5.19: Mix design for Phase B3.3 (kg/m^3)

	Phase B3.3			
Material (kg/m^3)	Mix 24b	Mix 3b	Mix 13b	Mix 21b
Coarse aggregates	941	858	776	609
Fine aggregates	442	520	597	754
Slag	259	259	259	259
Fly ash	394	394	394	394
Sodium silicate solution	81	81	81	81
Sodium hydroxide solution (8 Molar)	69	69	69	69
Water	125	125	125	125

5.3.2.4. Phase B4: Binder

The goal of Phase B4 was to investigate the influence on the compressive strength when the fine aggregates is decreased and the binder increased. The binder to fine aggregate ratio is influenced when the sand is decreased and the binder increased or vice versa. The amount of alkaline liquid remained the same. The phase consists of two categories. Each category consists of a binder with different slag content. The mass of coarse aggregates and the alkaline solution content remained the same for all the mixes. 10% of the alkaline solution was substituted by water for all the mixes in this phase.

The mixes for Phase B4 include the following:

Phase B4.1: Binder with 40% slag

- Mix 2b – Binder to fine aggregate: 1.26
- Mix 14b – Binder to fine aggregate: 1.05
- Mix 17b – Binder to fine aggregate: 0.89

Phase B4.1: Binder with 23% slag

- Mix 6b – Binder to fine aggregate: 1.22
- Mix 15b – Binder to fine aggregate:1.02
- Mix 18b – Binder/ fine aggregate: 0.86

Note that the reason for the slight difference in binder to fine aggregate ratio is due to the relative density of slag. The material make up were designed per volume and then converted to mass.

The mix design for Phase B4 is shown in Tables 5.20 and 5.21.

Table 5.20: Mix design for Phase B4.1 (kg/m^3)

	Phase B4.1		
Material (kg/m^3)	Mix 2b	Mix 14b	Mix 17b
Coarse aggregates	858	858	858
Fine aggregates	520	572	624
Slag	259	239	219
Fly ash	394	364	333
Sodium silicate solution	98	98	98
Sodium Hydroxide solution (8 Molar)	82	82	82
Water	104	104	104

Table 5.21: Mix design for Phase B4.2 (kg/m^3)

	Phase B4.2		
Material (kg/m^3)	Mix 6b	Mix 15b	Mix 18b
Coarse aggregates	858	858	858
Fine aggregates	520	572	624
Slag	148	137	125
Fly ash	485	448	410
Sodium silicate solution	98	98	98
Sodium hydroxide solution (8 Molar)	82	82	82
Water	104	104	104

5.3.2.5. Phase B5: Sodium silicate to sodium hydroxide ratio

The goal of Phase B5 was to investigate the influence of the sodium silicate to sodium hydroxide ratio on the compressive strength of the geopolymer concrete. The ratio was chosen according to the volume of the solutions and then converted to a mass ratio. The binder used in the phase consisted of 60% fly ash and 40% slag by mass, the sodium hydroxide concentration was 8 Molar and 25% of the alkaline solution was replaced by additional water.

The mixes for Phase B5 include the following:

- Mix 25b – Sodium silicate to sodium hydroxide ratio: 0.59
- Mix 3b – Sodium silicate to sodium hydroxide ratio: 1.18
- Mix 26b – Sodium silicate to sodium hydroxide ratio: 1.78
- Mix 27b – Sodium silicate to sodium hydroxide ratio: 2.37

The mix design for Phase B5 is shown in Table 5.22.

Table 5.22: Mix design for Phase B5 (kg/m^3)

Material (kg/m^3)	Mix 25b	Mix 3b	Mix 26b	Mix 27b
Coarse aggregates	858	858	858	858
Fine aggregates	520	520	520	520
Slag	259	259	259	259
Fly ash	394	394	394	394
Sodium silicate solution	54	81	101	110
Sodium hydroxide solution (8 Molar)	92	69	57	47
Water	125	125	125	125

5.3.2.6. Phase B6: Sodium hydroxide concentration

Phase B6 investigated the sodium hydroxide concentration in the matrix. The material make up were similar to Mix 3b with only the sodium hydroxide concentration varying.

The mixes for Phase B6 include the following:

- Mix 28b - 6 Molar concentration
- Mix 3b - 8 Molar concentration
- Mix 29b - 12 Molar concentration
- Mix 30b - 16 Molar concentration

The mix design for Phase B6 is shown in Table 5.23.

Table 5.23: Mix design for Phase B6 (kg/m^3)

Material (kg/m^3)	Mix 28b	Mix 3b	Mix 29b	Mix 30b
Coarse aggregates	858	858	858	858
Fine aggregates	520	520	520	520
Slag	259	259	259	259
Fly ash	394	394	394	394
Sodium silicate solution	81	81	81	81
Sodium hydroxide solution	65	69	75	80
Water	125	125	125	125

Note that the increase in mass of the sodium hydroxide solution is due to the increase in density. A higher sodium hydroxide concentration results in a higher relative density as more sodium hydroxide flakes, which are denser than water, are added to the solution once the concentration increase.

5.4. Mix designs for modulus of elasticity tests

To ensure comparable results, only mixes from Phase B were considered for the modulus of elasticity tests. Different parameters were investigated to determine their influence on the stiffness of the fly ash/slag based geopolymer concrete. Note that only the parameters are illustrated as the material make-up of the mixes is already described in Section 5.3.2. A total of 12 mix designs were used to determine the modulus of elasticity of the fly ash/slag based geopolymer concrete mixes. Three specimens were tested and the average was taken as the modulus of elasticity of a certain mix design.

5.4.1. Slag content

The following mixes were used to investigate the influence of the slag content on the stiffness of the geopolymer concrete:

- Mix 3b – 40% slag of the binder mass
- Mix 7b – 23% slag of the binder mass

5.4.2. Alkaline solution replaced by water

The influence of the alkaline content on the stiffness of the geopolymer concrete was investigated by using the following mixes.

- Mix 19b – 0% alkaline solution replaced by water
- Mix 20b – 10% alkaline solution replaced by water
- Mix 21b – 25% alkaline solution replaced by water

5.4.3. Percentage of coarse aggregates in the matrix

The following mixes were used to investigate the influence of the course aggregate on the stiffness of the geopolymer concrete:

- Mix 20b - 26.41% coarse aggregates of the total mass of concrete
- Mix 23b - 40.57% coarse aggregates of the total mass of concrete

5.4.4. Sodium silicate to sodium hydroxide ratio

The following mixes were used to investigate the influence of the sodium silicate to sodium hydroxide ratio on the stiffness of the geopolymer concrete:

- Mix 25b – Sodium silicate to sodium hydroxide ratio: 0.59
- Mix 3b – Sodium silicate to sodium hydroxide ratio: 1.18
- Mix 26b – Sodium silicate to sodium hydroxide ratio: 1.78
- Mix 27b – Sodium silicate to sodium hydroxide ratio: 2.37

5.4.5. Sodium hydroxide concentration

The influence of the sodium hydroxide concentration, on the stiffness of the geopolymer concrete, was investigated by using the following mixes:

- Mix 28b - 6 Molar concentration
- Mix 3b - 8 Molar concentration
- Mix 29b - 12 Molar concentration
- Mix 30b - 16 Molar concentration

5.5. Fibre reinforced mixes for three point bending- and round panel tests

The second part of the experimental program is to investigate the addition of fibres in fly ash/slag based geopolymer concrete. The first goal is to investigate how the addition of macro fibres increase the ductility of a low strength and high strength fly ash/slag based geopolymer concrete matrix respectively, followed by a comparison between the ductile behaviour of low strength fibre reinforced geopolymer concrete (FRGC) and low strength fibre reinforced OPC concrete (FROC). Unreinforced concrete mixes for each of the designs were cast to compare the ductile behaviour of unreinforced concrete and fibre reinforced concrete (FRC). Thus, two fly ash/slag based geopolymer mix designs were used and one OPC concrete mix design. The same mix designs were used for both the three point bending tests and the round panel tests. A total of six beam specimens per mix design were cast for the three point bending test and three round panels were cast for the round panel tests.

Both macro steel- and polypropylene fibres, with two different dosages, were investigated. A lower volume of 0.4% and a higher volume of 0.8% fibres per volume were used. The steel fibres were obtained from Fibsol (Fibre Reinforcing Solutions), South Africa and the polypropylene fibres were obtained from Geotex, South Africa.

Important properties of the fibres are shown in Tables 5.24. The mix designs of the FRGC and FROC are shown in Tables 5.25 and 5.26.

Table 5.24: Properties of the two fibre types

Properties	Steel	Polypropylene
Fibre name	Dramix RL-45/50-BN	CB Series 500
Fibre length	50 mm	50 mm
Fibre diameter	1.05 mm	0.9 mm
Specific gravity	7.8	0.91
Tensile strength	1115 MPa	295 MPa
Mass per m^3		
0.4%	31.2 kg	3.64 kg
0.8%	62.4 kg	7.28 kg

Table 5.25: Mix design for FRGC (kg/m^3)

Material (kg/m^3)	Mix 3b	Mix 7b
Coarse aggregates	858	858
Fine aggregates	520	520
Slag	259	148
Fly ash	394	485
Sodium silicate solution	81	81
Sodium Hydroxide solution (8 molar)	69	69
Water	125	125

Table 5.26: Mix design for FROC (kg/m^3)

Material (kg/m^3)	Mix 7-OPC
Water	205
Binder (Cem I 52.5)	205
Coarse aggregates	1020
Fine aggregates	972

5.6. Mix designs for single fibre pull-out tests

Four fly ash/slag based geopolymer concrete mixes were compared with four OPC concrete mixes. The compressive strength was used as the base line for the comparison. Thus, the compressive strengths of the four geopolymer concrete mixes were used to design the respective OPC concrete mixes. The compressive strength of the OPC concrete specimens had to be in a range of ±5 MPa to that of the geopolymer concrete specimens, to ensure comparable results. Both steel and polypropylene fibres were embedded in the two different concrete types. For simplicity, the OPC concrete mixes will have the same mix number as the corresponding geopolymer mixes to which they were compared with. A total of eight specimens per mix design were tested.

The material make up is shown in Tables 5.27 and 5.28

Table 5.27: Mix design for geopolymer concrete fibre pull-out specimens (kg/m^3)

Material (kg/m^3)	Mix 7b	Mix 16b	Mix 24b	Mix 3b
Coarse aggregates	858	858	941	858
Fine aggregates	520	572	442	520
Slag	148	116	259	259
Fly ash	485	465	394	394
Sodium silicate solution	81	98	81	81
Sodium hydroxide solution (8 Molar)	69	82	69	69
Additional water	125	104	125	125

Table 5.28: Mix design for OPC concrete fibre pull-out specimens (kg/m^3)

Material (kg/m^3)	Mix 7-OPC	Mix 16-OPC	Mix 24-OPC	Mix 3-OPC
Water	205	205	205	205
Binder (Cem I 52.5)	205	332	363	394
Coarse aggregates	1020	1020	1020	1020
Fine aggregates	972	864	838	811

5.7. Mix designs for setting time tests

Setting time tests were carried out on three specific geopolymer concrete specimens and the material make up is shown in Table 5.29. The three mixes include Mix 10a, Mix 3b and Mix 7b. Mix 10a contains no additional water in the matrix, thus a higher alkaline solution content. The two mixes of Phase B both contained additional water in the matrix. The setting time of two specimens of each mix design was measured and the average was taken as the setting time of the specific geopolymer concrete mix design.

Mix 10a and Mix 3b had similar binder content, thus a good comparison was drawn on the influence of alkaline solution content on the setting time. Mix 3b and Mix 7b had the same alkaline content, thus a good comparison was drawn on the influence of slag on the setting time of geopolymer concrete.

Mix 3b and Mix 7b contained a sodium hydroxide solution with an 8 M concentration and a sodium silicate solution that had a SiO_2:Na_2O ratio of 2 while Mix 10a contained a sodium hydroxide solution with a 6 M concentration and a sodium silicate solution that had a SiO_2:Na_2O ratio of 3.34.

Table 5.29: Geopolymer concrete mix designs for setting times and temperature tests (kg/m^3)

Material (kg/m^3)	Mix 7b	Mix 3b	Mix 10a
Coarse aggregates	858	858	1008
Fine aggregates	520	520	432
Slag	148	259	265
Fly ash	485	394	397
Sodium silicate solution	81	81	213
Sodium hydroxide solution	69	69	85
Additional water	125	125	0

5.8. Mix designs for concrete temperature development test

The same mixes, as used for the setting time tests (Section 5.7), were used for the temperature development tests. The temperature development for one specimen of each mix design was measured.

Mix 10a and Mix 3b had similar binder content, thus a good comparison was drawn on the influence of alkaline solution content/water content on the curing temperature. Mix 3b and Mix 7b had the same alkaline content, thus a good comparison was drawn on the influence of slag content on the temperature development. The temperature development of an OPC concrete mix (Mix 3-OPC) with a corresponding compressive strength to Mix 3b (50 MPa) was also investigated. The influence on the temperature, due to hydration is compared to geopolymer concrete. The mix design of the OPC concrete specimen is shown in Table 30.

Table 5.30: OPC concrete mix design for the temperature development test (kg/m^3)

Material (kg/m^3)	Mix 3-OPC
Water	205
Binder (Cem I 52.5)	394
Coarse aggregates	1020
Fine aggregates	811

Chapter 6
Results

The results of all the tests conducted, as described in Chapter 5, are reported in this chapter. This includes tests on the workability, compressive strength, modulus of elasticity, three point bending tests, round panel tests, single fibre pull-out tests, setting time tests and temperature development tests. All the tests were carried out on the age specified, except if stated differently.

6.1. Workability

The diameter slump of the fresh fly ash/slag based geopolymer concrete was determined immediately after mixing. The average diameter slump of the geopolymer concrete of Phase A was lower than the diameter slump of Phase B, mainly due to the additional water that was added to Phase B. The viscosity of the geopolymer concrete of Phase A was relatively high and vibration was needed to ensure adequate compaction, while no vibration was needed for the mixes of Phase B.

The diameter slump readings of 43 mixes ranged between 350 mm and 750 mm. Segregation was observed when the diameter slump reading was greater than 650 mm. An indication of segregation during the slump test is when a heap of stone is situated in the middle part of the slump circle. This result is due to the binder not having a proper bind to the coarse aggregates, due to a low viscosity or due to a large amount of stone in the matrix.

The amount of water and fly ash in the matrix had a great influence on the workability and the results are shown in Figure 6.1 and Figure 6.2. The workability increased when the fly ash to slag ratio increased or the water content increased.

As stated in Chapter 2, fly ash has a spherical shape, making it more mobile than the sharper particles of the slag. The workability increased significantly when the binder consisted of only 20% slag and segregation was usually found for the majority of these mixes.

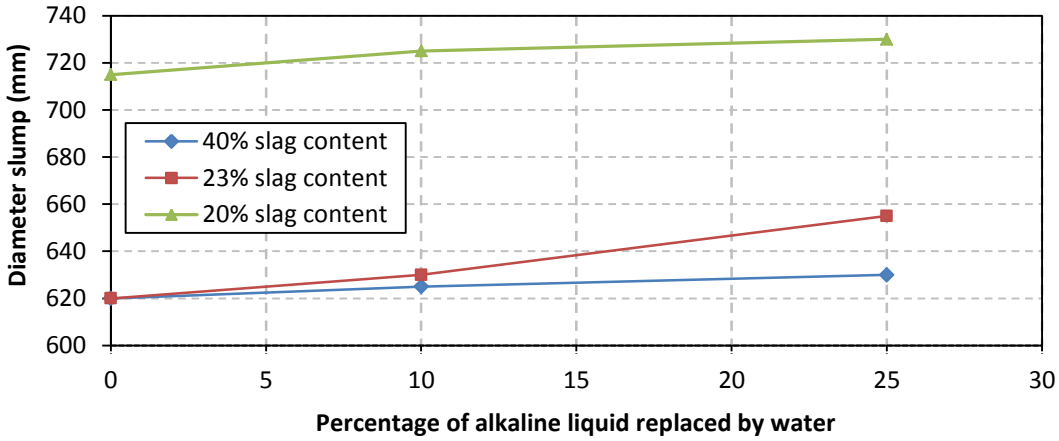

Figure 6.1: Influence of additional water on the workability

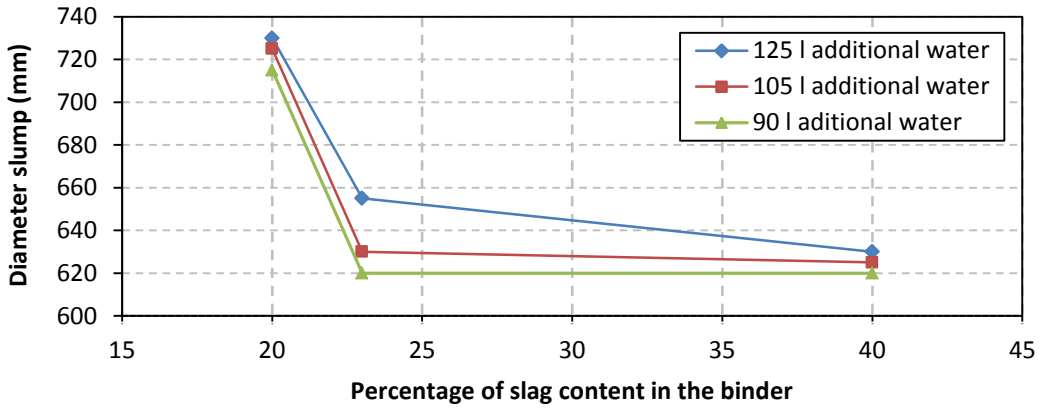

Figure 6.2: Influence of slag on the workability

Although it was not significant, the sodium hydroxide concentration influenced the workability of the fresh geopolymer concrete and the results are shown in Figure 6.3.

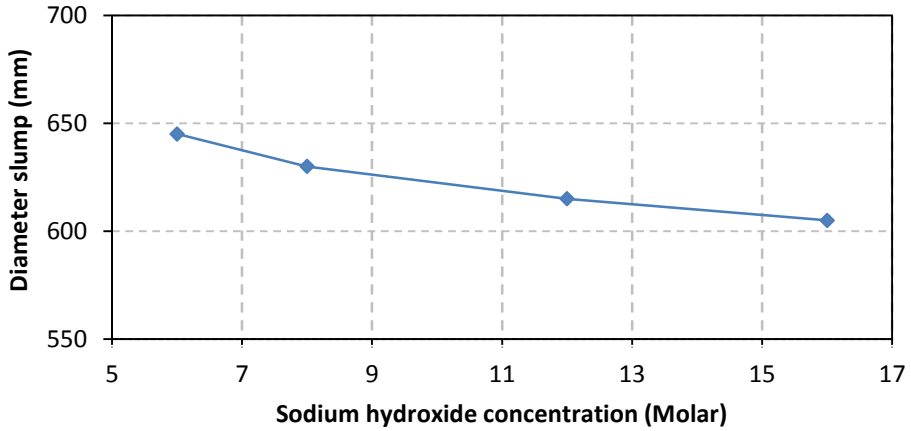

Figure 6.3: Influence of sodium hydroxide concentration on the workability

As shown in Figure 6.4, the aggregate content in the matrix also influenced the workability of the fly ash/slag based geopolymer concrete. The workability decreased when the aggregate content increased. By adding more aggregates, the binder content and the alkaline content decreased, resulting in less water in the matrix. This method is also used to adjust the slump test reading of OPC concrete in which a specific amount of water and binder can be reduced while increasing the sand content.

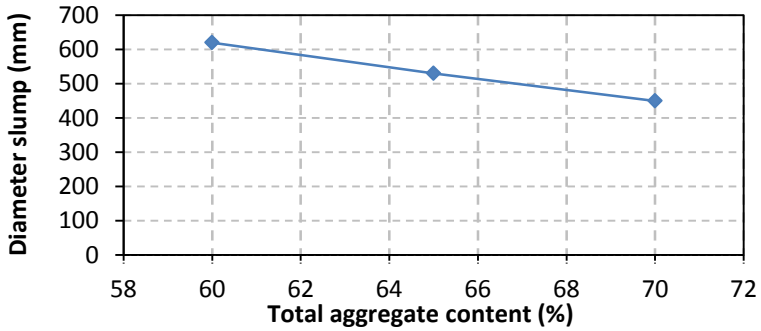

Figure 6.4: Influence of the amount of aggregate on the workability

6.2. Compressive strength test results

Compressive strength test results are discussed in the following sections. There was a significant variation in compressive strengths, varying from 6 MPa to 72 MPa. No results were obtained for two of the 44 mixes, i.e. Mix 9a (too compact) and Mix 4b (did not harden). The results are discussed in the same format as the phases described in Chapter 5.

6.2.1. Compressive strength test results for Phase A

6.2.1.1. Phase A1: Sodium silicate to sodium hydroxide ratio

As shown in Figure 6.5, by increasing the sodium silicate to sodium hydroxide ratio results in a decrease in compressive strength. There was no significant decrease in strength observed between a ratio of 1 and 2, but the strength decreased drastically when the ratio was increased beyond this point. It can be concluded from the results that the compressive strength decreases if less sodium hydroxide solution is available in the matrix.

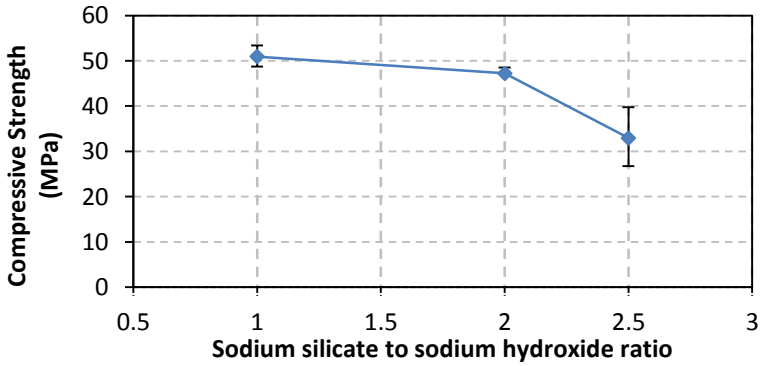

Figure 6.5: Influence of sodium silicate to sodium hydroxide ratio on the compressive strength

6.2.1.2. Phase A2: Fly ash/slag content

The influence of the slag content in the matrix is illustrated in Figure 6.6. The compressive strength increased when the slag content increased (fly ash content decreased). The slag content was increased in increments of 20%. Although the increase in strength was not significant, there was a higher strength gain for the first 20% increment than for the second 20%.

It must be noted that the cubes of the mix designs containing 0% slag were only demoulded three days after casting as it did not harden after one day. As mentioned in Chapter 2, the increase in slag accelerates the setting time of the fly ash/slag based geopolymer concrete.

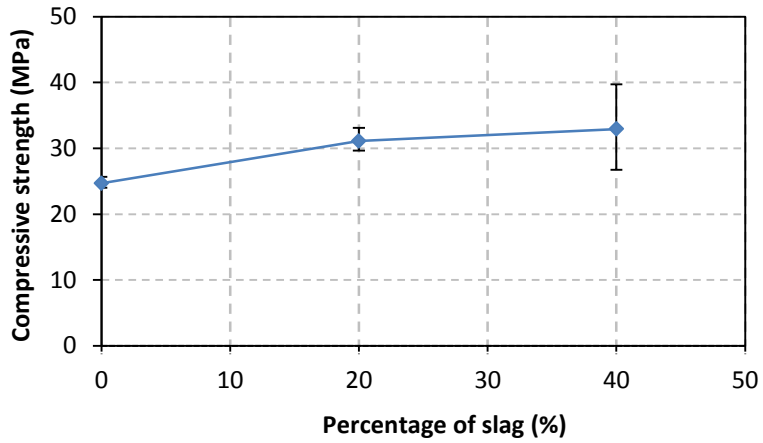

Figure 6.6: Influence of slag on the compressive strength

6.2.1.3. Phase A3: Aggregate content

Figure 6.7 illustrates the influence of the aggregate content in the matrix. The increase of aggregates did not yield significant changes, although a slight increase in the compressive strength was noticed when the aggregate content increased. The alkaline to binder ratio remained the same for all the mixes.

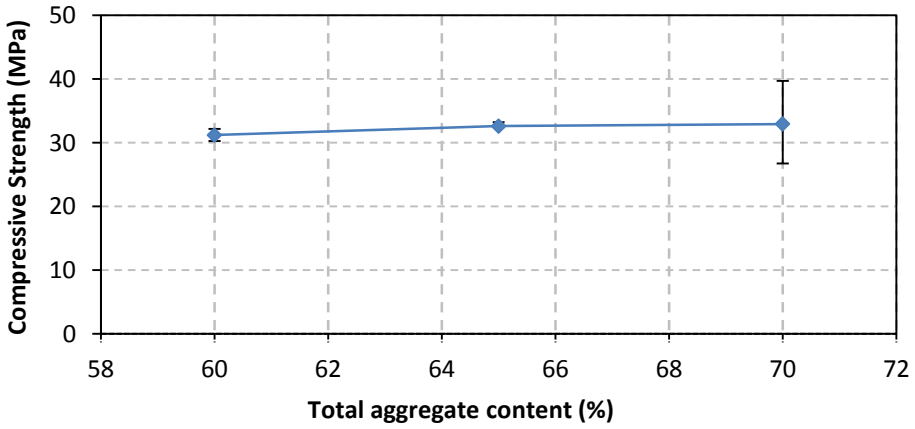

Figure 6.7: Influence of the amount of aggregates on the compressive strength

6.2.1.4. Phase A4: Influence of fine aggregates in the aggregate content

The results of the compressive strength tests are shown in Figure 6.8. An increase in strength was observed up to a ratio of 0.4, followed by a strength decrease beyond this point. The coarse aggregate content for the mix with a fine aggregate to total aggregate ratio of 0.3 was significantly high (1176 kg). If the coarse aggregate content is too high, segregation tends occur. Another possible explanation for the low compressive strength of the mix with a ratio of 0.3 is due to an inadequate amount of fine particles that can bind with the large amount of coarse aggregate.

From the results obtained the fine aggregate to total aggregates ratio of 0.4 yields the highest compression strength.

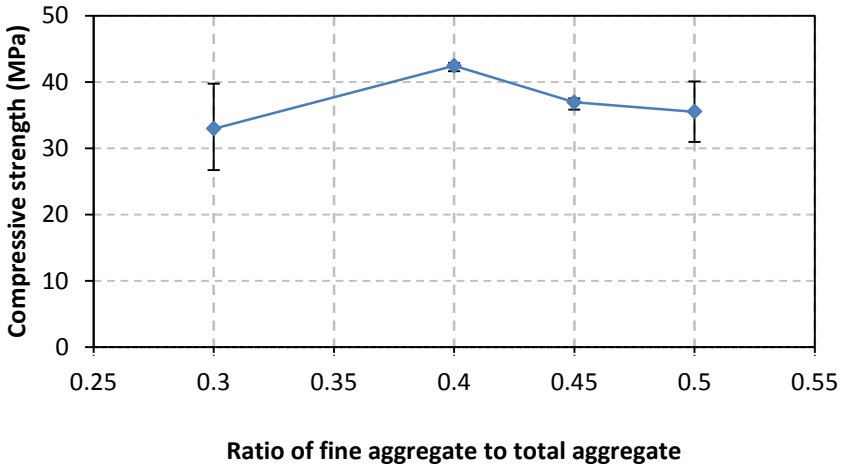

Figure 6.8: Influence of the fine aggregate to total aggregate ratio on the compressive strength

6.2.1.5. Phase A5: Alkaline to binder ratio

The alkaline to binder ratio in the matrix was investigated and the compressive strength results are shown in Figure 6.9. Initially three mixes were designed for this phase, but the mix with a ratio of 0.35 was too dry. This concludes that, for a mix with no additional water, an alkaline to binder ratio of 0.35 or less is too compact to cast. The results obtained for the other two mixes indicate that the compressive strength increases when the alkaline to binder ratio decreases. An inadequate amount of mixes were designed to obtain an optimum ratio.

The ratio had a significant influence on the workability of the fresh fly ash/slag based geopolymer concrete and this must be taken into consideration when deciding on the alkaline to binder ratio. The diameter slump readings of Mix 10a (0.45 ratio) and Mix 6a (0.55 ratio) were 450 mm and 620 mm.

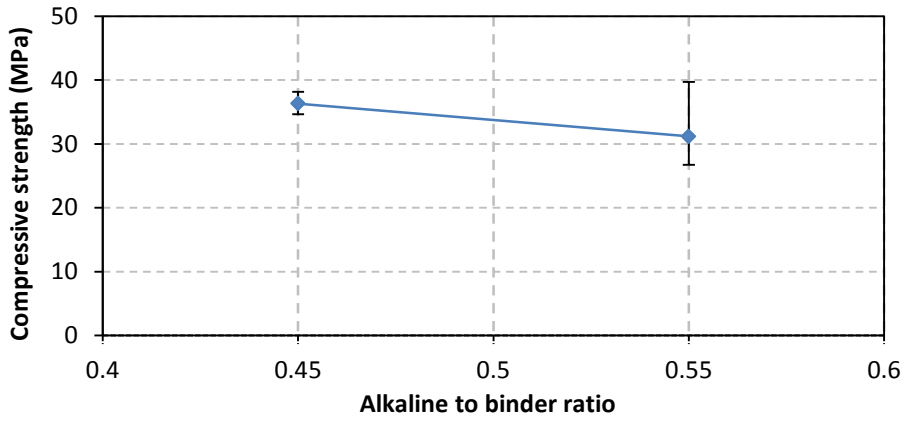

Figure 6.9: Influence of the alkaline to binder ratio on the compressive strength

6.2.1.6. Phase A6: Sodium hydroxide concentration

Figure 6.10 illustrates the influence on the compressive strength when the concentration of the sodium hydroxide solution was changed. The figure indicates that the compressive strength increased when the molarity of the sodium hydroxide concentration increased. There was no significant increase between a molarity of 3 M and 6 M, as the compressive strength only increased by 9%. The strength increased by approximately 28% when the molarity was increased to 8 M.

The dissolution process is more sufficient with a higher sodium hydroxide concentration, yielding higher compressive strengths.

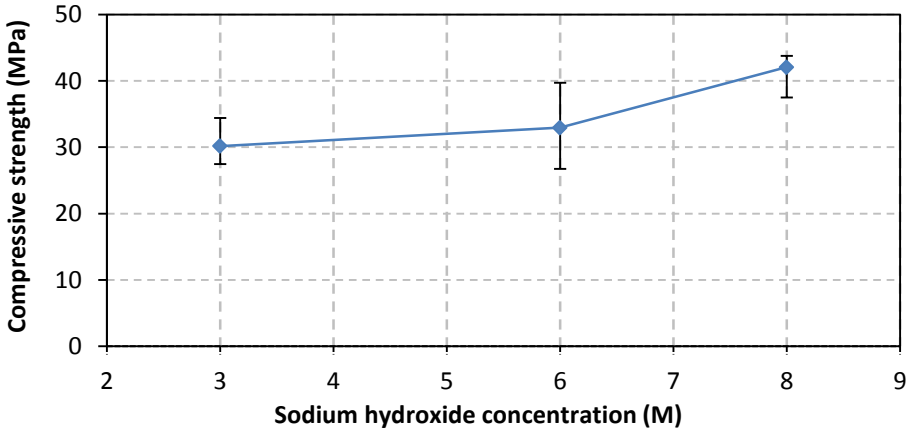

Figure 6.10: Influence of the sodium hydroxide concentration on the compressive strength

6.2.1.7. Concluding summary

All the results, except the sodium silicate to sodium hydroxide ratio, showed similar trends to results found by other researchers. The slag content and the concentration of the sodium hydroxide solution had the largest influence on the compressive strength of the fly ash/slag based geopolymer concrete.

6.2.2. Compressive strength test results for Phase B

The results of the mixes designed in Phase B are given in the following section.

6.2.2.1. Phase B1: Alkaline solution replaced by water

A fraction of the alkaline solution (by mass) was replaced by tap water and the results of the compressive tests are shown in Figure 6.11. Logically, the strength of the fly ash/slag based geopolymer concrete will decrease when the alkaline solution is decreased. The molarity of the concentration decreases when more water is added to the matrix, resulting in less sodium hydroxide ions available to dissolve the aluminosilicate. The matrix with a binder content consisting of 40% slag showed a slight increase in strength when 10% of the alkaline solution was replaced by water, followed by a decrease in strength when more alkaline liquid was replaced. The matrix with a binder content consisting of 23% slag and 20% slag by mass respectively showed a decrease in strength when both fractions of alkaline solution were replaced by water.

As stated in Section 2.2.3.3, calcium silicate hydrate (CSH) gel forms in conjunction with the geopolymeric gel when slag is added to the matrix. The CSH gel causes a significant increase in strength and it is suggested that more CSH gel forms when the slag content in the matrix is increased. Thus, even if 10% of the alkaline liquid is replaced by water, enough hydroxide ions are available to form an adequate amount of CSH gels that will yield similar strengths compared to a matrix that had no alkaline liquid replaced.

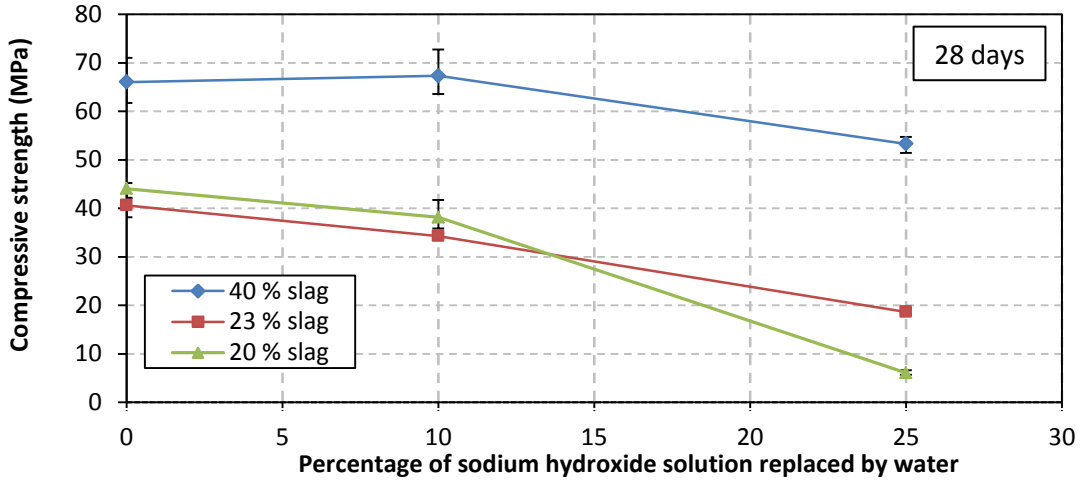

Figure 6.11: Influence of water replacement on the compressive strength at 28 days

Although it was not significant, the mixes with a binder content containing 20% slag (by mass) in the matrix yielded higher compressive strengths, than the mixes containing 23% slag, when the alkaline solution was replaced by 0% and 10% water. This result is counter intuitive. It must be noted that slag content is fairly similar, which may lead to a similar dissolution process and geopolymeric structure. Thus, the material makeup of the two mixes may be too similar to compare. As shown in Figure 6.12, more logical results were obtained for the 7 day compressive strength tests.

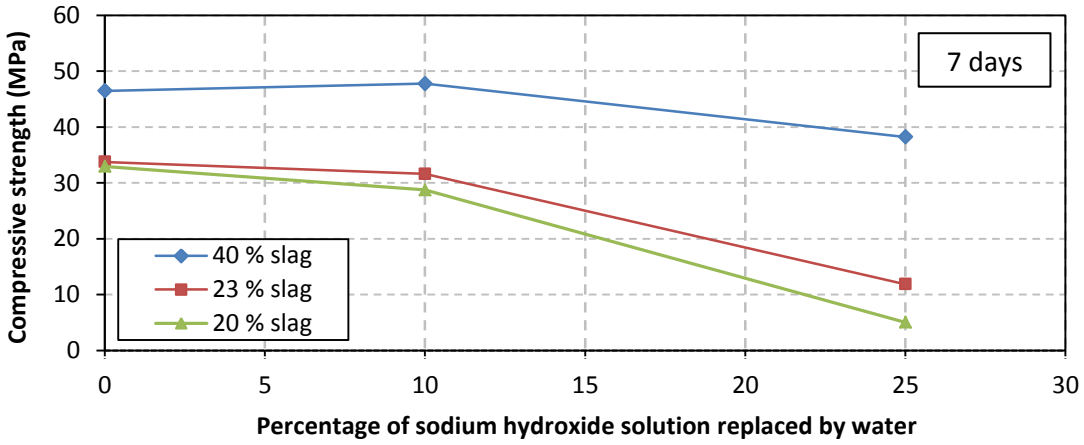

Figure 6.12: The 7 day compressive strength for Phase B1

Figure 6.13 shows the decrease in strength when the alkaline solution was replaced by water. The mixes in which no alkaline liquid were replaced, was taken as the reference mix and 100% strength was allocated to them. The strength, when alkaline solution was replaced by water, was taken as a percentage of the original strength. The figure shows that the strength decreased by a steeper gradient when the slag content decreased. A possible explanation is that the amount of CSH gel that is formed depends of the slag content. The CSH gel contributes to the strength of the fly ash/slag based geopolymer concrete and less gel will form when the slag content reduces, resulting in an overall lower compressive strength.

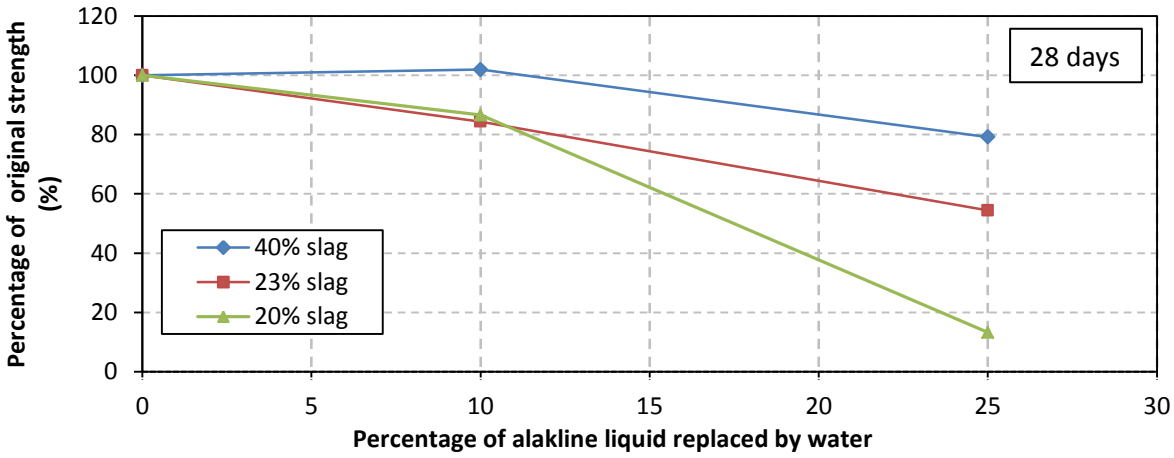

Figure 6.13: Compressive strength decrease at 28 days when alkaline liquid is substituted

6.2.2.2. Phase B2: Slag content

Figure 6.14 shows the Phase B2 compressive test results. The overall conclusion that was drawn from the results is that the compression strength of the fly ash/slag based geopolymer concrete increases if the slag content increases. Again, the mixes of which 0% and 10% sodium hydroxide solution was replaced by additional water did not show a logical trend when the slag content was increased from 20% to 23%.

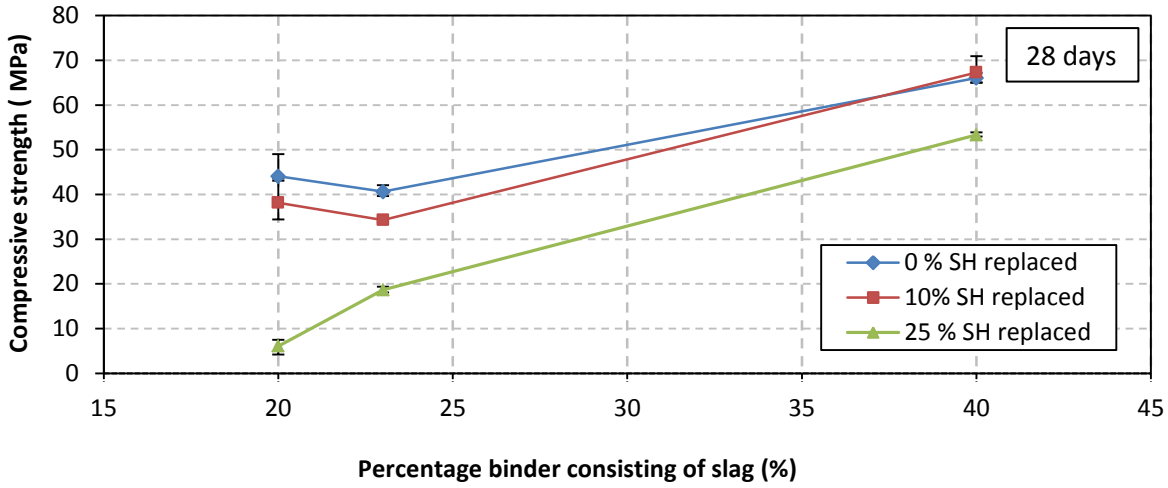

Figure 6.14: Influence of slag on the compressive strength at 28 days

It is yet inconclusive why the slight decrease in strength was found with the increase of slag from 20% to 23% and a suggestion is that the microstructure of the four mixes (first two of the blue line and first two of the red line) is fairly the same due to similar material composistition. This decrease could also be attributed to experimental scatter. However, there was a significant increase in strength when the slag content was increased to 40% of the binder mass. The 7 day strength curve (Figure 6.15) for the same phase was also more logical than that of the 28 day curve. The contradiction in the two figures indicates that the aging of the fly ash/slag based geopolymer concrete is inconsistent.

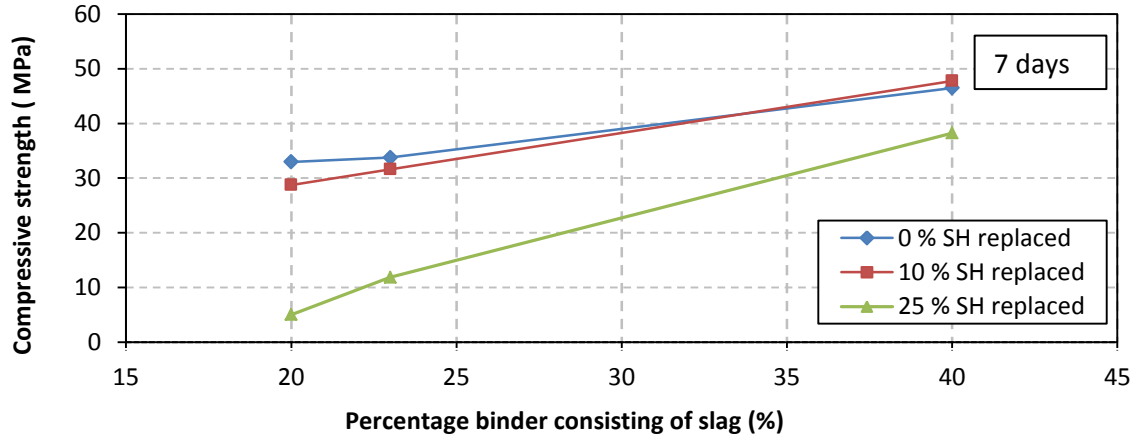

Figure 6.15: The 7 day compressive strength curve for Phase B2

A turquoise colour was observed in the fly ash/slag geopolymer concrete when slag was added to the matrix. The colour depended mainly on the amount of slag in the matrix, as the colour became darker when the slag content increased. It was also found that the darkness of the colour decreased when more water was added. The turquoise colour faded with age. Figure 6.16 shows the turquoise colour in the fly ash/slag based geopolymer concrete. The water content increased from left to right in the

figure. A significant difference in colour was observed between 25% additional water in the matrix (left) and 0% additional water in the matrix (right). The geopolymer concrete cylinder in the middle contained 10% additional water. The photograph was taken directly after the specimens were demoulded.

Figure 6.16: Turquoise colour in the geopolymer concrete specimens

6.2.2.3. Phase B3: Fine aggregate to total aggregate ratio

Figure 6.18 shows the compressive test results for Phase B3. The same trend was found for each of the three curves. The compressive strength increased when the ratio increased from 0.32 to 0.43, but a decrease in strength was observed when more fine aggregates were added. The binder material consisted of 40% slag by mass. The compressive strength for the mixes containing 10% additional water yielded similar or slightly higher compressive strengths than the mixes that contained 0% additional water. The matrix containing 25% additional water showed a significant lower strength.

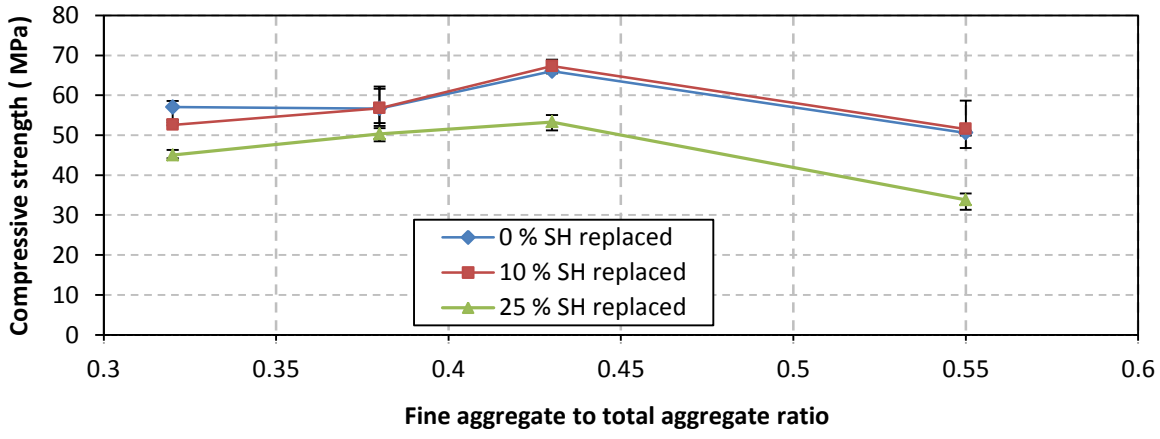

Figure 6.17: Influence of the fine aggregate to total aggregate ratio on the compressive strength

6.2.2.4. Phase B4: Binder

Figure 6.18 shows the results of compressive tests for Phase B4. The phase investigated the influence on the compressive strength when a fraction of the fine aggregates were replaced by additional binder. The compressive strength of the specimens, with a binder that consisted of 40% slag, increased when

the binder in the matrix increased. The increase in strength was only observed from a ratio of 1.05 to 1.26. The specimens with a binder consisting of 23% slag showed no significant change in strength.

This result indicates that the slag content has a major influence on the compressive strength and therefore no significant change in strength was observed when a binder material, consisting of 20% slag, was increased by the respective amounts. Thus, the binder to sand ratio only has an influence on the strength if an adequate amount of slag is present in the matrix.

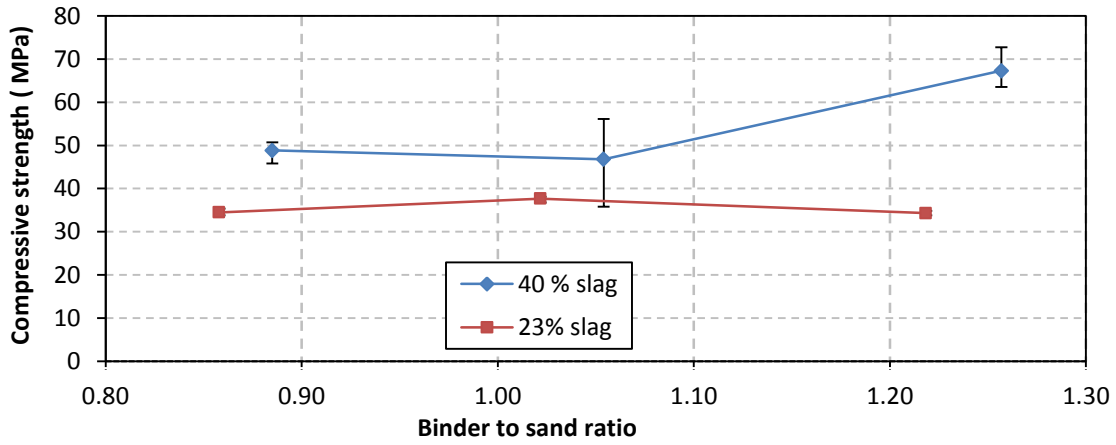

Figure 6.18: Influence of binder to sand ratio on the compressive strength

6.2.2.5. Phase B5: Sodium silicate to sodium hydroxide ratio

The influence of the sodium silicate to sodium hydroxide ratio is shown in Figure 6.19. According to the results obtained, a ratio of 1.18 yielded the highest compression strength.

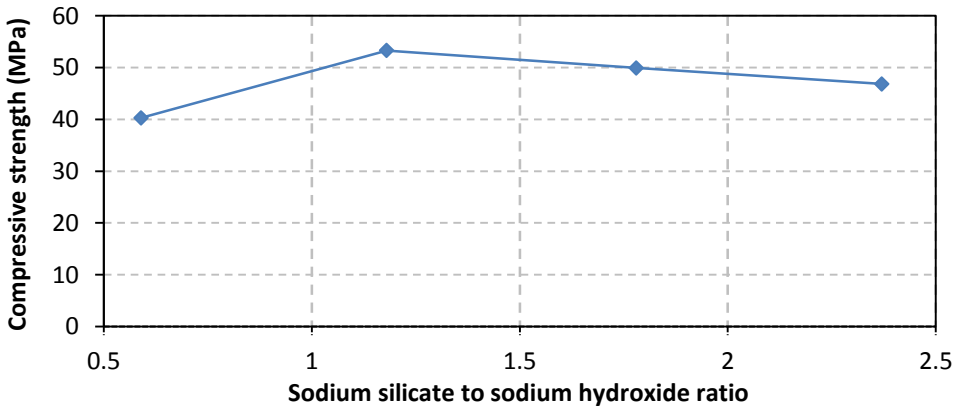

Figure 6.19: Influence of the sodium silicate to sodium hydroxide ratio on the compressive strength

6.2.2.6. Phase B6: Sodium hydroxide concentration

Figure 6.20 shows that the compressive strength of the geopolymer concrete increased when the concentration of the sodium hydroxide solution increased. A rapid increase in strength was observed for a concentration between 6 M and 8 M followed by a more gradually increase onwards up to 16 M.

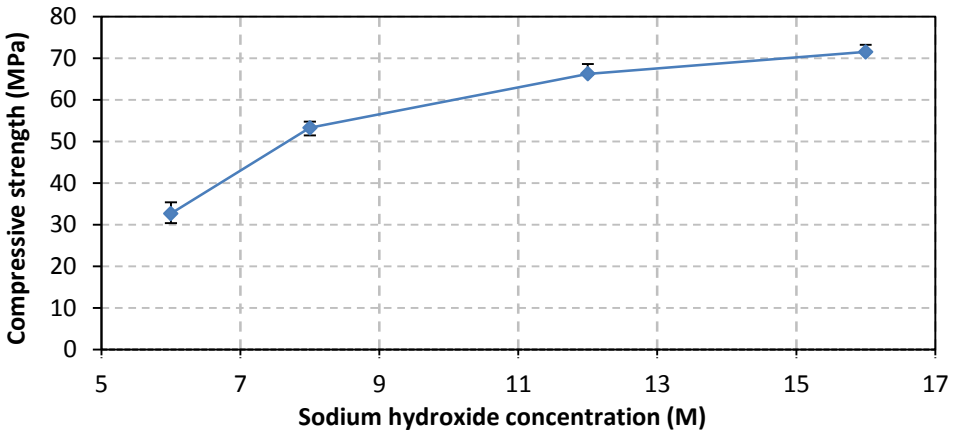

Figure 6.20: Influence of the sodium hydroxide concentration on the compressive strength

6.2.2.7. Concluding summary

It is clear from the results of Phase B that adequate compressive strengths can be achieved with a lower alkaline liquid content. The influence of the various parameters was also more significant compared to the results found in Phase A. The compressive strength of geopolymer concrete was significantly influenced by the sodium hydroxide concentration, the slag content and the amount of water in the matrix. There was no significant difference in strength when 10% of the alkaline solution was replaced by water when binder consisted of 40% slag by mass. A significant decrease in strength was observed when 25% of the alkaline solution was replaced by additional water.

6.3. Modulus of elasticity test results

The modulus of elasticity test was conducted to obtain information regarding the stiffness of the fly ash/slag based geopolymer concrete. The average of three specimens was taken as the modulus of elasticity for a certain mix design. The test was carried out, 28 days after casting, for a total of twelve different mix designs and the results are shown in the following section.

6.3.1. Slag content

The results of the modulus of elasticity tests are shown in Figure 6.21. The stiffness of the geopolymer concrete decreased when the slag content increased. A possible explanation for the decrease in stiffness is that the microstructure is affected when slag is added to the matrix. CSH gel forms in conjunction with the geopolymeric gel which hinders the original geopolymer microstructure. Note that the compressive strength actually increased from 18.65 MPa to 53.3 MPa when the slag content increased from 23% to 40% of the binder content by mass. It must be noted that limited tests were done and therefore more research is required to obtain a better understanding of the influence of slag on the modulus of elasticity of fly ash/slag based geopolymer concrete.

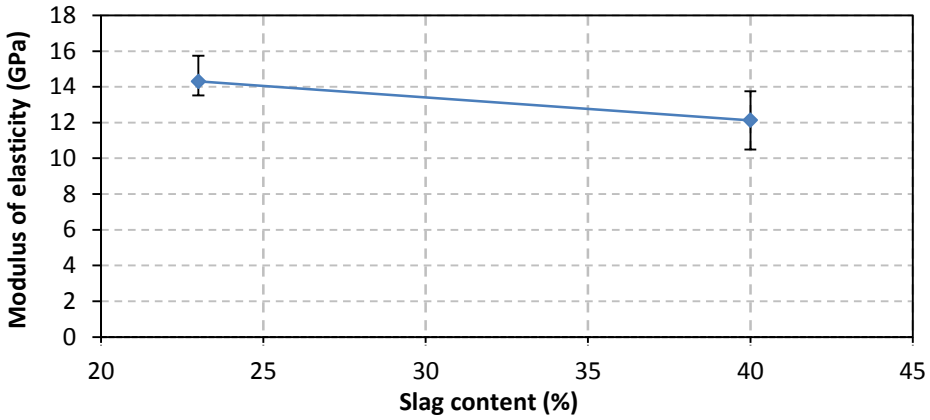

Figure 6.21: Influence of the slag on the modulus of elasticity

6.3.2. Alkaline solution replaced by water

As shown in Figure 6.22, the modulus of elasticity decreased when the amount of additional water increased. The amount of sodium hydroxide ions, available in the solution, decreased when a fraction of the alkaline solution was substituted by water, resulting in a lower concrete strength and also a lower elastic modulus. This result is due to less sodium hydroxide ions that can participate in the dissolution process.

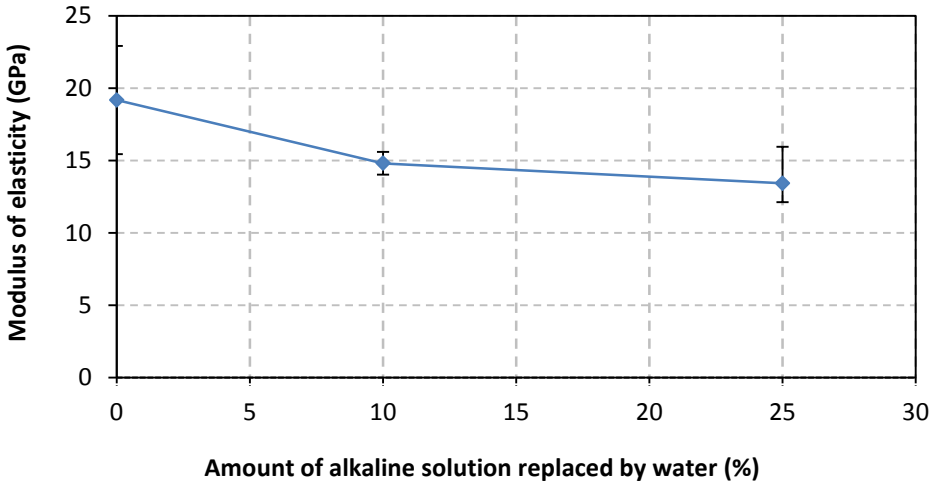

Figure 6.22: Influence of the alkaline solution on the modulus of elasticity

6.3.3. Percentage of coarse aggregates in the matrix

The results of the modulus of elasticity test are shown in Figure 6.23. A slight decrease in stiffness was observed when the amount of coarse aggregates increased. This is a contradictory trend compared to OPC concrete. Aggregates have a higher stiffness than the binder. Thus, the increase in coarse aggregate content must increase the elastic modulus of the geopolymer concrete. A possible explanation is that the bond between the coarse aggregates and the binder differs from that of OPC concrete. More research is required in this field as only two mix designs were tested.

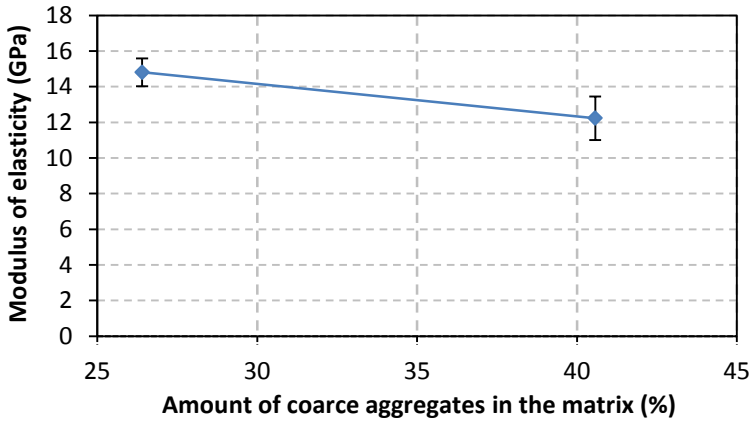

Figure 6.23: Influence of coarse aggregates on the modulus of elasticity

6.3.4. Sodium silicate to sodium hydroxide ratio

The influence of the sodium silicate to sodium hydroxide ratio, on the modulus of elasticity, is shown in Figure 6.24. The elastic modulus of the geopolymer concrete decreased when the ratio increased. It must be noted that the sodium hydroxide decreases when the ratio increases which, yet again, confirms the sodium hydroxide solution has a significant influence on the stiffness of the geopolymer concrete.

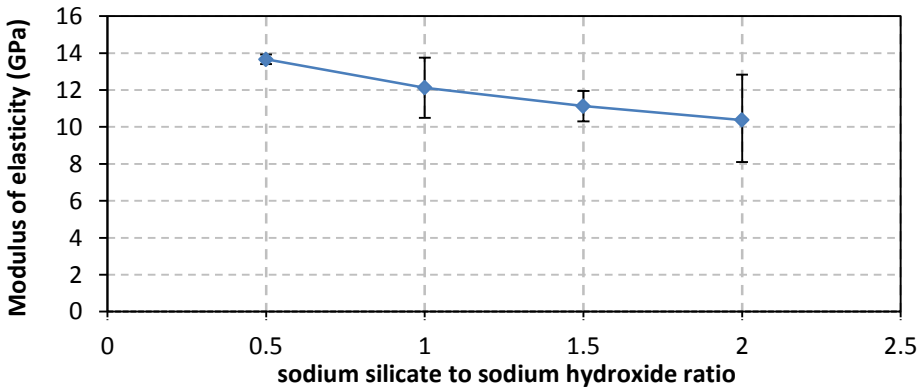

Figure 6.24: Influence of the sodium silicate to sodium hydroxide ratio on the modulus of elasticity

6.3.5. Sodium hydroxide concentration

The influence of the sodium hydroxide concentration on the elastic modulus of the geopolymer concrete is shown in Figure 6.25. The figure shows that the stiffness of the geopolymer concrete increased when a higher sodium hydroxide concentration was used. A concentration of 12 M yielded the highest stiffness while a decrease was observed when the concentration increased beyond 12 M.

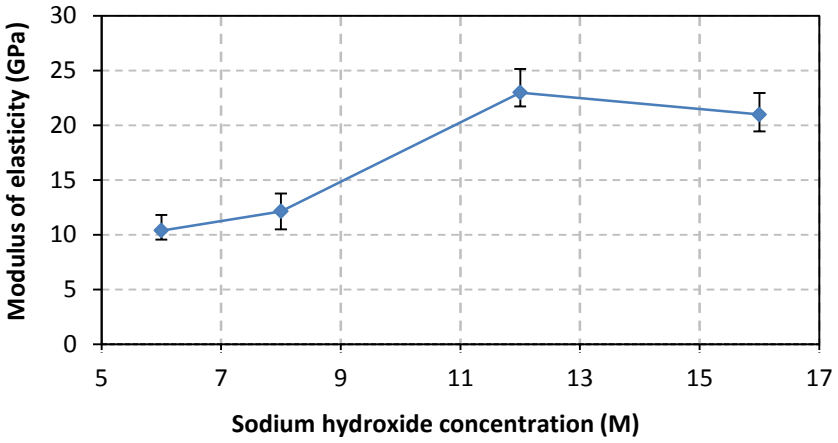

Figure 6.25: Influence of the sodium hydroxide solution concentration on the modulus of elasticity

6.3.6. Concluding summary

The results for the majority of the specimens showed a relatively low modulus of elasticity, ranging between 9.4 GPa and 23 GPa. However, it was found that the stiffness of fly ash/slag based geopolymer concrete is influenced by different parameters of which the sodium hydroxide solution had the largest influence. The modulus of elasticity for a low strength (20 MPa) OPC concrete mix was determined and it yielded an elastic modulus of 24.3 GPa. This result was higher than any of the twelve geopolymer concrete specimens regardless of the higher compressive strengths.

This is insufficient from a structural point of view as the size of the elements will have to be relatively large to avoid large deflections. However, as mentioned, various parameters influence the stiffness of the fly ash/slag based geopolymer concrete and it is suggested that if an optimum mix is designed, promising stiffness may be obtained.

6.4. Fibre reinforced concrete test results

The results of the fibre reinforced concrete tests are discussed in the following sections. Three mix designs were used to conduct three point bending tests and round panel tests. The three mixes include a higher strength fly ash/slag based geopolymer concrete, a lower strength fly ash/slag based geopolymer concrete and an OPC concrete with a similar compressive strength compared to the lower strength geopolymer concrete.

The mix names were allocated according to the corresponding mix designs used from the compression test results, the volume of fibres and the type of fibres. For example:

Mix 3b.4PP

- 3b – The mix design used is Mix 3b from the compression test results
- .4 – 0.4% fibres per volume in the matrix
- PP – Polypropylene fibres

Other important information:

- S – Steel fibres
- .8 – 0.8% fibres per volume in the matrix

The OPC concrete specimens were named exactly the same except they were clearly marked with the term "OPC" for example Mix 7-OPC.4PP. Note that the unreinforced concrete mixes have the same names as described in Chapter 5 for the compressive strengths.

The compressive strength of the various FRC specimens is shown in Table 6.1.

The compressive strength of the concrete (geopolymer and OPC) containing polypropylene fibres was lower than the strength of the unreinforced concrete. An opposite result was found for the steel fibre reinforced concrete specimens as the strength was higher than that of the unreinforced concrete. It must be noted that the change in strength was not significant and therefore it can be concluded that the addition of fibres do not have a significant influence on the compressive strength of both fly ash/slag based geopolymer concrete and OPC concrete.

Table 6.1: Compressive strength of FRC in MPa

Mix Name	Polypropylene	Steel	Plain
Mix 3b.4	49.01	56.05	53.30
Mix3b.8	49.69	53.62	
Mix 7b.4	16.18	21.28	18.65
Mix 7b.8	16.24	21.20	
Mix 7.4 - OPC	16.29	17.92	18.52
Mix 7.8 - OPC	16.48	18.97	

6.4.1. Three point bending test results

The results of the three point bending tests are shown in the following sections. The stress-deflection curves for all the beam specimens are shown in Figures A.1 to A.15 in the appendix. Figure 6.26 shows the typical results of the three point bending tests.

The stress-deflection curves for all the polypropylene fibre reinforced geopolymer concrete (PFRGC) specimens and the polypropylene fibre reinforced OPC concrete (PFROC) specimens showed deflection-softening behaviour (Figure 6.26a).

The higher volume steel fibre reinforced concrete (SFRC) mixes showed deflection-hardening behaviour for both geopolymer concrete mix designs and the OPC concrete mix (Figure 6.26b). Deflection-hardening was also found for the lower strength steel fibre reinforced geopolymer concrete

(SFRGC) specimens and the steel fibre reinforced OPC concrete (SFROC) specimens containing the lower volume fibres in the matrix.

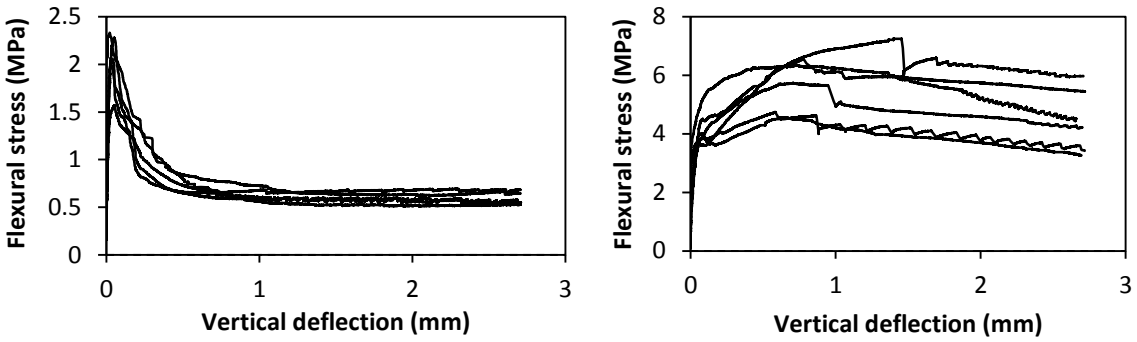

a) Deflection-softening behaviour **b) Deflection-hardening behaviour**

Figure 6.26: Load-deflection curves of the three point bending tests

6.4.1.1. Higher strength FRGC vs. lower strength FRGC

The results of the two fibre reinforced geopolymer concrete mix designs (higher strength and lower strength) are discussed in the following section. Steel- and polypropylene fibres were added to the respective mixes at two different dosages (0.4% and 0.8% by volume).

i. Polypropylene fibre reinforced geopolymer concrete

The properties of the PFRGC are shown in Table 6.2.

Table 6.2: Properties of higher strength PFRGC and lower strength PFRGC

Mix Name	Limit of proportionality (MPa)	δ at LOP (mm)	Equivalent flexural strength $F_{e,3}$ (MPa)	R_{e3}	Compressive strength (MPa)
Mix 3b.4PP	3.40	0.047	0.88	0.30	49.01
Mix3b.8PP	3.56	0.059	1.74	0.49	49.69
Mix 7b.4PP	2.06	0.039	0.65	0.32	16.18
Mix 7b.8PP	2.20	0.046	1.56	0.71	16.24

The LOP of Mix 3b was higher than that of Mix 7b, which indicates that the LOP of geopolymer concrete is related to its compressive strength. The amount of fibres in the matrix did not have a significant influence on the LOP of the geopolymer concrete, although there was a slight increase in strength when the fibre volume increased. According to Hsie et al. (2008), fibres do not have a significant influence on the elastic region (before cracking) of concrete and therefore the flexural strength of the geopolymer concrete is not likely to be influenced.

Neither the compressive strength nor the fibre volume had an influence on the deflection at LOP, although the higher fibre volume mixes showed a slightly higher deflection.

The equivalent flexural strength of Mix 3b was higher than that of Mix 7b. This result indicates that the bond strength between the fibres may be influenced by the compressive strength of geopolymer concrete.

Mix 7b obtained higher R_{e3} values than that Mix 3b. The R_{e3} value of the geopolymer concrete increased when more fibres were added to the matrix. This result is mainly due to a higher equivalent flexural strength provided by the larger amount of fibres.

As shown in Figures A.1 to A.4, the stress distribution of the higher fibre volume PFRGC mixes was better compared to that of the lower volume fibre specimens. After the LOP have been reached, the lower volume PFRGC specimens showed a steeper and quicker decrease in strength compared to the higher volume PFRGC. This result is illustrated by the "sharper" point at LOP on the graph.

ii. Steel fibre reinforced geopolymer concrete

It was more challenging to determine the LOP of a specimen when the stress-deflection curve showed deflection-hardening behaviour. It is considered as perfect deflection-hardening when there is no clear indication of a decrease in strength after the first crack. Thus, a LOP value and its corresponding deflection was estimated and used as the ultimate strength before the first crack. As mentioned, the LOP is the ultimate elastic stress that the specimen can withstand before cracking. This estimation is graphically shown in Figure 6.27.

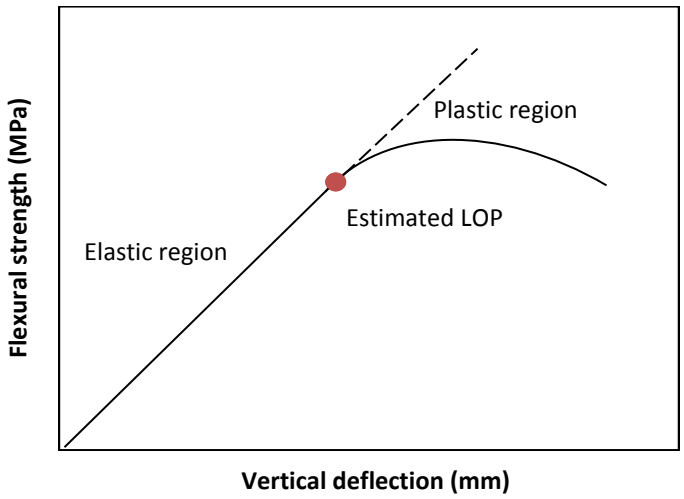

Figure 6.27: Example of the LOP value estimation in a deflection-hardening load-deflection curve

The properties of the SFRGC are shown in Table 6.3. The LOP of Mix 3b was higher than the LOP of Mix 7b. This trend is similar to the results found for the PFRGC. The equivalent flexural strength of the geopolymer concrete increased when more steel fibres were added to the matrix. Mix 3b showed a higher equivalent flexural strength compared to Mix 7b. Thus, the flexural strength and the equivalent flexural strength of the geopolymer concrete are related to the compressive strength.

The R_{e3} values for the specimens of Mix 3b were lower than that of Mix 7b. This results show a similar trend found for the PFRGC in which the lower strength geopolymer concrete yielded higher R_{e3} values.

Table 6.3: Properties of higher strength SFRGC and lower strength SFRGC

Mix Name	Limit of proportionality (MPa)	δ at LOP (mm)	Equivalent flexural strength $F_{e,3}$ (MPa)	R_{e3}	Compressive strength (MPa)
Mix 3b.4S	3.72	0.066	1.81	0.48	56.05
Mix3b.8S	3.89	0.068	3.08	0.81	53.62
Mix 7b.4S	2.36	0.026	1.57	0.68	21.28
Mix 7b.8S	2.68	0.034	2.51	0.94	21.20

An example of the fibre distribution in a specimen of Mix 7b.8S and Mix 7b.4S is shown in Figure 6.28. The figure clearly shows that the fibres in Mix 7b.8S are significantly more than the fibres in Mix 7b.4S and better distributed. Segregation of the steel fibres was observed for some of the specimens of Mix 7b.4S. It must be noted that segregation was not observed for all of the specimens as there was mainly two specimens (green and red line in Figure A.9) that showed signs of probable segregation. The results of these two specimens were not included in the calculations.

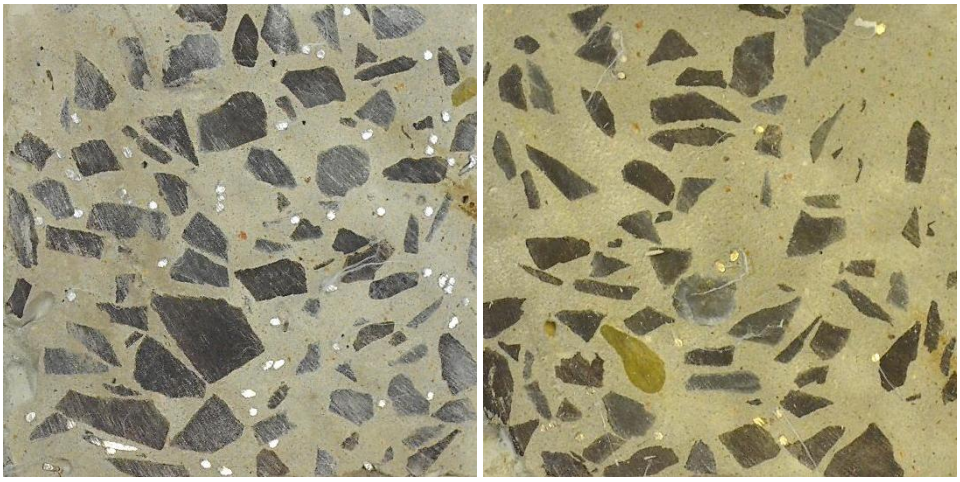

Figure 6.28: Mix 7b.8S (Left) and Mix 7b.4S (Right)

iii. Concluding summary

The ductility of fibre reinforced geopolymer concrete was improved when fibres were added to the matrix. The same trend was found for both fibre types. Neither the fibre volume nor fibre type had a significant influence on the LOP of the geopolymer concrete although the SFRGC obtained a higher LOP values than the PFRGC.

Higher equivalent flexural strengths were obtained for the specimens that obtained steel fibres compared to the addition of polypropylene fibres. The equivalent flexural strength increased when more fibres were added to the matrix.

There was no significant influence on the deflection, corresponding to the LOP, when fibres were added to the matrix, although a slightly higher deflection was found for the specimens that contained a larger amount of fibres.

The results of the three point bending tests for the PFRGC showed a lower coefficient of variance compared to that of the SFRGC. This result is clearly shown in the respective figures (Figures A.1 to A.10) in which the steel fibre graphs are more scattered compared to the polypropylene fibre graphs. A possible explanation for the higher variance is due to the fibre pull-out behaviour of steel fibres. The hooked end of the steel fibre may cause the fibre to pull out differently, depending on the environment surrounding it. The coarse aggregates can anchor the hooked end of the fibre, resulting in a higher pull-out resistance.

6.4.1.2. Fibre reinforced geopolymer concrete vs. fibre reinforced OPC concrete

The three point bending test results of a similar strength fibre reinforced fly ash/slag based geopolymer concrete specimen and a fibre reinforced OPC concrete specimen are compared in the following section. Steel and polypropylene fibres were added to the respective mixes at two different dosages (0.4% and 0.8% by volume).

i. PFRGC vs. PFROC

Table 6.4 shows the properties of the PFRGC and the PFROC.

Table 6.4: Properties of the PFRGC and PFROC

Mix Name	Limit of proportionality (MPa)	δ at LOP (mm)	Equivalent flexural strength $F_{e,3}$ (MPa)	R_{e3}	Compressive strength (MPa)
Mix 7b.4PP	2.06	0.039	0.65	0.32	16.18
Mix 7b.8PP	2.20	0.046	1.56	0.71	16.24
Mix 7-OPC.4PP	2.97	0.015	0.96	0.32	16.29
Mix 7-OPC.8PP	3.08	0.016	2.05	0.67	16.48

The LOP of the PFROC concrete was higher than that of the PFRGC for both fibre volumes. This result indicates that, for these specific mixes, the flexural strength of the OPC concrete is higher than that of the geopolymer concrete when polypropylene fibres are added to the matrix. The equivalent flexural strength of the PFROC was also higher than that of the PFRGC for both fibre volumes.

The fact that the R_{e3} values are similar, indicates that the ratio of LOP and equivalent flexural strength are the same for the two concrete types. The vertical deflection, at LOP, was approximately 3 times larger for the PFRGC specimens compared to that of the PFROC specimens. Thus, it is clear that the OPC concrete is much stiffer than the geopolymer concrete. This result confirms the low modulus of elasticity of the fly ash/slag based geopolymer concrete as discussed in Section 6.3.

As shown in the load-deflection curves of Figures A.5 and A.6, the PFROC did not have a smooth deflection-softening curve like most of the PFRGC specimens. The graphs show a slight increase in strength followed by a significant drop before increasing again. Mix 7-OPC.4PP showed rapid but smaller changes in strength while Mix 7-OPC.8PP had more gradual but larger changes in strength. The significant drop in strength is due to the rupture of the fibres. The same result was observed for Mix 7b.8PP.

ii. SFRGC vs. SFROC

The properties of the SFRGC and the SFROC are shown in Table 6.5.

Table 6.5: Properties of SFRGC and SFROC

Mix Name	Limit of proportionality (MPa)	δ at LOP (mm)	Equivalent flexural strength $F_{e,3}$ (MPa)	R_{e3}	Compressive strength (MPa)
Mix 7b.4S	2.36	0.026	1.57	0.68	21.28
Mix 7b.8S	2.68	0.034	2.51	0.94	21.20
Mix 7-OPC.4S	3.16	0.031	2.21	0.68	17.92
Mix 7-OPC.8S	3.17	0.030	2.88	0.92	18.97

Although the compressive strengths were slightly higher for the SFRGC, the LOP and the equivalent flexural strength of the SFROC was higher than that of the SFRGC. The R_{e3} values were similar for the two concrete types, for both fibre volumes.

The deflection corresponding to the LOP was similar for both the SFRGC and SFROC specimens. Neither the fibres nor the flexural strength influenced the deflection corresponding to LOP.

It must be noted that the LOP value was estimated for the majority of the specimens (geopolymer concrete and OPC concrete). According to RILEM TC 163 (2002) the LOP value of a steel fibre reinforced concrete specimen must be taken either as the value where the gradient of the graph is zero (peak value) or the highest value up until a vertical deflection of 0.05 mm. For the purpose of comparing the two concrete types it was decided to estimate the value closest to where the first crack appeared, rather than taking the values corresponding to a deflection of 0.05 mm. This estimation explains the similar deflection, as it was difficult to accurately pin point the LOP value.

iii. Concluding summary

OPC concrete yielded better flexural properties compared to the fly ash/slag based geopolymer concrete with the same compressive strength. The LOP and the equivalent flexural strength were higher for the FROC specimens, for both fibre volumes and fibre types. The R_{e3} values were similar which indicate that the ratio between the LOP and the equivalent flexural strength is similar for the two concrete types when fibres are added to the matrix.

The deflection at LOP were significantly lower for the OPC concrete specimens containing polypropylene fibres, compared to the corresponding geopolymer concrete specimens. This result indicates that OPC concrete is much stiffer than the fly ash/slag based geopolymer concrete. The deflection corresponding to the specimens containing steel fibres were inadequate to compare due to the estimation of the LOP value.

It must be noted that only one mix design for each concrete type was investigated, making it difficult to draw an adequate comparison on the flexural properties between geopolymer concrete and OPC concrete. More research is required in this field.

6.4.1.3. Fibre reinforced concrete vs. unreinforced concrete

Beam specimens without any fibres were cast for the two fly ash/slag based geopolymer concrete mix designs (high strength and low strength) to compare the flexural behaviour of unreinforced geopolymer concrete and fibre reinforced geopolymer concrete. Unreinforced OPC concrete specimens were also cast to compare the ductility improvement between geopolymer concrete and OPC concrete when fibres are added to the matrix. The results of the LOP, the energy absorption and compressive strength of the respective specimens are shown in the following section.

As mentioned in Section 4.7 (clear area on Figure 4.4), the energy absorption of unreinforced concrete is determined as the LOP force times by a value of 0.3. This value was taken as an estimate of the typical energy absorption of unreinforced concrete.

i. Polypropylene fibre reinforced concrete vs. unreinforced concrete

The properties of the unreinforced concrete specimens and the polypropylene fibre reinforced concrete specimens are shown in Table 6.6. The LOP of the unreinforced geopolymer concrete was higher than both the corresponding PFRGC mixes (Mix 3b and Mix 7b) while the LOP of the unreinforced OPC concrete was lower than the corresponding PFROC mix (Mix 7-OPC). In both cases the unreinforced geopolymer concrete mixes yielded a higher LOP than any of the fibre reinforced mixes. However, the LOP increased slightly when the fibre volume in both geopolymer matrices increased. There was a clear increase in LOP when more polypropylene fibres were added to the OPC concrete matrix.

Table 6.6: Polypropylene fibre reinforced concrete vs. unreinforced concrete

Mix name	Limit of proportionality (MPa)	Energy absorption (J)	Compressive strength (MPa)
Mix 3b	4.01	1.85	53.30
Mix 3b.4PP	3.40	7.94	49.01
Mix3b.8PP	3.56	13.63	49.69
Mix 7b	2.24	1.03	18.65
Mix 7b.4PP	2.06	5.10	16.18
Mix 7b.8PP	2.21	12.74	16.24
Mix 7-OPC	2.83	1.33	18.52
Mix 7-OPC.4PP	2.97	7.54	16.29
Mix 7-OPC.8PP	3.08	15.77	16.48

The energy absorption was significantly influenced by the fibres. The same trend was found for all the mix designs (geopolymer concrete and OPC concrete) in which the energy absorption increased significantly when polypropylene fibres were added to the respective matrices. The compressive strength of the respective specimens (geopolymer concrete and OPC concrete) did not influence the energy absorption. This is proved by the similar energy absorption of Mix 3b and Mix 7b for both fibre volumes. The OPC concrete yielded a slightly higher energy absorption compared to the geopolymer concrete mix.

ii. Steel fibre reinforced concrete vs. unreinforced concrete

The properties of unreinforced concrete and steel fibre reinforced concrete are shown in Table 6.7. The addition of steel fibres did not significantly influence the LOP of both concrete types. However, the lower strength mixes (Mix 7b and Mix 7-OPC) yielded a higher LOP value when steel fibres were added to the matrix. Mix 3b showed contradictory results as the unreinforced concrete specimens yielded the highest LOP.

Table 6.7: Steel fibre reinforced concrete vs. unreinforced concrete

Mix name	Limit of proportionality (MPa)	Energy absorption (J)	Compressive strength (MPa)
Mix 3b	4.01	1.85	53.30
Mix 3b.4S	3.72	14.16	56.05
Mix3b.8S	3.82	27.43	53.62
Mix 7b	2.24	1.03	18.65
Mix 7b.4S	2.36	12.26	21.28
Mix 7b.8S	2.68	19.64	21.20
Mix 7-OPC	2.83	1.33	18.52
Mix 7-OPC.4S	3.16	17.09	17.92
Mix 7-OPC.8S	3.17	22.24	18.97

The energy absorption was again significantly influenced by the fibres. A clear increase in energy absorption was found when the fibre volume increased in both the geopolymer concrete specimens and the OPC concrete specimens.

The energy absorption was significantly higher for Mix 3b.8S (higher strength geopolymer concrete) compared to Mix 7b.8S and Mix 7-OPC.8S (both lower strengths), which indicate that the compressive strength does have an influence on the energy absorption when a large amount of steel fibres are present in the matrix. Note that the results of the specimens with 0.4% by volume did not show the same trend. This may be due to the inadequate amount of steel fibre distribution over the whole cross section. The results of the three specimens that contained the lower volume fibres were also much closer compared to the results of the specimens which contained more steel fibres.

A possible explanation is due to the geometry of the fibre. The hooked end of the steel fibre will provide better pull-out resistance when the matrix has a stronger bond, mainly due to better anchorage, as it will be more difficult for the fibre to deform in the stronger matrix. The specimens, containing polypropylene fibres, showed a similar increase in energy absorption for the higher strength and lower strength geopolymer concrete specimens. The polypropylene fibres are relatively straight compared to the hooked end steel fibres, providing overall less pull-out resistance. This explains why the steel fibres may show a higher increase in energy absorption in the specimens of the higher strength geopolymer concrete.

iii. Concluding summary

The flexural strength (LOP) of both the geopolymer concrete and OPC concrete was not significantly influenced when fibres (steel or polypropylene) were added to the matrix. However, the energy absorption of the both concrete types increased significantly with the addition of fibres. The compressive strength only influenced the energy absorption when a large amount of steel fibres were added to the matrix.

6.4.2. Round Panel test results

The round panel tests were carried out to determine the energy absorption, provided by the fibres, after the concrete had cracked. The same mix designs as used for the three point bending tests were used for the round panel tests, i.e. two geopolymer concrete mixes and one OPC concrete mix. The results of the round panel tests are presented in the following sections.

A vertical deflection of 40 mm was obtained for all the specimens to evaluate the performance of FRC for applications where large cracks can be tolerated (ASTM C1550 2012). The majority of the round panel specimens had the same crack pattern as shown in Figure 6.29. After failure, the panel will crack at angles of approximately 120º apart. This type of failure pattern consumes the least amount of energy, due to the type of support structure (Bernard and Pircher 2000).

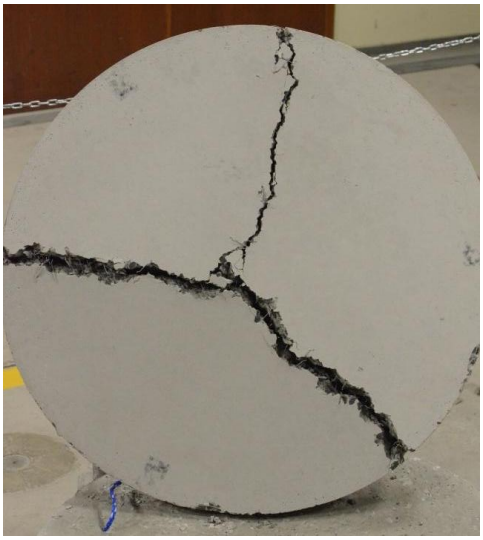

Figure 6.29: Crack pattern of the panels

Deflection-softening behaviour was found for all the specimens and an example of a load-deflection curve is shown in Figure 6.30.

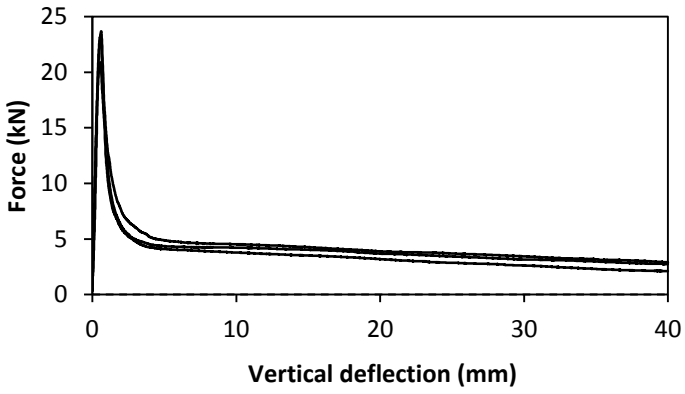

Figure 6.30: Example of a load-deflection curve of a round panel test

The results of all the panel tests are shown in Figure A.16 to Figure A.31 in the appendix.

6.4.2.1. Higher strength FRGC vs. lower strength FRGC

The results of the two fibre reinforced geopolymer concrete mixes (higher strength and lower strength) are discussed in the following section. Steel- and polypropylene fibres were added to the respective mixes at two different dosages (0.4% and 0.8% by volume).

i. Polypropylene fibre reinforced geopolymer concrete

The round panel test results of the PFRGC specimens are shown in Table 6.8. The LOP and the energy absorption of Mix 3b, for both fibre volumes, were higher compared to that of Mix 7b. This result again indicates that the flexural strength relates to the compressive strength of the geopolymer concrete. The deflection, corresponding to the LOP, was also higher for the specimens of Mix 3b. The

LOP showed a slight decrease in strength when more fibres were added to the matrix, while there was no significant difference in the deflection.

Table 6.8: Properties of higher strength PFRGC and lower strength PFRGC

Mix Name	Limit of proportionality (kN)	δ at LOP (mm)	Energy absorption (J)	Compressive strength (MPa)
Mix 3b.4PP	22.63	0.581	161.51	49.01
Mix 3b.8PP	20.62	0.556	282.06	49.69
Mix 7b.4PP	15.24	0.325	143.44	16.18
Mix 7b.8PP	12.92	0.3	232.59	16.24

The majority of the graphs in the figures showed a relatively small variance except for one graph on the load-deflection curve of for Mix 7b.8PP (red line of Figure A.20) which was significantly higher than the rest. A possible explanation for the higher energy absorption is due to more fibres being distributed in the bottom part of the panel or at critical areas, providing better post crack resistance. This result was not included in the results.

ii. Steel fibre reinforced geopolymer concrete

The round panel test results of the SFRGC are shown in Table 6.9. The LOP and the energy absorption were again higher for the specimens of Mix 3b compared to Mix 7b.

Table 6.9: Properties of higher strength SFRGC and lower strength SFRGC

Mix Name	Limit of proportionality (kN)	δ at LOP (mm)	Energy absorption (J)	Compressive strength (MPa)
Mix 3b.4S	22.69	0.500	224.89	56.05
Mix 3b.8S	20.94	0.867	393.88	53.62
Mix 7b.4S	17.10	0.394	200.86	21.28
Mix 7b.8S	18.44	0.923	309.83	21.20

The deflection corresponding to the LOP increased when the fibre volume increased. As shown in Figures A.23 to A.26, the load distribution before and after the LOP was better for the higher fibre volumes. The graphs of the lower fibre volume specimens had a “sharper” peak compared to the specimens that contained the higher volume of fibres. This result explains the higher vertical deflection obtained at the LOP for the larger volume fibres.

iii. Concluding summary

The LOP of the various mix designs was significantly influenced by the compressive strength of the geopolymer concrete. The specimens with a higher compressive strength yielded higher LOP values. The LOP of Mix 7b improved when the polypropylene fibres were replaced by steel fibres, while there was no influence for Mix 3b. The deflection corresponding to the LOP increased when more

steel fibres were added to the matrix, while there was no significant influence on the deflection for the specimens that contained polypropylene fibres. An overall increase in energy absorption was found when more fibres were added to the matrix. The compressive strength only influenced the energy absorption when the specimens contained the higher volume steel fibres.

6.4.2.2. Fibre reinforced geopolymer concrete vs. fibre reinforced OPC concrete

The round panel test results of a similar strength fibre reinforced fly ash/slag based geopolymer concrete specimen and a fibre reinforced OPC concrete specimen are compared in the following section. Steel and polypropylene fibres were added to the respective mixes at two different dosages (0.4% and 0.8% by volume).

i. PFRGC vs. PFROC

The results of the two concrete types are shown in Table 6.10. Regardless of their similar compressive strengths, the LOP of the PFROC was higher compared to that of the PFRGC, for both fibre volumes. The deflection corresponding to the LOP was similar for both types of concrete. This result is contradictory to the three point bending tests in which the PFROC specimens yielded a significantly lower deflection at LOP.

The energy absorption of Mix 7b.4PP was slightly higher than that of Mix 7-OPC.4PP while Mix 7-OPC.8PP yielded higher energy absorption compared to Mix 7b.8PP.

Table 6.10: Properties of PFRGC and PFROC

Mix Name	Limit of proportionality (kN)	δ at LOP (mm)	Energy absorption (J)	Compressive strength (MPa)
Mix 7b.4PP	15.24	0.33	143.44	16.18
Mix 7b.8PP	12.92	0.30	232.59	16.24
Mix 7-OPC.4PP	18.86	0.31	140.44	16.29
Mix 7-OPC.8PP	18.79	0.29	263.29	16.48

ii. SFRGC vs. SFROC

The results of the two types of concrete are shown in Table 6.11. The LOP of the SFROC, for both fibre volumes, was again higher than that of the SFRGC. The deflection of the SFRGC at the LOP increased when more fibres were added to the matrix. This result was not found for the SFROC, which may indicate that the stress distribution at the ultimate load was better for the SFRGC. This result is illustrated in Figure A.26, in the appendix, in which the peaks of the graphs are more "rounded" for Mix 7b.8S compared to the sharper peaks of Mix 7-OPC.8S as shown in Figure A.28.

The SFROC specimen, containing the lower volume fibres (Mix 7-OPC.4S), yielded higher energy absorption than the SFRGC specimen (Mix 7b.4S), while opposite results were observed for the higher volume fibre specimens.

Table 6.11: Properties of SFRGC and SFROC

Mix Name	Limit of proportionality (kN)	δ at LOP (mm)	Energy absorption (J)	Compressive strength (MPa)
Mix 7b.4S	17.10	0.394	200.86	21.28
Mix 7b.8S	18.44	0.923	309.83	21.20
Mix 7-OPC.4S	20.25	0.304	238.52	17.92
Mix 7-OPC.8S	22.10	0.311	296.81	18.97

iii. Concluding summary

The OPC concrete yielded overall higher LOP values compared to geopolymer concrete, for both fibre volumes. The deflection corresponding to the LOP was fairly similar except for Mix 7b.8S which was larger than the rest. The energy absorption was fairly similar for the two concrete types, although the OPC concrete specimens yielded the highest energy absorption for the majority of the specimens.

6.4.2.3. Fibre reinforced concrete vs. unreinforced concrete

Unreinforced fly ash/slag based geopolymer concrete round panels (both higher strength and lower strength) and a corresponding lower strength unreinforced OPC concrete round panel were tested. The only comparison available between unreinforced concrete and FRC was the LOP and the deflection corresponding to the LOP. The results are shown in the following section.

i. Polypropylene fibre reinforced concrete vs. unreinforced concrete

The properties of the unreinforced concrete and PFRC specimens are shown in Table 6.12. The LOP of the unreinforced concrete specimens and PFRC specimens were fairly similar although the unreinforced concrete specimens of Mix 3b yielded slightly higher strengths. The deflection at LOP increased when fibres were added to both the geopolymer concrete mixes and the OPC mix. This result is due to the stress distribution provided by the fibres.

Table 6.12: Polypropylene fibre reinforced concrete vs. unreinforced concrete

Mix Name	Limit of proportionality (kN)	δ at LOP (mm)	Compressive strength (MPa)
Mix 3b	23.86	0.382	53.30
Mix 3b.4PP	22.63	0.581	49.01
Mix 3b.8PP	20.62	0.556	49.69
Mix 7b	14.24	0.282	18.65
Mix 7b.4PP	15.24	0.325	16.18
Mix 7b.8PP	12.92	0.300	16.24
Mix 7-OPC	19.05	0.247	18.52
Mix 7-OPC.4PP	18.86	0.310	16.29
Mix 7-OPC.8PP	18.79	0.290	16.48

i. Steel fibre reinforced concrete vs. unreinforced concrete

The properties of the unreinforced concrete and SFRC specimens are shown in Table 6.13. The LOP of the two lower strength concrete mixes (Mix 7b and Mix 7-OPC) increased, when fibres were added to the matrix, while a decrease in LOP was found for Mix 3b. The same result was found for the three point bending tests in which the addition of steel fibres increased the LOP for both the lower strength geopolymer concrete and the OPC concrete.

The deflection at LOP increased for both concrete types when steel fibres were added.

Table 6.13: Steel fibre reinforced concrete vs. unreinforced concrete

Mix Name	Limit of proportionality (kN)	δ at LOP (mm)	Compressive strength (MPa)
Mix 3b	23.86	0.382	53.30
Mix 3b.4S	22.69	0.500	56.05
Mix 3b.8S	20.94	0.867	53.62
Mix 7b	14.24	0.282	18.65
Mix 7b.4S	17.10	0.394	21.28
Mix 7b.8S	18.44	0.923	21.20
Mix 7-OPC	19.05	0.247	18.52
Mix 7-OPC.4S	20.25	0.304	17.92
Mix 7-OPC.8S	22.10	0.311	18.97

iii. Concluding summary

Compared to the unreinforced concrete, the LOP increased for the majority of SFRC specimens while there was no significant change when polypropylene fibres were added to the matrix. The deflection corresponding to the LOP increased when either steel or polypropylene fibres were added to the matrix. This result indicates that the fibres provide stress distribution at LOP, resulting in a rounder peak compared to a sharper peak found for the unreinforced concrete specimens.

6.5. Fibre pull-out test results

Fibre pull-out tests were conducted to obtain some information regarding the fibre to matrix interface. The fibre pull-out tests were only introductory to what can, in the future, be an important investigation. It was decided to only use an embedment length of 25 mm for all the tests.

The main focus of the fibre pull-out tests was to obtain the bond strength between the fibre and the specific concrete matrix. Steel- and polypropylene fibres were used respectively and four geopolymer concrete specimens were compared with four OPC concrete specimens. The comparison between the compressive strength and the fibre bond strength was investigated. Figure 6.31 illustrates the typical fibre pull-out behaviour of a polypropylene fibre (Figure 6.31a) and steel fibre respectively (Figure 6.31b).

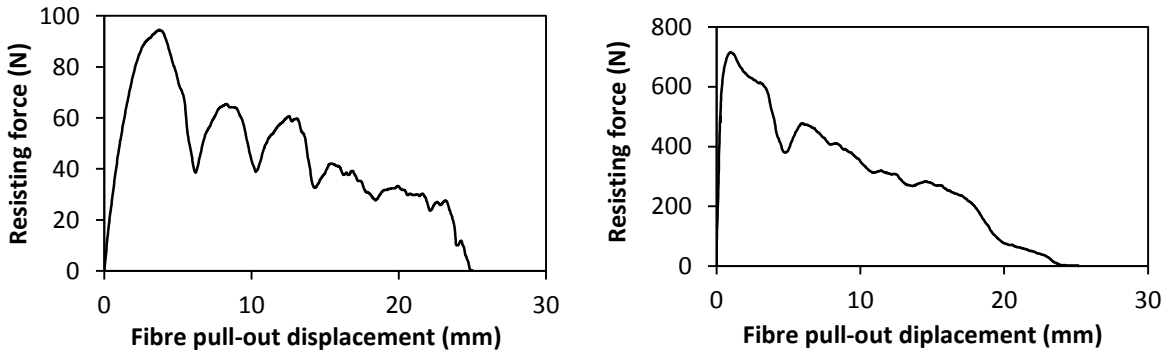

a) Polypropylene fibre pull-out behaviour **b) Steel fibre pull-out behaviour**

Figure 6.31: Fibre pull-out behaviour

A repeated sudden drop in strength followed by an increase was observed for the polypropylene fibre pull-out behaviour. This result is due to the fibre unravelling as shown Figure 6.33a. The unravelling of the fibre provides additional resistance against pull-out, causing the resisting pull-out force to increase. The unravelling of the fibre can be beneficial to fibre reinforced concrete if the majority of the fibres pull out successfully.

As indicated in Figure 6.31, the steel fibre provides a significantly higher pull-out resistance. This result is due to the hooked end of the steel fibre, providing additional anchorage. The tensile strength of the steel fibre is also significantly higher than that of the polypropylene fibre. As shown in Figure 6.31b, the graph reaches a maximum resistance, followed by a decrease in strength. The decrease in strength occurs when the first bend, of the two on each side of the fibre, straightens. After a certain deflection the strength starts to increase again. The second increase in strength is due to the second bend straightening. The straitening of the steel fibre is schematically illustrated in Figure 6.32.

Figure 6.33b illustrates the shape of the steel fibre after pull-out. The top fibre was pulled out of a high strength geopolymer concrete specimen (52.8 MPa) and the middle fibre was pulled out of a lower strength geopolymer concrete specimen (18.65 MPa). The bottom fibre is before any pull-out.

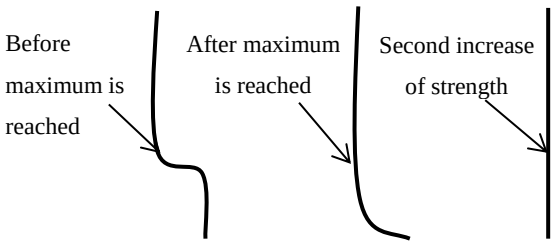

Figure 6.32: Schematically illustration of the bending of a steel fibre

a) Polypropylene fibres **b) Steel fibres**

Figure 6.33: Respective fibres after successful pull-out.

6.5.1. Polypropylene fibre pull-out results

The results of the polypropylene fibre pull-out tests are shown in Figure 6.34.

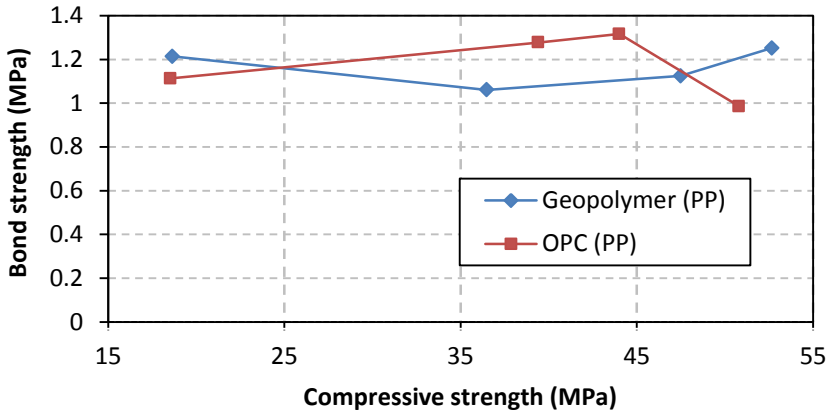

Figure 6.34: Results of the polypropylene fibre pull-out test

A strange result was found for the lower strength (18.65 MPa) geopolymer concrete specimen as it yielded an unexpected high bond strength. It must be noted, as shown in Figure 6.35, that a high percentage of fibre rupture occurred when the polypropylene fibre was pulled out of this specific specimen. However, the surface of geopolymer concrete specimens was significantly smooth and dense. This was particularly the case when the geopolymer concrete matrix contained a large amount of fly ash (more rounded particles and better compaction). The smooth and dense surface may have provided additional resistance against pull-out. Another explanation may be due to experimental error.

There was an increase in bond strength between the 36.5 MPa geopolymer concrete specimens and the 52.6 MPa geopolymer concrete specimens. The OPC concrete showed an increase in bond strength between compressive strengths of 18.5 MPa and 44 MPa, followed by a decrease in bond strength. The 50 MPa OPC concrete specimens only had one successful fibre pull-out and due to the large percentage of fibre rupture, it was difficult to explain the low bond strength. Note that when the fibres rupture, the bond strength is not measured anymore and the resisting force will be equal to the

tensile strength of the fibre. A possible explanation may be due to the high percentage of fibre rupturing.

The percentage of polypropylene fibre rupture for all the specimens is shown in Figure 6.35. The OPC concrete specimens yielded a better pull-out success rate, compared to the geopolymer concrete. The OPC concrete specimens also showed a more realistic fibre rupture trend. The percentage of rupture for the OPC concrete specimens was directly dependent of the respective compressive strength as more fibres ruptured when the compressive strength of the OPC concrete increased. This trend was not as clear for geopolymer concrete. A typical example of a polypropylene fibre that ruptured is shown in Figure 6.36.

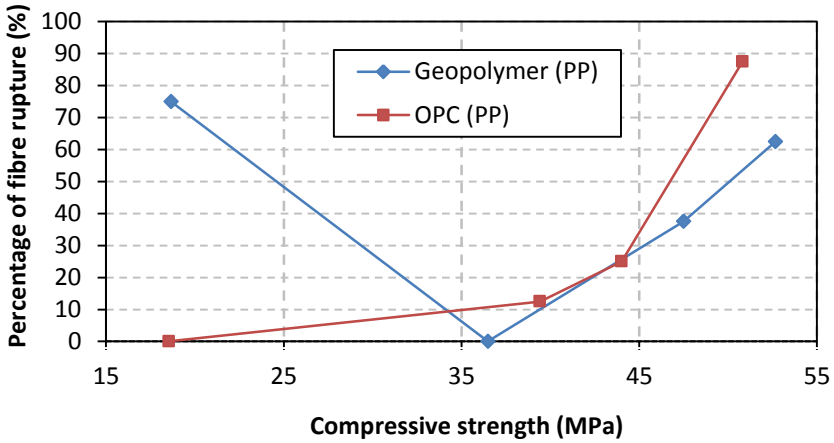

Figure 6.35: Percentage of polypropylene fibre rupture

The majority of the fibres ruptured near the fastening mechanism.

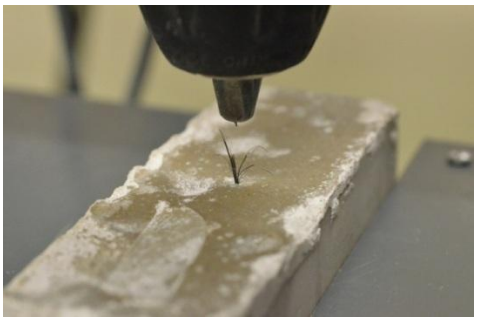

Figure 6.36: Polypropylene fibre rupture

6.5.2. Steel fibre pull-out results

The results of the steel fibre pull-out tests are shown in Figure 6.37. The percentage of fibre rupture is shown in Figure 6.38. The bond strength of the geopolymer concrete specimens was almost twice as high compared to that of the OPC concrete specimens.

The same trend, as for the polypropylene fibre pull-out tests, was found for the respective matrices. The lower strength (18.6 MPa) geopolymer concrete, again, obtained a relatively high bond strength, compared to the 36.5 MPa mix design. The bond strength decreased as the compressive strength increased form 18.6 MPa to 36.5 MPa followed by an increase up to a compressive strength of 52.6 MPa. This result shows some indication that the bond strength may be dependent to the compressive strength. As shown in Figure 6.38, the highest percentage of fibre rupture was 50% (four from eight) for the geopolymer concrete specimens. The polypropylene fibre- and the steel fibre pull-out specimens were cast from the same concrete batch and therefore the high bond strength observed for lower strength (18.6 MPa) geopolymer concrete specimens may also be due to experimental error.

An increase in bond strength was found for the OPC concrete specimens between a compressive strength of 18.5 MPa and 44 MPa followed by, again, a strange decrease for the 50 MPa mix design. The percentage of fibre rupture cannot be attributed to the low bond strength as only 25% (two from eight) of the steel fibres ruptured for the 50 MPa mix design, which indicates that the results obtained are fairly accurate in terms of the failure mechanism.

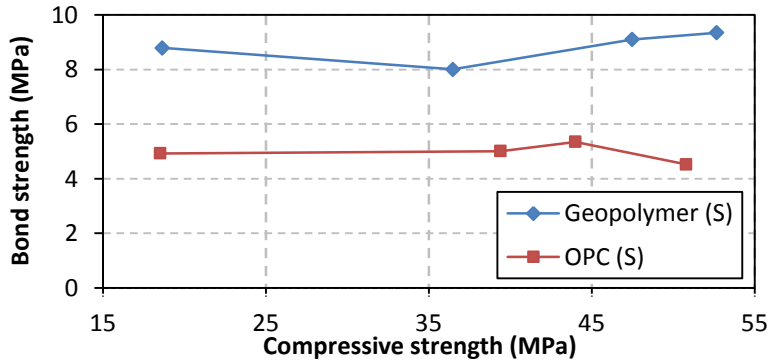

Figure 6.37: Results of the steel fibre pull-out test

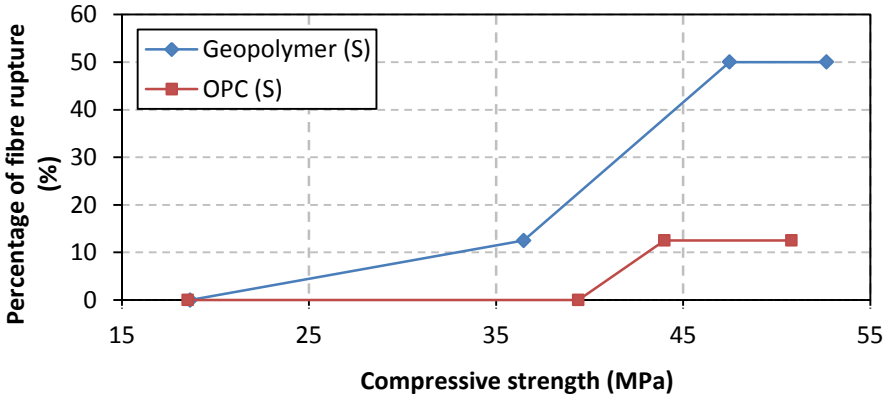

Figure 6.38: Percentage of steel fibre rupture

Overall, the percentage of fibre rupture was higher for the geopolymer concrete specimens. This result can be attributed to the fastening mechanism. Due to the higher force required to pull the steel fibre out of the geopolymer concrete, the fibre had to be gripped tighter than in the case of the OPC concrete specimens, causing the fibre to be more damaged. Due to the damaged caused to the fibre, more fibre rupture occurred. Note that the fibres had to be gripped tighter to prevent slipping. An example of a ruptured fibre is shown in Figure 6.40. The fastening mechanism must be improved in future studies to ensure that it does not have an influence on the results. All the steel fibres ruptured at the fastening mechanism.

Figure 6.40: Steel fibre rupture

6.5. 3. Concluding summary

The results of the fibre pull-out tests did provide some information regarding the fibre-matrix interface of the two concrete types. The geopolymer concrete specimens yielded significantly higher bond strengths when steel fibres were pulled out, while mixed results were found for the polypropylene fibre pull out. Overall, it was found that polypropylene fibres have the same bond strength in geopolymer concrete and OPC concrete, while the hooked end steel fibres had approximately double the bond strength in the geopolymer concrete compared to the OPC concrete.

The OPC concrete yielded slightly better pull-out behaviour for both the polypropylene fibre pull-out and steel fibre pull-out tests, as less fibres ruptured during pull-out. A relative trend was found between the bond strength and compressive strength of both the geopolymer concrete and the OPC concrete, with one outlier for each concrete type.

An embedment length of 25 mm proved to be slightly too deep as a significant amount of fibres, especially polypropylene, ruptured during the execution of tests. The higher strength geopolymer concrete and the lower strength geopolymer concrete showed a significant amount of fibre rupture. This result is not ideal fibre pull-out behaviour in concrete as it yields a lower energy absorption.

Various embedment lengths must be investigated to obtain the critical embedment length of the various fibres. However, the results obtained can act as introductory results which can be used to improve on. The steel fibre fastening mechanism must be improved to ensure that less damage is caused by the gripping device, while ensuring that slipping does not occur.

6.6. Setting time test results

Setting time tests were conducted on three specific fly ash/slag based geopolymer concrete mix designs. Mix 10a and Mix 3b had similar binder content, thus a good comparison was drawn on the influence of alkaline solution content on the setting time. Mix 3b and Mix 7b had the same alkaline solution content, thus a good comparison was drawn on the influence of slag content on the setting time of geopolymer concrete. Mix 10a contained no additional water in the matrix, thus a higher alkaline solution content. The two mixes of Phase B both contained additional water in the mix.

The results of the setting time tests are shown in Figure 6.41. The blue bar (bottom part of bar) represents the initial setting time while the red bar (top part of bar) represents the final setting time. The initial setting time corresponds to the top of the blue bar while the final setting time of a specific specimen corresponds to the top of the red bar.

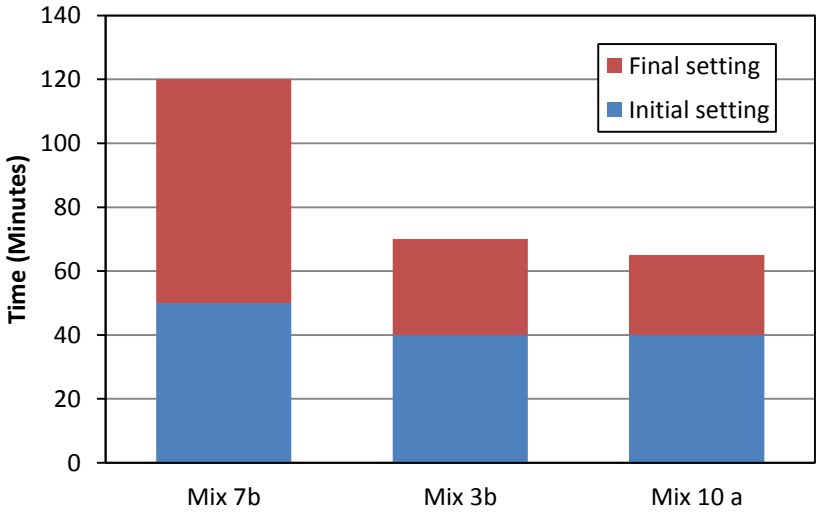

Figure 6.41: Setting time test results

The initial setting time of the three mixes was fairly similar, although Mix 7b (lower slag content) yielded a slightly longer initial setting time. Mix 10a and Mix 3b yielded the same initial setting time and very similar final setting times. The final setting time of Mix 3b was 70 minutes while the final setting time of Mix 10a was 65 minutes. The final setting time of Mix 7b was 120 minutes.

6.6.1. Concluding summary

The final setting time was significantly influenced by the slag content in the matrix. The increase in slag resulted in a quicker final setting time. The amount of alkaline solution in the matrix did not have

a significant influence on neither the initial- nor the final setting time of the fly ash/slag based geopolymer concrete. It must be noted that a limited amount of tests was done on the setting time of fly ash/slag based geopolymer concrete. This is certainly an area that needs to be investigated to obtain more knowledge regarding the rapid setting time of the fly ash/slag based geopolymer concrete.

6.7. Temperature development test results

The results of the temperature development tests are shown in Figure 6.42. The temperature development of three geopolymer specimens and one OPC concrete specimen were obtained. The results of the three geopolymer concrete mix designs ensured that the influence on the temperature development, due to the slag content and the alkaline content, could be obtained. The slag content investigation is presented by Mix 3b (40% slag content) and Mix 7b (23% slag content). The maximum curing temperature for Mix 3b was 21.7 ℃ and 19.5 ℃ for Mix 7b. The results confirm that the temperature development of the geopolymer concrete increase when slag is added to the matrix.

The influence of the alkaline liquid content on the curing temperature is presented by Mix 10a (298 kg alkaline solution) and Mix 3b (150 kg alkaline solution). The curing temperature increased when more alkaline solution was present in the matrix. The maximum temperature of Mix 10a was 25.4℃ compared to 21.7 ℃ of Mix 3b. Thus, a significant increase in temperature was observed when the alkaline solution increased. The measured peak temperature of Mix 10a was almost as high as that of the OPC concrete mix. This result indicates that the increase in temperature may be similar in geopolymer concrete containing a high slag content and high alkaline content, compared to that of OPC concrete.

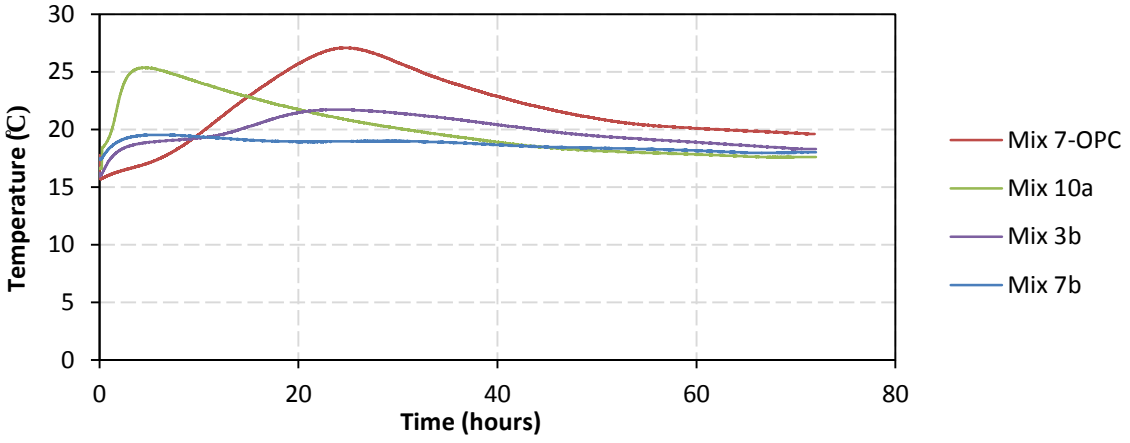

Figure 6.42: Temperature development during the initial hardening process

The time corresponding to the maximum temperature is shown in Table 6.14.

Table 6.14: Peak time of temperature development

Mix Name	Maximum Temperature (˚C)	Hours after casting
Mix 7b	19.52	4.37
Mix 3b	21.70	22.18
Mix 10a	25.35	4.18
Mix 3-OPC	27.08	24.12

The temperature development was different for the two concrete types. The majority of the geopolymer concrete specimens showed a steeper increase in temperature development compared to the more gradual increase of the OPC concrete specimen. Mix 10a (4hours and 12 minutes) and Mix 7b (4 hours and 18 minutes) reached their respective maximum temperatures in the first 5 hours after casting. Mix 3b reached its maximum after 22 hours while the OPC concrete specimen reached its maximum after 24 hours. The longer temperature development of Mix 3b may be due to less alkaline solution available to ensure a rapid dissolution process, as in the case of Mix 10a, resulting in a more gradual increase.

Large cracks were found on the surface of the specimens of Mix 10a while almost no cracks (few minor cracks) were observed on the specimens of Mix 3b. The binder content was very similar which may indicate that the rapid temperature development during curing had an influence on the size and amount of cracks formed on the geopolymer concrete surface. There were no cracks found on the cubes of Mix 7b. The temperature development of Mix 7b was the lowest.

6.7.1. Concluding summary

The curing temperature of fly ash/slag based geopolymer concrete was significantly influenced by the alkaline content and the slag content. The maximum temperature peak increased when either the slag or the alkaline liquid increased. The high temperatures may have contributed to the cracks formed on the surface of geopolymer concrete. The fact that the temperature increased when more slag was added to the matrix may indicate that heat was generated due to the hydration of slag.

The peak temperature time of the fly ash/slag based geopolymer concrete was significantly influenced by the amount of alkaline solution present in the matrix. The temperature development peak was reached faster when more alkaline solution was available for the dissolution process. It must be noted that limited tests was done and therefore more research is required in this field.

Chapter 7
Discussion

In this chapter, the experimental results as given in Chapter 6 are discussed. The objective of the workability tests, compressive tests, elastic modulus tests, setting time tests and temperature development tests was to obtain a better understanding of the mechanical properties of the fly ash/slag based geopolymer concrete. The objective of the three point bending tests and round panel tests was to obtain some information regarding the flexural behaviour and the ductility of the geopolymer concrete matrix when fibres were added. The objective of the fibre pull-out tests was to obtain some information regarding the fibre-matrix interface. The 7 to 28 day aging of the geopolymer concrete is discussed in this chapter. Lastly, all the problems that were experienced and dealt with during the course of the experimental study are discussed to ensure that these problems are avoided in the future.

The obvious trends that were found during the experimental study are discussed under their respective headings.

7.1. Mechanical properties of fly ash/slag based geopolymer concrete

The following section discusses all the information gathered regarding the mechanical properties, except the flexural behaviour, of fly ash/slag based geopolymer concrete. The mechanical properties includes the workability of the geopolymer concrete, compressive strength, modulus of elasticity, setting times, and temperature development of the geopolymer concrete during the initial stage of its curing process.

7.1.1. Workability

As stated in Section 6.1, the water, fly ash/slag content, sodium hydroxide concentration and the aggregate content influenced the workability. The compressive strength was significantly influenced when one of these parameters, except the aggregate content, were changed. The workability of the various mix designs is shown in Figures 7.1 and 7.2. The mixes of Phase A yielded an overall lower diameter slump reading than that of Phase B. This result is mainly due to the additional water in the mixes of Phase B. However, it was found that the fresh geopolymer concrete tends to segregate once the diameter slump reading was close to or more than 650 mm. It is recommended that the slump flow

must be in the rage of 600 ± 30 mm to ensure adequate self-compacting workability and to avoid segregation.

A conclusion can be drawn that fresh fly ash/slag based geopolymer concrete shows signs of self-compacting which, from a construction point of view, is promising. Careful attention must be given to ensure that the geopolymer concrete does not segregate. It was found that, although the diameter slump readings of some of the specimens were over 550 mm, their slump flow seemed to be relatively viscous and sticky as the flow ability tests took longer than usual. Note that the viscosity was not measured scientifically and this is an aspect that can be investigated in the future. This usually occurred when the fine aggregate to total aggregate ratio increased. This result is a logical trend as more fine materials are present in the matrix.

The strength of the geopolymer concrete was not significantly influenced when the aggregate content increased or decreased. However, the workability decreased when the amount of aggregates increased. This trend can be used to obtain a desired diameter slump reading, as one can simply increase the aggregate content if a lower slump is required or vice versa, without having a significant influence on the compressive strength.

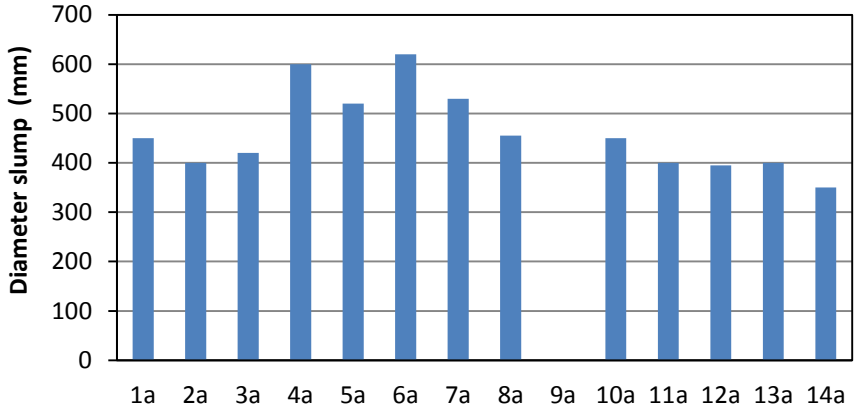

Figure 7.1: Geopolymer concrete workability of Phase A

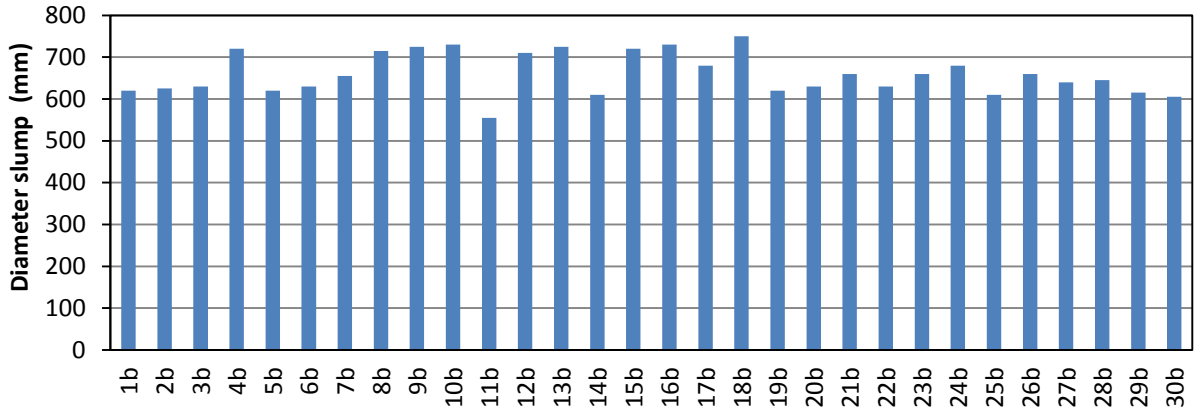

Figure 7.2: Geopolymer concrete workability of Phase B

7.1.2. Compressive strengths

In the following section, the results and observations found in Section 6.2 are discussed. The main goal was to obtain adequate geopolymer concrete strengths while investigating the influence that the various parameters, present in the matrix, had on the strength of the geopolymer concrete. As mentioned in Section 4.1.1, the average compressive strength of three cubes was taken as the strength for a specific mix design. Due to the small number of specimens used for the tests, no outlier was defined and the results of all three specimens were used. This result explains the large variation in some of the results. It is recommended that more cubes are tested per mix design in order to ensure enough results to accommodate for an outlier to be adopted and to determine whether a lower characteristic strength must be adopted for geopolymer concrete.

A total of nine different parameters were investigated including:

- Fly ash/slag content
- Binder
- Aggregate content
- Fine aggregate content
- Alkaline to binder ratio
- Sodium hydroxide concentration
- Sodium silicate to sodium hydroxide ratio
- Additional water in the matrix

7.1.2.1. Fly ash/slag content

Both the results obtained in Phase A and Phase B showed a similar trend regarding the slag content in the matrix. Higher compressive strengths were obtained when the slag content increased or the fly ash content decreased.

In most of the research investigated during the literature review, only low calcium based source materials, for example fly ash, metakaolin etc., were used as the binder. The curing process required heat activation in order to accelerate the geopolymerisation process. As described in Section 2.1.2, the low calcium based geopolymer concrete structure consists of only Si-O-Al bonds. The geopolymer concrete will not yield significant strengths or cure properly when low calcium based geopolymer concrete is cured at ambient temperature.

However, the geopolymer concrete type that was investigated in this study had a different hardening process due to the addition of corex slag in the matrix. When slag is alkali activated it forms calcium silicate hydrate gel in conjunction with geopolymeric gels. The CSH gel ensures that geopolymer concrete hardens at ambient temperature. The geopolymer concrete strength is also significantly higher compared to when low calcium based geopolymer concrete is cured at ambient temperatures.

Yip et al (2008) explained that the rapid hardening and strength gain of the geopolymer concrete is due to the CSH that is present in the fresh concrete, providing nucleation sites which trigger the geopolymer gel formation.

Thus, a possible explanation for the increase in strength, when slag is added or increased, is that more CSH gels form during the hardening process. A larger amount of CSH gels, present in the matrix, will ensure higher ambient temperature fly ash/slag based geopolymer concrete strengths. It must be noted that when adding corex slag to the matrix, the original geopolymer microstructure is hindered as the structure not only consist of an interaction between silicon and aluminium ions, but also the interaction of additional calcium ions.

The strength of the geopolymer concrete was also highly dependent on the concentration of the alkaline solution. It is argued that the alkali activation of the sodium aluminosilicate materials is the first step of the geopolymerisation process (Yip and Van Deventer 2003, Davidovits 2011). During a study done by Yip et al (2003), in which a microanalysis was conducted on CSH gel that forms within a geopolymeric binder, they concluded that the dissolution process is also the first step when slag and metakaolin was mixed together in an alkaline solution. Silicon and aluminium were dissolved from the surface of metakaolin, in this case fly ash, while silicon and calcium were dissolved from the slag. This explains the origin of additional calcium ions in the microstructure. They also concluded that the rate of dissolution of the two materials depended on the alkaline concentration. This conclusion confirms the statement that the strength of the geopolymer concrete was mainly influenced by the concentration of the alkaline activator.

The influence of the slag content on the compressive strength of all the mix designs is shown in Figure 7.3a and the same information regarding the fly ash is shown in Figure 7.3b. The “R-squared” value is given in each figure. If a clear trend is found, the “R-squared” value will be close to one. If no trend is found, the “R-squared” value will be close to zero. This value will be used to compare the influence of the various materials on the compressive strength of the geopolymer concrete. Note that linear regression was used. The “R-squared” value is significantly higher for the influence of slag content, which indicates that slag has a more significant influence on the compressive strength of fly ash/slag based geopolymer concrete compared to that of fly ash. This result is due to the slow rate of the dissolution process of fly ash in the absence of heat.

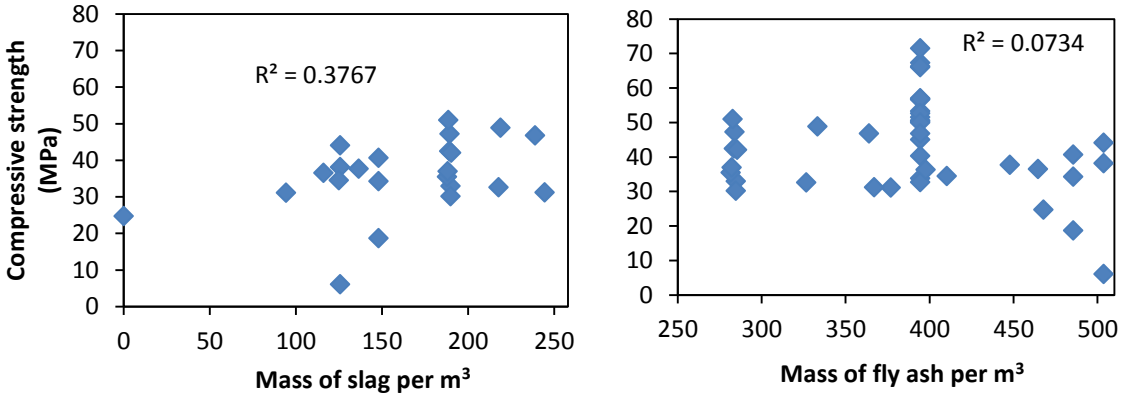

a) Mass of slag per m^3 of geopolymer concrete **b) Mass of slag per m^3 of geopolymer concrete**

Figure 7.3: Mass of binder vs. compressive strength

7.1.2.2. Binder to fine aggregate

From the results obtained in Phase B4 it is clear that the slag content has a significant influence on the compressive strength gain. A possible explanation for the difference in the two curves is that the dissolution process is not efficient enough, in ambient conditions, to yield promising strengths when the slag content is low. Thus, even by increasing the binder, the strength remains the same. For the higher slag content, higher strengths were obtained when the binder was increased. This result is due to more CSH gel that can precipitate during the dissolution process.

This investigation was another confirmation that the slag content in the matrix has an influence on the compressive strength of fly ash/slag based geopolymer concrete, cured at ambient temperatures.

7.1.2.3. Aggregate content

The aggregate content did not have a significant influence on the compressive strength of the geopolymer concrete. It must be noted that the alkaline solution to binder ratio remained the same. Thus, when the aggregate content increased, the alkaline solution and the binder content decreased and vice versa. This similar behaviour is observed in OPC concrete. In OPC concrete, the strength is determined by the water to binder ratio. Thus, when increasing the amount of aggregates in the mix and decreasing the water and cement, ensuring the same ratio, the OPC concrete strength is not influenced significantly.

This result is also observed in geopolymer concrete, although there is significantly more constituents and ratios that have to be kept constant to ensure that the strength does not change significantly when aggregates are added or subtracted. Thus, when the concentration of the sodium hydroxide is constant, the ratio between sodium hydroxide and sodium silicate is constant and the fly ash to slag ratio is constant, it is safe to conclude that the alkaline to binder ratio determines the compressive strength of the geopolymer concrete for a specific mix. However, this result is only valid if there is no additional water present in the matrix.

During a study done by Joseph and Mathew (2012) they found that the strength of the geopolymer concrete had a slight increase when the amount of aggregates increased. Although not by much, this was also experienced in this study.

Figure 7.4 shows the mass of aggregates versus the compressive strength in the various mixes. The mass of aggregates was fairly constant for all the mixes and therefore all the data points are mostly in vertical lines. The large variation in compressive strength for a certain mass of aggregates, indicates that the aggregates do not have a significant influence on the compressive strength of the geopolymer concrete. It can be seen from Figure 7.4 that the aggregates do not have a significant influence on the compressive strength of the geopolymer concrete.

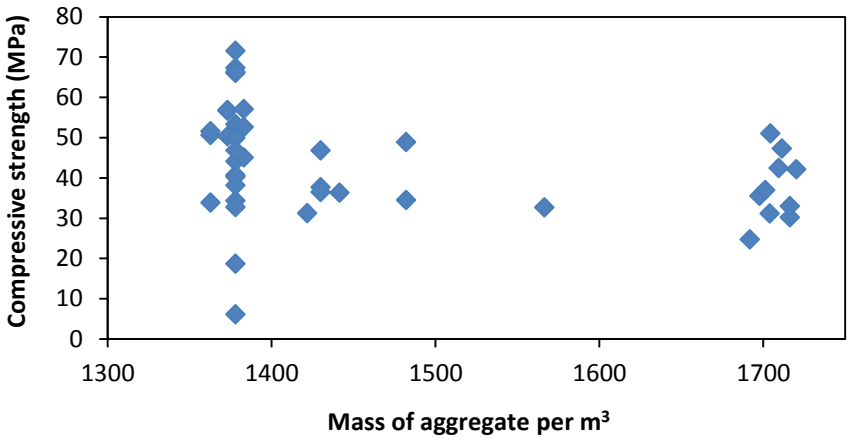

Figure 7.4: Mass of aggregate per m^3 of geopolymer concrete

7.1.2.4. Fine aggregate content to total aggregate ratio

The same trend was found in the results of Phase A4 and Phase B3 in which a peak value was obtained. According to Joseph and Mathew (2012) the behaviour is similar to OPC concrete. The ratio of fine aggregates to total aggregates plays a role in the binding properties and the optimum ratio yields the most efficient binding characteristics in the geopolymer concrete, resulting in the highest compression strength. Thus, with the specific type of sand and stone as used in this study, the highest peak was found when the ratio was between 0.40 and 0.45. The optimum fine aggregate to total aggregate ratio obtained by Joseph and Mathew (2012) was 0.35.

Overall the fine aggregate content, as shown in Figure 7.5, did not have a significant influence on the compressive strength of the geopolymer concrete.

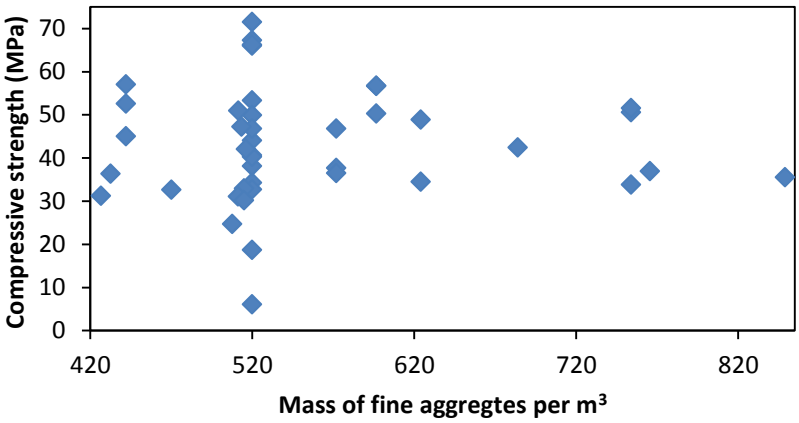

Figure 7.5: Mass of fine aggregate content per m^3 of geopolymer concrete

7.1.2.6. Alkaline to binder ratio

The results found in Phase A5 agree with that found by Joseph and Mathew (2012). The compressive strength of the geopolymer concrete decreased as the alkaline to binder ratio increased. Although the alkaline solution is the important aspect when considering the dissolution process, an adequate amount of aluminosilicate materials must be available to ensure that there is enough Si, Al and Ca ions to participate in the dissolution process. Thus, it is important to ensure that the ratio between the alkaline liquid and the binder is of such nature that it ensures an adequate dissolution process.

A problem considering this ratio is that the decrease in alkaline liquid results in a lower fresh geopolymer concrete workability, as less water is present in the matrix. Thus, an optimum ratio must be found that will ensure a good workability while yielding adequate compressive strengths.

The ratio becomes inadequate when additional water is added to the matrix. Even if the alkaline to binder ratio remains the same, the compressive strength decreases if additional water is added to the matrix.

However, the ratio can be adjusted to a liquid to binder ratio. The liquid then consists of the alkaline solution and the additional water, while the binder remains the same (fly ash and slag). Figure 7.6 shows the compressive strength corresponding to the liquid to binder ratio. An overall decrease in compressive strength was found when more liquid was added to the matrix. This ratio can adequately be used if the mass of sodium hydroxide solids and the mass of sodium silicate solids is constant.

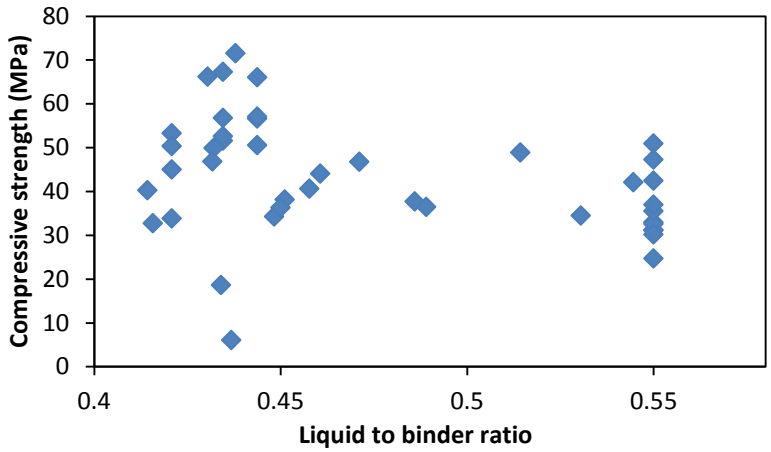

Figure 7.6: Influence of the liquid to binder ratio

7.1.2.7. Sodium hydroxide concentration

Similar results, regarding the sodium hydroxide solution, were obtained in Phase A6 and Phase B6. The compressive strength increased when the molarity of the sodium hydroxide concentration increased. This trend is familiar in the geopolymer research field and similar results are found by most researchers. The amount of sodium hydroxide solution and its concentration can be considered as the most important factor in the geopolymerisation process, as the hydroxide ions dissolves the aluminosilicate during the dissolution process. Therefore, it is of most importance to ensure that an adequate amount of hydroxide ions are available in the fresh concrete matrix.

The dissolution process dependents on the amount of sodium hydroxide and binder material present in the matrix. Joseph and Mathew (2012) concluded that an optimum amount of 10 M sodium hydroxide concentration yields the best results while the results of this study concludes that a molarity of 16 still yielded an increase in strength. The amount of binder material used in this study was significantly higher than the binder material used by Joseph and Mathew (2012). The binder in this study also included slag which was not present in the mixes designed by Joseph and Mathew (2012). Wallah et al. (2006) designed mixes containing sodium hydroxide solutions with a molarity of 14 M. Thus, it can be concluded that the optimum sodium hydroxide concentration depends on the amount of aluminosilicate materials that need to be dissolved.

A 8 M sodium hydroxide solution was used for the majority of the mixes in Phase B and according to the sodium hydroxide concentration trend, higher strengths can be obtained when the concentration is increased. It must be noticed that sodium hydroxide is a hazardous chemical and must be handled with safety equipment. The safety issues, regarding sodium hydroxide, must be taken into account when a concentration is chosen.

The compressive strength corresponding to mass of sodium hydroxide solution (Figure 7.7) and the compressive strength corresponding to the mass of sodium hydroxide solid flakes (Figure 7.8) are

shown. The mass of sodium hydroxide flakes may differ in a sodium hydroxide solution, depending on the concentration, and therefore it was decided to investigate the influence of only the sodium hydroxide flakes. The "R-squared" value is higher when only the mass of the sodium hydroxide flakes are taken into account. Thus, a better trend is found when only taking into account the mass of sodium hydroxide flakes in the alkaline solution.

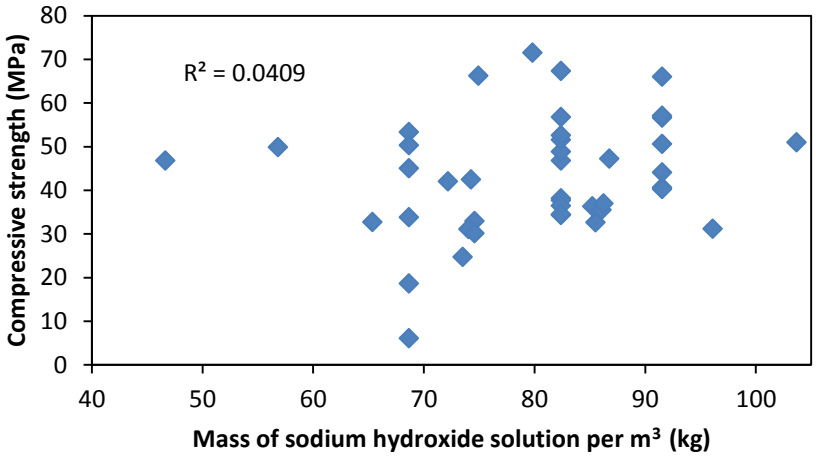

Figure 7.7: Mass of sodium hydroxide solution per m^3 of geopolymer concrete

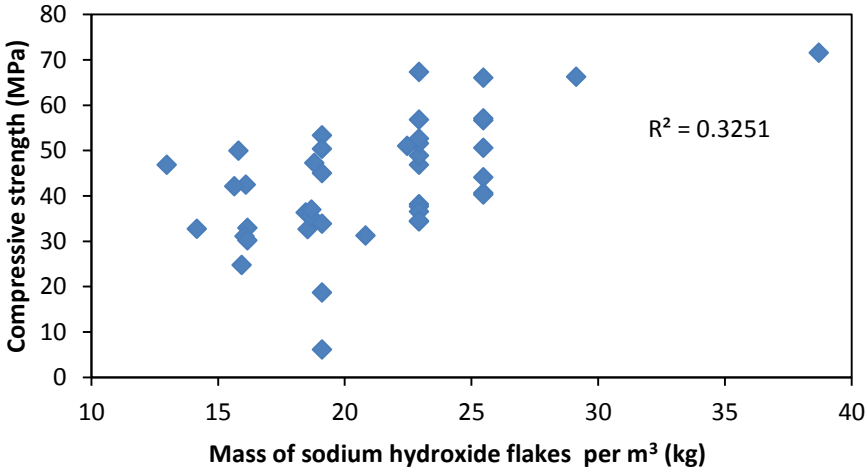

Figure 7.8: Mass of sodium hydroxide flakes per m^3 of geopolymer concrete

7.1.2.8. Sodium silicate to sodium hydroxide ratio

According to results found in previous studies, the optimum sodium silicate to sodium hydroxide ratio is approximately 2.5 (Joseph and Mathew 2012, Hardjito and Rangan 2005). However, the results found in both Phases A and B showed that the highest strength were yielded when a ratio of approximately 1 was used. A possible explanation for the lower value is due to the high aluminosilicate to sodium hydroxide ratio. Thus, the dissolution of the silicate and aluminate is inadequate, causing problems in the microstructure (Sagoe-Crentsil and Weng 2007). It must also be

noted that the value of 2.5 was used for geopolymer concrete with only fly ash as binder and it was heat cured. As mentioned, the geopolymerisation process changes when slag is added to the matrix.

The reason for the addition of sodium silicate in the matrix is to increase the silica content. Sodium hydroxide is required for the dissolution process and when the matrix has a high silica content, more sodium hydroxide is required to ensure an adequate geopolymerisation process. A low amount of sodium hydroxide solution in a matrix may lead to a less efficient dissolution process (Weng and Sagoe-Crentsil 2007, Sagoe-Crentsil and Weng 2007).

Figure 7.9 shows the influence of the sodium silicate to sodium hydroxide solution ratio on the compressive strength of the geopolymer concrete. Most of the mixes of Phase A had a sodium silicate to sodium hydroxide ratio of 2.5 while the ratio for most of the mixes of Phase B was 1.18. The large variation in compressive strength for these two values illustrates that the water and the binder also have a significant influence on the compressive strength. Regardless of the large variation in the two values, a trend is still noticalble, as the compressive strength decrease when the amount of sodium hydroxide solution decrease.

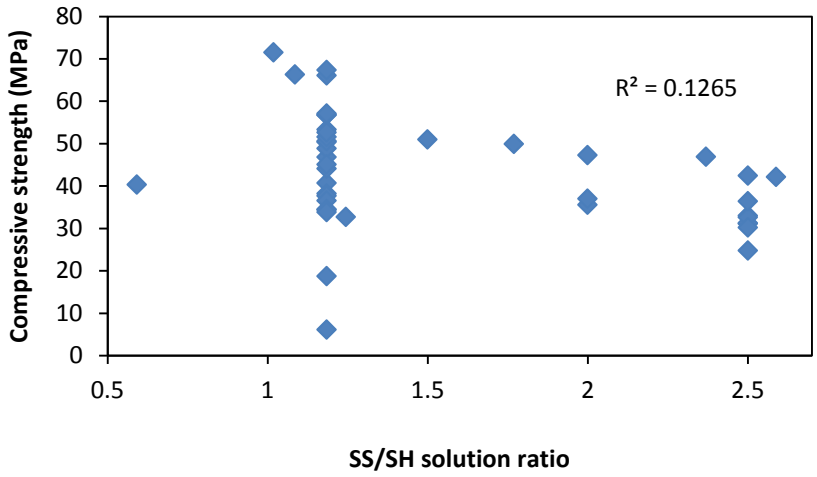

Figure 7.9: Influence of the sodium silicate to sodium hydroxide solution ratio

Figure 7.10 illustrates the ratio of only the mass of the solids in the respective solutions, thus no water was taken into account. There was no significant difference in the "R-squared" value when only the mass of solids were taken into account.

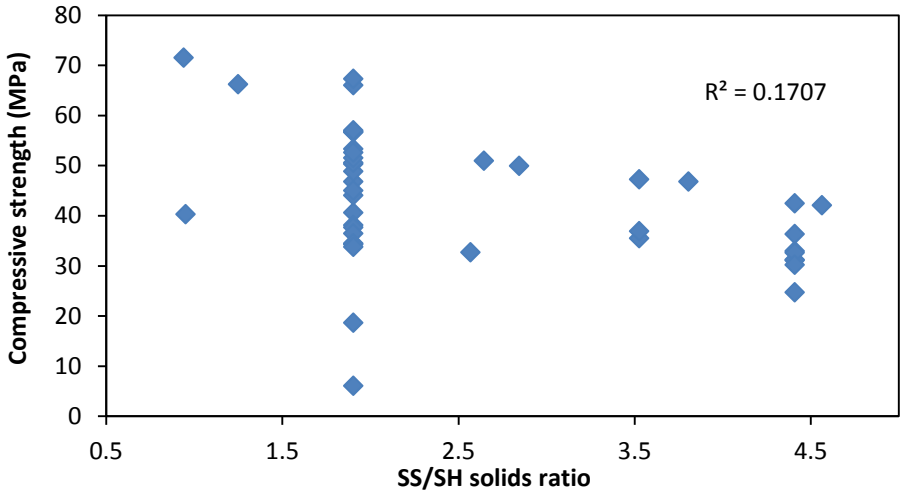

Figure 7.10: Influence of the sodium silicate to sodium hydroxide solids ratio

7.1.2.9. Mass of water in the matrix

The compressive strength, corresponding to the mass of water in the matrix, is shown in Figure 7.11 (Phase A) and in Figure 7.12 (Phase B). The reason for plotting the phases on different graphs is due to the additional water that was added to the mixes of Phase B. It is clear from the two figures that the additional water had a significant influence on the compressive strength of the geopolymer concrete, while the water in Phase A did not have a large influence. The mass of water includes the water present in the alkaline solution and the additional water, if any. This observation is also confirmed by the higher "R-squared" value for the mixes of Phase B.

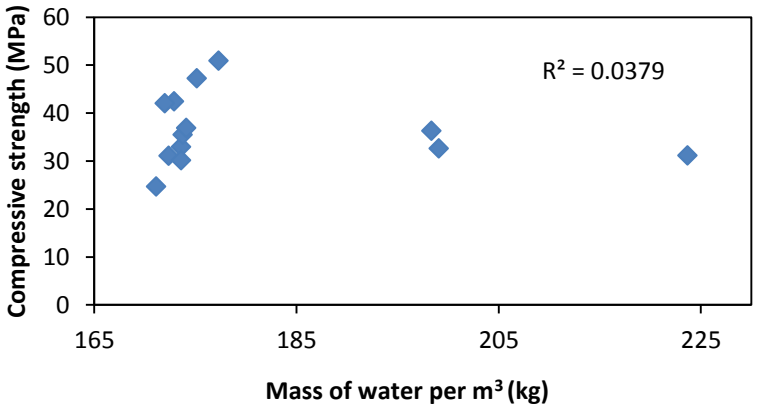

Figure 7.11: Mass of water per m^3 of geopolymer concrete for Phase A

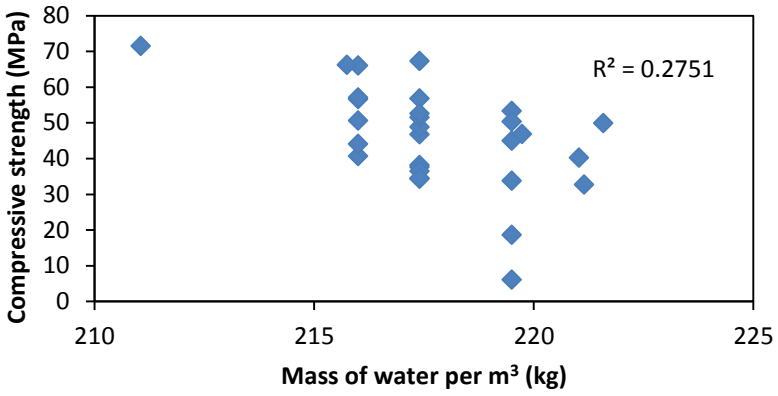

Figure 7.12: Mass of water per m^3 of geopolymer concrete for Phase B

7.1.2.10. Concluding summary

The compressive strength of the fly ash/slag based geopolymer concrete is mainly influenced by the slag content, additional water and mass of sodium hydroxide solids per m^3 of fly ash/slag based geopolymer concrete. The aggregate content did not have a significant influence on the compressive strength of the geopolymer concrete.

7.1.3. Modulus of elasticity

The results of Section 6.3 are discussed in the following section. The stiffness of concrete is an important aspect in the construction industry. The deflection of a concrete element is directly dependent on the stiffness of the concrete and a low stiffness yields large deflections when a load is applied.

According to the SANS 10100, the modulus of elasticity of OPC concrete is determined by taking into account the stiffness of the aggregates and the strength of the OPC concrete itself. The modulus of elasticity of OPC concrete, with certain strength, is shown in Table 7.1.

Table 7.1: Modulus of elasticity of normal-density OPC concrete (SANS-10100 2000)

Characteristic strength F_{cu} (MPa)	Static modulus E_c (GPa)
20	25
25	26
30	28
40	31
50	34
60	36

Figure 7.13 indicates that the elastic modulus of geopolymer concrete is also relatively influenced by the compressive strength. However, the fly ash/slag based geopolymer concrete showed significantly lower stiffness compared to OPC concrete.

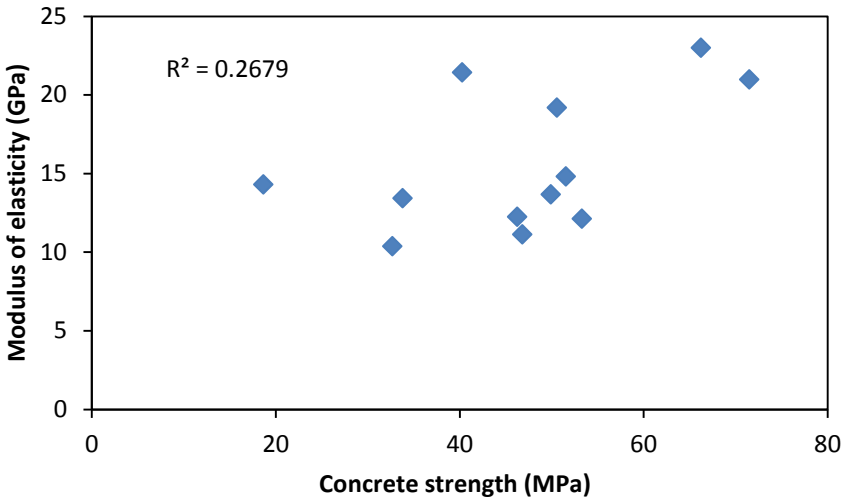

Figure 7.13: Modulus of elasticity of geopolymer concrete

There were only three mixes (out of 12) that yielded an elastic modulus of more than 20 GPa. Two of which the compressive strength was approximately 70 MPa. When compared, an OPC concrete specimen with a strength of 20 MPa typically yields a stiffness of more than 20 GPa.

The stiffness of fly ash/slag based geopolymer concrete was significantly influenced by the amount and concentration of the sodium hydroxide solution available in the matrix. It was found that the elastic modulus increased when a higher sodium hydroxide concentration was used. Thus, from the results obtained, it is clear that sodium hydroxide improves the compressive strength of the geopolymer concrete and ensures better bond strength between the aggregates and the binder, ensuring a higher stiffness. If more hydroxide ions are available to participate, the geopolymerisation process is more efficient, resulting in better interlocking between the Si, Al and Ca ions. The influence of the mass of sodium hydroxide flakes on the modulus of elasticity of the geopolymer concrete is shown in Figure 7.14.

The “R-squared” value of Figure 7.14 is significantly higher than that in Figure 7.13, which indicates that the mass of sodium hydroxide flakes has a larger influence on the modulus of elasticity compared to the compressive strength of the geopolymer concrete. This result confirms the statement that the amount of sodium hydroxide, present in the matrix, influences the modulus of elasticity of fly ash/slag based geopolymer concrete.

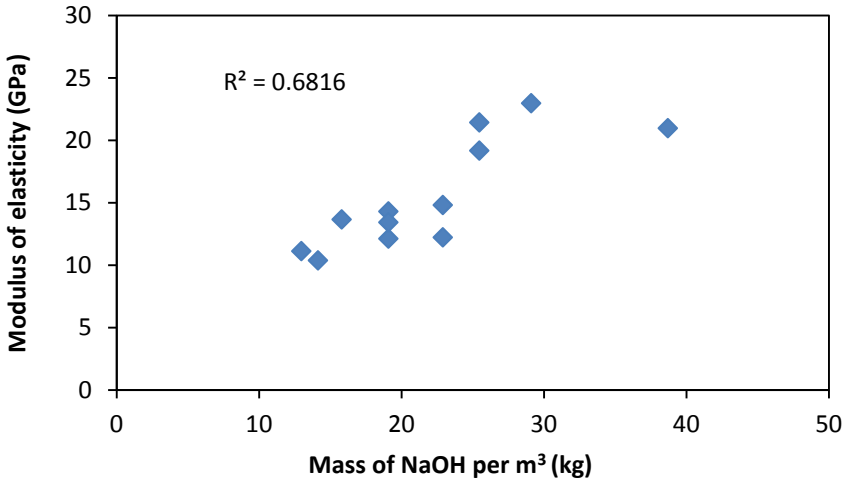

Figure 7.14: Influence of the mass of sodium hydroxide flakes on the modulus of elasticity

Unexpected results were found when the course aggregates were increased in the matrix. The stiffness of the geopolymer concrete decreased when more course aggregates were added. This is contradictory compared to OPC concrete where the elastic modulus increases when more stone is added.

Joseph and Mathew (2012) and Hardjito et al. (2005) concluded that the modulus of elasticity of geopolymer concrete can be brought equal to that of OPC concrete by selecting the appropriate aggregate content as well as the optimum fine aggregate to total aggregate ratio. Fernandez-Jimenez et al. (2006) obtained very similar modulus of elasticity values as in this study, yielding stiffness of less than 20 GPa for geopolymer concrete specimens with strengths above 30 MPa. They also found that the sodium hydroxide solution had an influence on the modulus of elasticity. This proves to be a conformation for the results and conclusions made in this study regarding the modulus of elasticity of geopolymer concrete. The modulus of elasticity values found by Lee and Lee (2013), for fly ash/slag based geopolymer concrete, was between 10 GPa and 21 GPa.

The difference between the geopolymer concrete investigated by Joseph and Mathew (2012) and Hardjito et al. (2005) and the geopolymer concrete investigated in this study, by Fernandez-Jimenez (2006) and by Lee and Lee (2006) is the addition of slag in the matrix. Thus, from the results obtained in this study and by other researches it is suggested that the addition of slag in the matrix reduces the stiffness of geopolymer concrete.

Contradictory results have been found by researchers and an in-depth study must be conducted to find solutions on how to improve the modulus of elasticity of fly ash/slag based geopolymer concrete.

7.1.4. Flexural properties

The results of Section 6.4 are discussed in this section. Two fly ash/slag based geopolymer concrete mix designs were used during this investigation, one that had a relatively high compressive strength (53 MPa) and one that had a relatively low compressive strength (19 MPa). The lower strength

geopolymer concrete was compared to a similar strength OPC concrete. Two different kinds of fibres were investigated and two different fibre dosages. The flexural properties of geopolymer concrete were obtained by means of three point bending tests and round panel tests.

The addition of polypropylene fibres decreased the compressive strength of both the OPC concrete and geopolymer concrete, while the addition of the steel fibres increased the compressive strength. The increase or decrease in strength was significantly small, which conclude that the addition of fibres do not have a significant influence on the compressive strength of the geopolymer concrete.

7.1.4.1. Flexural strength

The LOP of fly ash/slag based geopolymer concrete was directly dependent to its compressive strength (Figure 7.15). This trend is similar to that of OPC concrete in which higher strength concrete yields higher flexural strengths. The steel fibre reinforced geopolymer concrete (SFRGC) specimens yielded slightly higher flexural strengths compared to polypropylene fibre reinforced geopolymer concrete (PFRGC). The energy absorption provided by the fibres (steel or polypropylene) were mainly influenced by the amount of fibres that were added to the geopolymer concrete.

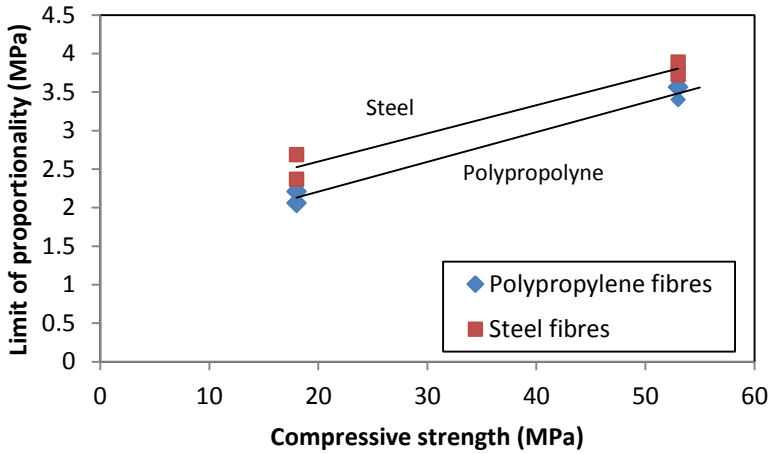

Figure 7.15: Compressive strength vs. flexural strength

7.1.4.2. R_{e3} value

The R_{e3} values of the lower strength geopolymer concrete specimens were higher than that of the higher strength geopolymer concrete. A simple explanation for this result is illustrated in Figure 7.16 which shows the stress-deflection curve of a higher strength and lower strength polypropylene fibre reinforced geopolymer concrete specimen. As described in Section 4.7, the R_{e3} value is determined by the LOP and the equivalent flexural strength of the geopolymer concrete. The equivalent flexural strength is determined by the area under the curve. The figure clearly shows that the post cracking resisting stress is similar, which results in a similar equivalent flexural strength for the two mixes.

Thus, when dividing the equivalent flexural strength with the LOP, it is logical that the specimen with the highest LOP value yields the lowest R_{e3} value.

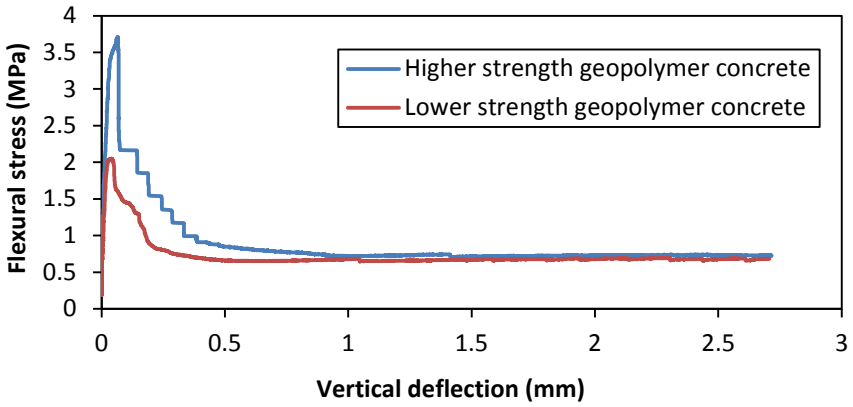

Figure 7.16: Example of a high and low strength geopolymer concrete load-deflection curve

7.1.4.3. Comparison of geopolymer concrete and OPC concrete with the addition of fibres

The OPC concrete specimens showed better ductility behaviour, when fibres were added, compared to that of geopolymer concrete. A possible explanation for the result is that the fibre pull-out behaviour in the fibre reinforced OPC concrete (FROC) matrix is better than that found in the fibre reinforced geopolymer concrete (FRGC) matrix.

Figure 7.17 compares PFROC with PFRGC. Figure 7.18 compares SFROC with SFRGC. For both fibre types, the LOP of the FROC was significantly higher compared to the LOP of FRGC, while the R_{e3} values of the two specimens were similar. This result indicates that the equivalent flexural strength was also significantly higher for the FROC specimens.

It is clear from the two figures that, regardless of fibre type, the OPC concrete tends to have better flexural properties compared to geopolymer concrete. The average flexural strength to compressive strength ratio was 0.12 and 0.17 for geopolymer concrete and OPC concrete respectively.

The deflection corresponding to the LOP was significantly smaller for the OPC concrete specimens compared to that of the geopolymer concrete specimens, when polypropylene fibres were added to the respective matrices. Due to the estimation of the LOP when steel fibres were added to the respective matrices, it was difficult to draw a comparison on the deflection corresponding to the LOP between the OPC concrete specimens and geopolymer concrete specimens with the addition of steel fibres. However, the results obtained from the modulus of elasticity tests of the geopolymer concrete specimens and the deflection corresponding to LOP when polypropylene fibres were added to the matrix, provides enough evidence that the OPC concrete specimen is significantly stiffer compared to that of fly ash/slag based geopolymer concrete.

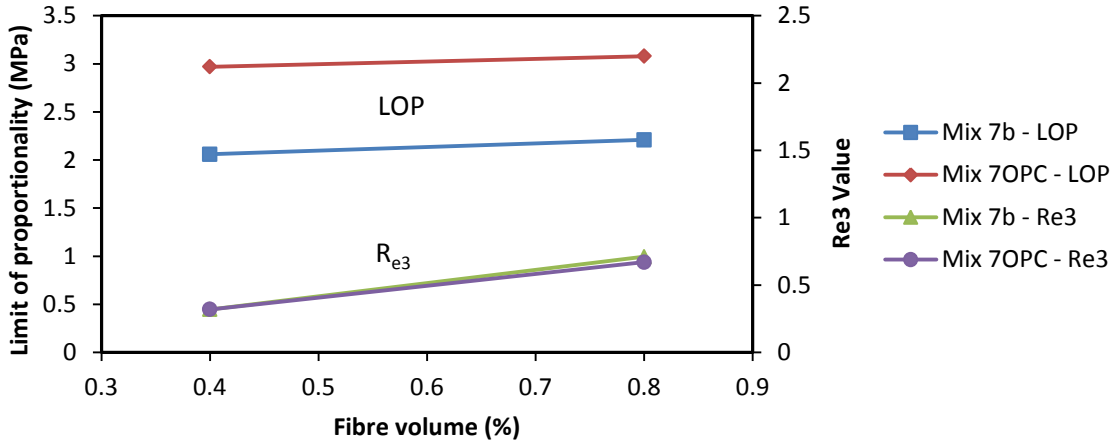

Figure 7.17: Comparison of PFRGC and PFROC

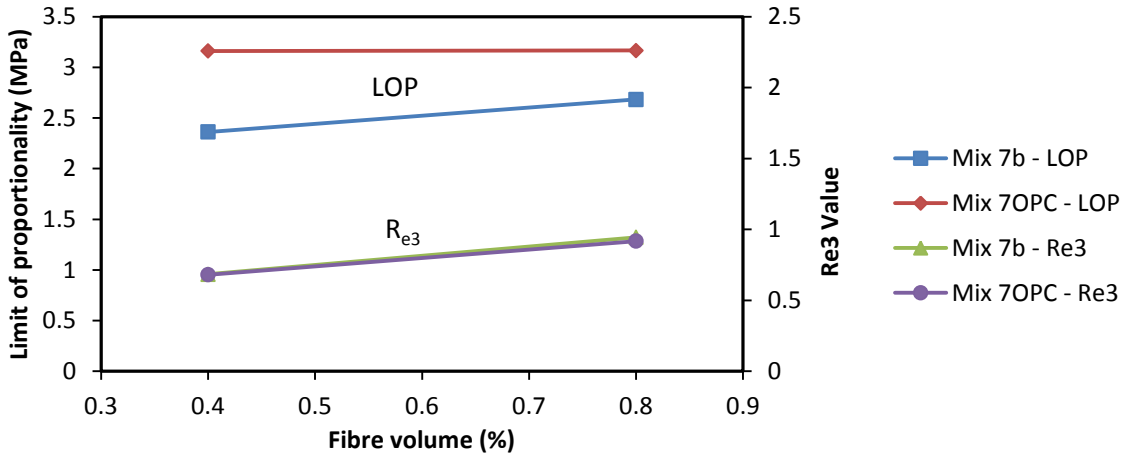

Figure 7.18: Comparison of SFRGC and SFROC

7.1.5. Aging of the geopolymer concrete

The strength gain behaviour, due to aging of geopolymer concrete, showed similar characteristics compared to the aging of OPC concrete. The aging of all the specimens is illustrated in Figure 7.18. A rapid strength gain was observed in the first seven days followed by a more gradual increase in strength up to 28 days. This is a good result for practical purposes. When a structure is built, form work is used as a mould for the part of the structure, slab for example, which is cast. The faster the slab can manage its own weight, the faster the formwork and false work can be removed. This characteristic increases both the cost efficiency and the time needed to construct the building.

It is inconclusive to comment on the strength gradient between 7 days and 28 days as no tests has been carried out on any day between 7 and 28 days. This is a matter that can certainly be investigated in future studies to find out when or if the strength gain reaches a point where there is no significant increase in strength. The strength gain beyond 28 days is also an aspect that can be investigated in the future.

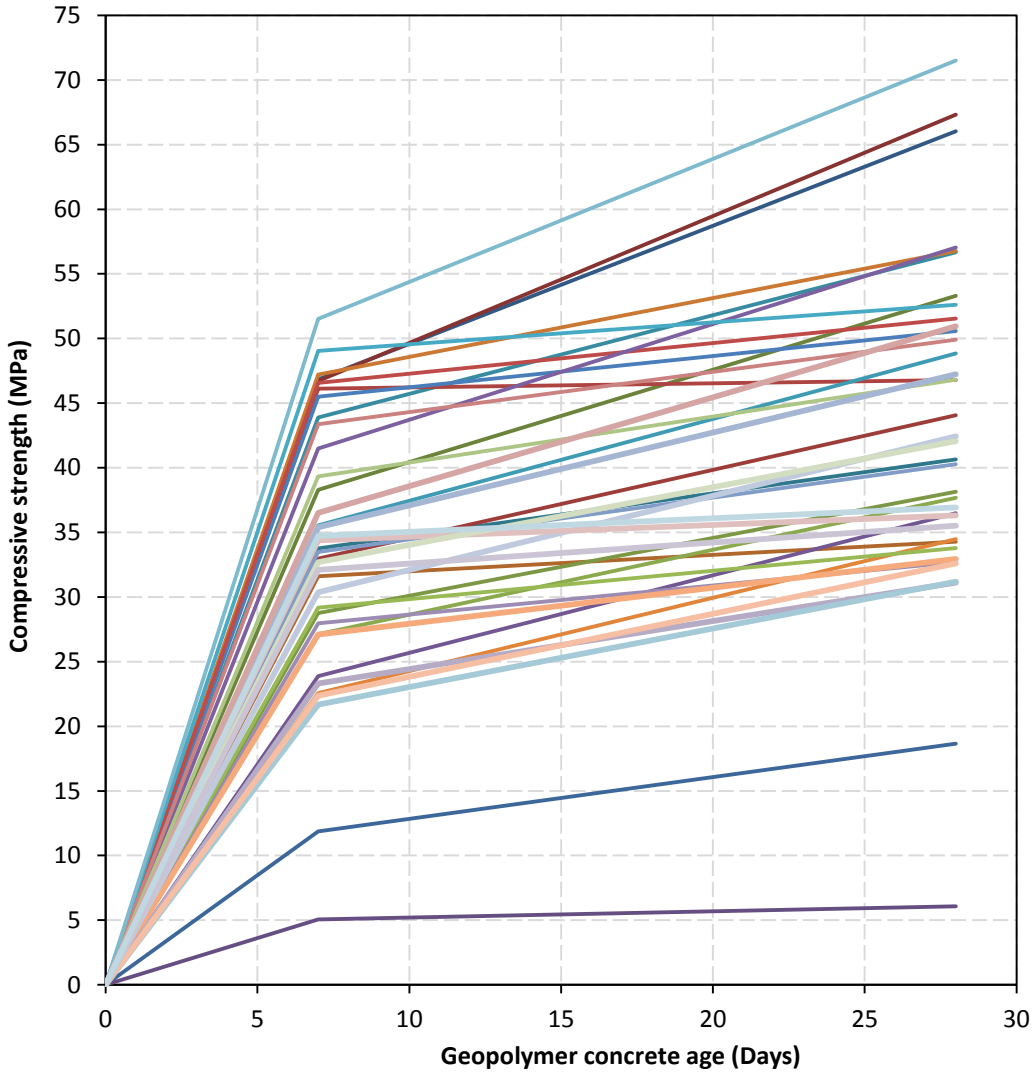

Figure 7.19: The effect of aging on the compressive strength

The percentage of strength gain between 7 days to 28 days was inconsistent, ranging from 2% to 65%. Thus, from the mixes designed in this study, it is inconclusive to provide a 28 day strength estimation after 7 days.

7.1.6. Density of geopolymer concrete

The density of the geopolymer concrete varied from 2093 kg/m^3 to 2302.3 kg/m^3, depending on the constituents in the matrix. The aggregate content had the largest influence on the density of geopolymer concrete, especially the fine aggregate content which increased the density when more were added to the matrix.

7.2. Occurring problems

The problems that were experienced and dealt with during the experimental part of the study are discussed in this section. The reason for discussing these problems is to ensure that they are avoided in future studies. The problems mostly occurred in the mixes of Phase A. The most significant

problem was cracking of the early age concrete. Attempts were made to avoid or reduce these problems when the mixes of Phase B were designed. The problems that occurred include, surface cracking, leeching of sodium bicarbonate and significant rapid setting times of the fly ash/slag based geopolymer concrete.

7.2.1. Rapid setting of fly ash/slag based geopolymer concrete

Rapid setting of the geopolymer concrete was a significant problem, experienced during the trial mixing period. Due to the rapid hardening, there was no time to adequately cast the fresh geopolymer concrete into the moulds. Figure 7.20 shows an example of a cube that was casted when rapid hardening occurred. The time of setting was estimated to be approximately 10 minutes. After mixing, only a slump flow test was carried out before the cubes were cast. The geopolymer concrete already hardened to such an extent that it was impossible for the cubes to be cast in the moulds after the execution of the slump flow test. This proved to be a significant problem for the casting of the moulds, as well as for the cleaning of the mixer. The mixer and mixing equipment had to be cleaned directly after the cubes were cast, to ensure that the geopolymer concrete material did not get stuck to the equipment.

Figure 7.20: Rapid setting of geopolymer concrete

The first identification of a possible problem was the fact that the sodium hydroxide and sodium silicate solutions were mixed together a day prior to mixing. According to Davidovits (2011), the dissolution of the silica, present in the sodium silicate solution, starts the moment when the two solutions are mixed together, resulting in an accelerated geopolymerisation process. This is usually done when a low calcium based source material e.g. fly ash is used as the binder, i.e. no slag or any material containing a high amount of calcium. The setting time of the fly ash/slag based geopolymer concrete increased significantly when the two alkaline solutions were separately added to the mixer. Although the casting process and cleaning process still had to be done relatively quickly, there was enough time to ensure adequate compaction. The initial setting time increased to approximately

40 minutes, depending on the amount of slag available in the mix and the temperature of the laboratory.

The slag content had a significant influence on the final setting times. This result is due to the amount of CSH gel that is formed in conjunction with the geopolymeric gels. If less slag is available, less CSH gels form, resulting in a longer final setting time.

The viscosity also played a role in the casting process. The mixes of Phase A had a high viscosity, making it even more challenging to cast. The workability was improved when additional water was added to the matrix, which lowered the viscosity.

7.2.2. Cracks on the geopolymer concrete specimens

Surface cracking on the geopolymer concrete specimens was a major concern in Phase A. The majority of the cubes, for the mix designs of Phase A, showed surface cracks as few as two days after casting. Considering the durability, the cracking of any concrete is a major concern as it may influence both the short term and the long term properties of the specific concrete. It is suggested that slag is the cause for these cracks, as it has a strong tendency to hydrate, i.e. forming a turquoise green crystalline gel. When slag is alkaline activated it starts to hydrate and this hydrate then moves through dehydroxylation (loss of water) into polycondensation. The loss of water causes an uneven volume change, resulting in cracks (Attwell 2014).

It was found that the amount and size of the cracks increased when more slag were added to the matrix. The binder material consisted of 40% slag for the majority of the mix designs of Phase A. Figure 7.21 illustrate the difference in colour between a matrix that consisted of a binder material with 20% slag and 40% slag. The green colour was only observed in the specimens with a binder that consisted of 40% slag by mass.

a) Binder material consist of 20% slag **b) Binder material consists of 40% slag**

Figure 7.21: Concrete colour for different slag contents

The temperature tests confirmed that a specimen with the same slag content, but a higher alkaline solution content, yielded higher temperatures during the initial stages of the hardening process. The cracks observed on the cubes, with a lower alkaline solution content, were significantly less than the cracks observed on the cubes with a higher alkaline solution content. Thus, the cracks may have formed due to the higher temperature development during the initial stages of the hardening process. The temperature increased rapidly within the first five hours after casting. However, temperature decreased when less slag was used in the matrix. The majority of the mix designs in Phase A contained a large amount of both slag and alkaline solution. Therefore, it is possible that the slag content and alkaline solution content, available to participate in the hydration process, may contribute to the amount- and size of the cracks on the surface of the fly ash/slag based geopolymer concrete specimens.

An example of the major cracks is shown in Figure 7.22. Major cracks occurred, in the top third of the specimens of Phase A, when the amount of aggregates decreased and the binder and alkaline solution increased. These cracks occurred when the aggregate content was between 60% and 65% of the total concrete mass, compared to the usual 70%. A decrease in aggregates resulted in the increase of slag content and sodium hydroxide solution and therefore more water was required for the hydration process. If there is a lack of water available in the fresh fly ash slag based geopolymer concrete matrix, the cube starts to crack due to uneven volume change (Attwell 2012).

An attempt was made to cure the geopolymer concrete specimens in water, but a decrease in strength was observed when the cubes were tested after 28 days. It must be noted that no cracks were observed on the surface of the cubes that were water-cured.

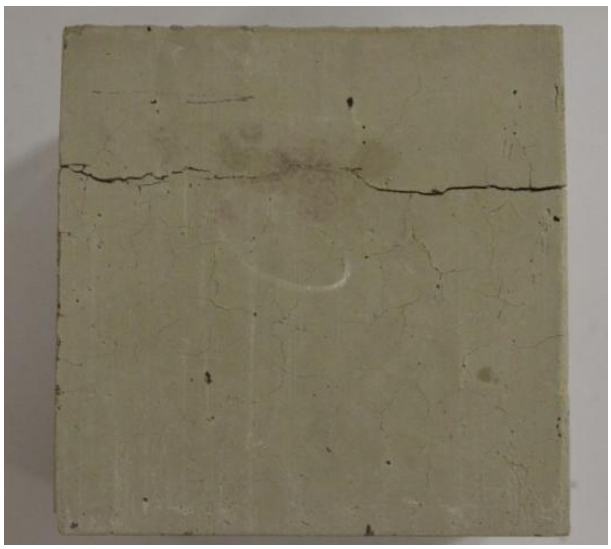

Figure 7.22: Major cracks in the top part of the cubes

Surface cracks, as shown in Figure 7.23, were a common ocurance on the cubes after five to seven days. The filtration of water, through the cracks, may result in larger cracks and even corrosion of the steel reinforcement if the water reaches the steel.

Figure 7.23: Surface cracks

Minor surface cracks, as shown in Figure 7.24, were another type of cracks that were found on the cubes after several days. Those cracks are aloso an indication that either the slag content is too high or the water content is too low.

Figure 7.24: Minor cracks on the cubes

Some of the cube results showed inconsistent results, i.e. there was a relative large variation between the individual results. A possible explanation for the variation is the large number of cracks on the surface of the cubes which may have formed weak spots in critical areas.

Two approaches were followed to find solutions for the cracks. Firstly, the slag content in the matrix was decreased and secondly, additional water was added to the matrix. Various mixes were designed in which the slag content was decreased, while additional water was added in the matrix. The majority of the cubes did not show any cracks, although segregation became a problem when a low slag content was used. It was challenging to find an optimum ratio between the slag content and additional water in the mix.

After the various experiments, it was concluded that a binder with slag content of 40% and 125 l/m^3 additional water yielded promising strengths while having few minor or even no cracks. Mix 3b is an example of such a mix design. All the mixes of Phase B contained at least 90 l/m^3 of additional water. This addition proved to be a promising solution for the major cracks that was observed on the specimens of Phase A. However, significantly more research must be done to ensure a fly ash/slag based geopolymer concrete with no cracks. A sodium hydroxide solution with a concentration of 8 M was used for the majority of the mixes. The concentration can be increased to ensure that a binder with 20% slag content yields higher strengths.

7.2.3. **Leaching of sodium bicarbonate**

As illustrated in Figure 7.25, a white efflorescence was observed on some of the cubes, five to seven days after casting. It is a type of crystalline that forms on the surface of the cube. According to the geopolymer institute, the white crystalline is sodium bicarbonate which forms when there is an excess amount of sodium hydroxide in the matrix which has not reacted with the fly ash or slag (Davidovits 2011). The sodium hydroxide migrates to the surface during drying and reacts with CO_2 available in the atmosphere. This crystallization does not occur when potassium hydroxide is used as the alkaline activator, as potassium hydroxide does not form such a salt type crystal (Davidovits 2011).

Figure 7.25: Efflorescence on some of the cubes

After more research, it was found that the efflorescence on the cubes could have been reduced by changing the mixing procedures. The mixing procedure in this study was conducted according to published literature as described in Chapter 4. The same method, as for OPC, was followed in which all the dry materials were mix first, before adding the liquid and mixing it all together.

The problem experienced with this mixing procedure is that if the stone or sand particles have cracks or certain porosity, some of the alkaline solution is trapped inside these cracks or voids. The trapped alkaline solution does not participate in the reaction and is only released during drying. The sodium hydroxide then migrates to the surface of the geopolymer concrete, forming the white powder (Davidovits 2011).

According to Davidovits (2011), it is important to follow the correct mixing procedure as it may have an influence on the properties of the geopolymer concrete. The correct mixing procedure is to prepare the geopolymer cement first, before adding the fine and coarse aggregates. The reason for mixing the binder and alkaline liquid first is to ensure that the alkaline molecules are utilised efficiently. According to Davidovits (2011), the process can be enhanced by mixing the alkaline solutions together, one day prior to mixing. It must be noted that these observations were made for low calcium based geopolymer concrete only and it has already been confirmed that the alkaline solution must not be mixed together one day prior to mixing when slag is added to the matrix. The leaching of the sodium hydroxide only occurred in mixes that had a low slag content, i.e. lower strength concrete. This result suggests that the slag consumes a large amount of the sodium hydroxide.

7.2.4. Health concerns and safety awareness

Geopolymer concrete holds some health concerns which require the correct safety procedures when worked with. The most significant concern is the sodium hydroxide solution which is hazardous due

to its high alkalinity. Sodium hydroxide burns when coming in contact with bare skin or eyes. The solution not only burns the skin but also sets free hazardous vapours that must not be inhaled.

As stated in Section 2.1.4, only a concentration of less than 0.05 M typically holds no danger or irritation to skin or eyes (Evonik Industries 2010). Therefore, gloves had to be worn when working with the geopolymer concrete as molar concentrations of up to 16 M were used in this study. A sodium hydroxide solution with a concentration of 0.05 M, for a geopolymer mix, is insufficient to ensure a proper dissolution process and therefore it is difficult to avoid this danger.

The safety of employees is important and it must be ensured that the correct safety equipment is provided to the people that are working with the geopolymer concrete.

Chapter 8
Conclusions and recommendations

8.1. Conclusions

This study investigated fly ash/slag based geopolymer concrete, cured at ambient temperature. The aim of the study is to obtain a better understanding regarding the mechanical properties of fly ash/slag based geopolymer concrete and its flexural behaviour with the addition of macro steel- or polypropylene fibres. Tests were conducted on fly ash/slag based geopolymer concrete specimens to determine the compressive strength, modulus of elasticity, setting time and the temperature development during the initial stages of the hardening process. All of these tests contributed to characterise the mechanical properties. Three point bending tests and round panel tests were carried out to determine the flexural properties of the fly ash/slag based geopolymer concrete. Fibre pull-out tests were conducted to obtain some information regarding the fibre-matrix interface. The flexural properties of an OPC concrete mix, with a similar compressive strength, were compared to a lower strength fly ash/slag based geopolymer concrete mix.

Cracking was observed on the surface of the fly ash/slag based geopolymer concrete specimens, especially during Phase A, but it was improved significantly during Phase B.

Leaching of sodium bicarbonate was observed on the surface of the low strength fly ash/slag based geopolymer concrete specimens. The majority of the low strength mix designs contained a binder with relatively low slag content.

The final setting time of fly ash/slag based geopolymer concrete was highly dependent on the slag content in the matrix. The final setting time decreased significantly when the slag content increased.

The internal temperature development during the hardening process was influenced by the slag content and the amount of alkaline solution in the matrix. The temperature increased when more slag and alkaline solution was added in the matrix.

8.1.1. Compressive strength of fly ash/slag based geopolymer concrete

- Promising fly ash/slag based geopolymer concrete compressive strengths, of up to 72 MPa, were obtained in this study. Only ambient curing was carried out in this study.
- When the amount of slag in the matrix increased, higher compressive strengths were obtained.

- When increasing or decreasing the binder material (fly ash and slag), the compressive strength was only influenced if the slag content was relatively high (40%). This result is due to a slow dissolution of the fly ash particles at ambient temperatures.
- If the liquid to binder ratio was kept constant, the compressive strength of fly ash/slag based geopolymer concrete was not significantly influenced by the amount of aggregates in the matrix.
- The fine aggregate to total aggregate ratio influenced the compressive strength of the fly ash/slag based geopolymer concrete. A ratio of 0.40 to 0.45 proved to yield the highest strength.
- The alkaline to binder ratio influenced the compressive strength of the fly ash/slag based geopolymer concrete. However, this ratio is only valid when there is no additional water added to the matrix. The alkaline to binder ratio can be replaced by a liquid to binder ratio, which include the additional water. The compressive strength decreased when additional water was added to the fly ash/slag based geopolymer concrete mix. Thus, the compressive strength decreased when the liquid to binder ratio increased.
- The sodium hydroxide concentration had a significant influence on the compressive strength of the fly ash/slag based geopolymer concrete. A higher concentration yielded higher compressive strengths. Thus, if the mass of sodium hydroxide flakes is increased, higher compressive strengths are obtained.
- A value of approximately 1 was obtained as the optimum sodium silicate to sodium hydroxide ratio for the mix designs in this study. This ratio yielded the highest compressive strengths when a sodium hydroxide concentration of 8 M was used. The ratio will change if the sodium hydroxide concentration is changed.

An overall conclusion regarding the compressive strength of the fly ash/slag based geopolymer concrete is that the slag content, additional water and mass of sodium hydroxide solids per m^3 have the most significant influence on the strength.

8.1.2. Modulus of elasticity of fly ash/slag based geopolymer concrete

- The overall modulus of elasticity of fly ash/slag based geopolymer concrete was significantly lower than that of OPC concrete, yielding an elastic modulus of between 9.4 GPa and 23 GPa for compressive strengths of up to 72 MPa.
- Although not as significantly as in the case of OPC concrete, the modulus of elasticity of the fly ash/slag based geopolymer concrete is dependent on its compressive strength.
- The mass of sodium hydroxide flakes in the matrix had the largest influence on the modulus of elasticity. The modulus of elasticity will increase if more sodium hydroxide flakes are added to the alkaline solution, i.e. a higher sodium hydroxide concentration.

8.1.3. Flexural properties of fly ash/slag based geopolymer concrete

The ductility of the fly ash/slag based geopolymer concrete was improved when fibres were added to the matrix. Neither the limit of proportionality nor the compressive strength of the fly ash/slag based geopolymer concrete was significantly influenced by the addition of fibres in the matrix, although both increased slightly when steel fibres were added. The flexural toughness of the fly ash/slag based geopolymer concrete was significantly influenced by the fibre volume and fibre type. An increase in fibre volume resulted in a higher energy absorption provided by the fibres. The steel fibres yielded higher energy absorption compared to the polypropylene fibres.

The R_{e3} values of the lower strength (18.65 MPa) fly ash/slag based geopolymer concrete were higher than that of the higher strength (52 MPa) fly ash/slag based geopolymer concrete.

For the specific mixes that were compared, both the flexural strength and the equivalent flexural strength of fly ash/slag based geopolymer concrete was significantly lower compared to OPC concrete. Due to the better flexural properties of OPC concrete in the pre-crack and post-crack region, the R_{e3} values were fairly similar. The energy absorption provided by the fibres was also higher for the OPC concrete.

According to the single fibre pull-out results, the polypropylene fibre bond strength is similar for both the geopolymer concrete and the OPC concrete, while the hooked end steel fibre bond strength is almost twice as high in the geopolymer concrete as in the OPC concrete.

8.2. Recommendations

From the knowledge gained during this study, the following can be identified as important for further research:

- Further research must be conducted on the setting times of fly ash/slag based geopolymer concrete. The rapid setting of the fly ash/slag based geopolymer concrete made the casting of the various moulds a challenging task and an attempt must be made to ensure a longer setting time.
- The curing process of the fly ash/slag based geopolymer concrete must be investigated and a solution must be found that will eliminate possible cracking due to the hydration of the slag in the matrix.
- The drying shrinkage of fly ash/slag based geopolymer concrete must be investigated. This may provide important information regarding the cracking of the fly ash/slag based geopolymer concrete.
- The sodium hydroxide solution can be replaced by a potassium hydroxide solution. This substitution will avoid the leeching of sodium bicarbonate which forms the white efflorescence.

- More knowledge regarding the elastic modulus of fly ash/slag based geopolymer concrete must be obtained. The modulus of elasticity must be significantly improved before fly ash/slag based geopolymer concrete can serve as a construction material.
- Limited research was done on a single fibre pull-out level, which leaves significant room for a more in depth study. The critical embedment length of fibres must be obtained for certain strength fly ash/slag based geopolymer concrete specimen, in order to improve the energy absorption of the fibres. This result will improve the ductility of the fly ash/slag based geopolymer concrete.
- The flexural properties of more fly ash/slag based geopolymer concrete mix designs must be investigated to obtain more results. Only two different mix designs were investigated in this study, making it difficult to draw a proper conclusion. A more in-depth study can be carried out to draw a better comparison between the flexural properties of fly ash/slag based geopolymer concrete and OPC concrete.
- Most of the mix designs consisted of a sodium hydroxide solution with a concentration of 6 M or 8 M. This can be increased to 12 M or 14 M to yield even better mechanical properties. However, the necessary safety precautions must be carried out.
- This study only investigated the mechanical part of fly ash/slag based geopolymer concrete. Not much research was done on the molecular structure of the fly ash/ slag based geopolymer concrete matrix. The chemistry of fly ash/slag based geopolymer concrete is certainly an important aspect that needs significantly more research.

8.3. Concluding statement

A significant amount of knowledge was gained on the mechanical properties of fly ash/slag based geopolymer concrete during this study. The problems experienced, during the experimental part of the study, leaves room for further research. From the knowledge gained, it can be concluded that the use of fly ash/slag based geopolymer concrete, as an alternative binder material, is still some time away as there is many complications that need to be dealt with, especially the low modulus of elasticity. However, it can be concluded that fly ash/slag based geopolymer concrete has the potential if these complications can be improved.

References

ACI Committee 544. 1973. State-of-the-Art Report on Fiber Reinforced Concrete. Paper presented at ACI Journal Proceedings.

Ahmadi, B. 2000. Initial and Final Setting Time of Concrete in Hot Weather. *Materials and Structures*, 33(8).

Ahmed, S. 2013. Review of Mechanical Properties of Short Fibre Reinforced Geopolymer Composites.

Al Bakri, A.M., Kamarudin, H., Bnhussain, M., Nizar, I.K. & Mastura, W. 2011. Mechanism and Chemical Reaction of Fly Ash Geopolymer Cement-A Review. *Journal of Asian Scientific Research*, 1(5).

Alexander, M., Jaufeerally, H. & Mackechnie, J. 2003. Structural and Durability Properties of Concrete made with Corex Slag. *Research monograph*, (6).

Alzeer, M. & MacKenzie, K. 2013. Synthesis and Mechanical Properties of Novel Composites of Inorganic Polymers (Geopolymers) with Unidirectional Natural Flax Fibres (Phormium Tenax). *Applied Clay Science*, 75–76(0).

Arioz, E., Arioz, O. & Kockar, O.M. 2012. An Experimental Study on the Mechanical and Microstructural Properties of Geopolymers. *Procedia Engineering*, 42

ASTM International. 2010. ASTM C469/C469M – 10 "Standard Test Method for Static Modulus of Elasticity and Poisson's Ratio of Concrete in Compression".

ASTM International. 2012. *C1550: Standard test method for flexural toughness of fiber reinforced concrete (using centrally loaded round panel).* United States:

Astutiningsih, S. and Liu, Y. 2005. Geopolymerisation of Australian Slag with Effective Dissolution by the Alkali. Paper presented at Proceedings of the World Congress Geopolymer.

Attwell, 2014, C. Problems with geopolymer mix designs

Bakharev, T. 2005. Resistance of Geopolymer Materials to Acid Attack. *Cement and Concrete Research*, 35(4).

Bernal, S., De Gutierrez, R., Delvasto, S. & Rodriguez, E. 2010. Performance of an Alkali-Activated Slag Concrete Reinforced with Steel Fibers. *Construction and Building Materials*, 24(2).

Bernard, E.S. & Pircher, M. 2000. *Influence of geometry on performance of round determinate panels made with fibre reinforced concrete.* University of Western Sydney, Nepean, School of Civic Engineering and Environment

Bondar, D., Lynsdale, C.J., Milestone, N.B., Hassani, N. & Ramezanianpour, A.A. 2011. Engineering Properties of Alkali-Activated Natural Pozzolan Concrete. *ACI Materials Journal*, 108(1).

Boshoff, W.P. 2007. *Time-dependant behaviour of engineered cement-based composites. Unpublished thesis.* Stellenbosch University: Stellenbosch: University of Stellenbosch.Phd

Bothma, J. 2013. *The structural use of synthetic fibres: Thickness design of slabs on grade. Unpublished thesis.* Stellenbosch University.

Brandt, A.M. 2008. Fibre Reinforced Cement-Based (FRC) Composites After Over 40 Years of Development in Building and Civil Engineering. *Composite Structures,* 86(1).

British Standard. 2005. *BS EN 14651:2005+A1:2007: Test method for metallic fibre concrete. measuring the flexural tensile strength (limit of proportionality (LOP), residual).* BSI

Buratti, N., Mazzotti, C. & Savoia, M. 2011. Post-Cracking Behaviour of Steel and Macro-Synthetic Fibre-Reinforced Concretes. *Construction and Building Materials,* 25(5).

Cement & Concrete Association of New Zealand. 2009. Fibre Reinforced Concrete. http://www.ccanz.org.nz/files/documents/8426734f-acf3-411d-85b1-a3e242e8ee37/IB%2039.pdf

Cement and concrete association of New Zealand. 2013. *Fibre reinforced concrete.* [Online]. Available: http://www.ccanz.org.nz/files/documents/8426734facf3- 411d-85b1-a3e242e8ee37/IB%2039.pdf

Cement & Concrete institute. 2013. *Fibre reinforced concrete.* [Online]. Available: http://www.cnci.org.za/Uploads/Fibre%20Reinforced%2001102010.pdf

Chandramouli, K., Rao, S., Pannirselvam, N., Seshadri Sekhar, T. & Sravana, P. 2006. Strength Properties of Glass Fibre Concrete.

Clarke, J., Peaston, C. & Swannell, N. 2007. Guidance on the use of Macro-Synthetic-Fiber Reinforced Concrete. *The Concrete Society,*

Davidovits, J. 1989. Geopolymers and Geopolymeric Materials. *Journal of Thermal Analysis and Calorimetry,* 35(2).

Davidovits, J. 1991. Geopolymers. *Journal of Thermal Analysis,* 37(8).

Davidovits, J. 1994. High-Alkali Cements for 21st Century Concretes. *ACI Special Publication,* 144

Davidovits, J. 1999. Chemistry of Geopolymeric Systems, Terminology. Paper presented at Proceeding of Geopolymer.

Davidovits, J. 2011. *Geopolymer chemistry and applications.* France: Geopolymer Institute

Davidovits, J., Davidovits, M., Davidovits, F. & Davidovits, R. 2012. Geopolymer Cement of the Calcium Ferro-Aluminosilicate Polymer Type and Production Process.

Davidovits, Joseph. 2013. *Geopolymer cement: A review.* [Online]. Available: http://www.geopolymer.org/library/technical-papers/21-geopolymer-cement-review-2013

Davidovits, Joseph. 2014. *[Video] webinar spring 2014: Geopolymer web workshop.* [Online]. Available: http://www.geopolymer.org/conference/webinar/webinar-spring-2014-geopolymer-web-workshop-apr-8-9[26/05/2014]

Dimas, D., Giannopoulou, I. & Panias, D. 2009. Polymerization in Sodium Silicate Solutions: A Fundamental Process in Geopolymerization Technology. *Journal of Materials Science,* 44(14).

Duxson, P., Provis, J.L., Lukey, G.C. & van Deventer, J.S.J. 2007. The Role of Inorganic Polymer Technology in the Development of 'green Concrete'. *Cement and Concrete Research,* 37(12).

EN, B. 2007. 14651: 2005 a1: 2007. *Test method for metallic fibre concrete.Measuring the flexural tensile strength (limit of proportionality (LOP), residual),*

Evonik Industries. 2010. GPS Safety Summary for Sodium Hydroxide.

Fernández-Jiménez, A. & Palomo, A. 2003. Characterisation of Fly Ashes. Potential Reactivity as Alkaline Cements< sup>☆</sup>. *Fuel,* 82(18).

Fernández-Jiménez, A. & Palomo, A. 2005. Composition and Microstructure of Alkali Activated Fly Ash Binder: Effect of the Activator. *Cement and Concrete Research,* 35(10).

Fernandez-Jimenez, A.M., Palomo, A. & Lopez-Hombrados, C. 2006. Engineering Properties of Alkali-Activated Fly Ash Concrete. *ACI Materials Journal,* 103(2).

Fernández-Jiménez, A., Palomo, A., Sobrados, I. & Sanz, J. 2006. The Role Played by the Reactive Alumina Content in the Alkaline Activation of Fly Ashes. *Microporous and Mesoporous Materials,* 91(1–3).

Geopolymer Institute. 2013. *Geopolymer cement.* [Online]. Available: http://www.geopolymer.org/applications/geopolymer-cement

Geopolymer Institute. 2013. *New scientific word for metakaolin.* [Online]. Available: http://www.geopolymer.org/faq/new-scientific-word-for-metakaolin

Geopolymer Institute. 2014. *Applications: Geopolymer cement.* [Online]. Available: http://www.geopolymer.org/applications/geopolymer-cement

Girard, J. 2008. Introduction to GFRC (Glass Fibre Reinforced Concrete). http://www.concretecountertopinstitute.com/library.item.57/introduction-to-gfrc-glass-fiber-reinforced-concrete.html

Gourley, J. and Johnson, G. 2005. Developments in Geopolymer Precast Concrete. Paper presented at World Congress Ceopolymer.

Hajimohammadi, A., Provis, J.L. & van Deventer, J.S.J. 2011. The Effect of Silica Availability on the Mechanism of Geopolymerisation. *Cement and Concrete Research,* 41(3).

Haranki, B. 2009. *Strength, modulus of elasticity, creep and shrinkage of concrete used in florida. Unpublished thesis.* University of Florida.

Hardjito, D., Wallah, S.E., Sumajouw, D.M. & Rangan, B.V. 2004. On the Development of Fly Ash-Based Geopolymer Concrete. *ACI Materials Journal-American Concrete Institute,* 101(6).

Hardjito, D., Wallah, S., Sumajouw, D. and Rangan, B. 2005. Introducing Fly Ash-Based Geopolymer Concrete: Manufacture and Engineering Properties. Paper presented at 30th Conference on our World in Concrete and Structures.

Hardjito, D. & Rangan, B.V. 2005. Development and Properties of Low-Calcium Fly Ash-Based Geopolymer Concrete. *Perth, Australia: Curtin University of Technology,*

Hsie, M., Tu, C. & Song, P. 2008. Mechanical Properties of Polypropylene Hybrid Fiber-Reinforced Concrete. *Materials Science and Engineering: A,* 494(1).

Jiabiao, J., Loh, S. and Gasho, T. 2004. Synthetic Structure Fibers for Toughness and Crack Control of Concrete . August 2004.

Joseph, B. & Mathew, G. 2012. Influence of Aggregate Content on the Behavior of Fly Ash Based Geopolymer Concrete. *Scientia Iranica,* 19(5).

Khale, D. & Chaudhary, R. 2007. Mechanism of Geopolymerization and Factors Influencing its Development: A Review. *Journal of Materials Science,* 42(3).

Kong, D.L. & Sanjayan, J.G. 2010. Effect of Elevated Temperatures on Geopolymer Paste, Mortar and Concrete. *Cement and Concrete Research,* 40(2).

Labib, W. & Eden, N. 2006. An Investigation into the use of Fibres in Concrete Industrial Ground-Floor Slabs. *Liverpool John Moores University, Liverpool,*

Lawler, J.S., Connolly, J.D., Krauss, P.D. & Tracy, S.L. 2007. *NCHRP REPORT 566: Guidelines for concrete mixtures containing supplementary cementitious materials to enhance durability of bridge decks.* WASHINGTON, D.C.: Transportation Research Board

Lee, W. & Van Deventer, J. 2002. Structural Reorganisation of Class F Fly Ash in Alkaline Silicate Solutions. *Colloids and Surfaces A: Physicochemical and Engineering Aspects,* 211(1).

Lee, N.K. & Lee, H.K. 2013. Setting and Mechanical Properties of Alkali-Activated Fly ash/slag Concrete Manufactured at Room Temperature. *Construction and Building Materials,* 47(0).

Lewis, D.W. 1992. Properties and Uses of Iron and Steel Slags. http://www.nationalslag.org/archive/legacy/nsa_182-6_properties_and_uses_slag.pdf

Li, V., van Zijl, G. & Wittmann, F.H. 2011. *Durability of strain-hardening fibre-reinforced cement-based composites (SHCC): State of the art report.* Springer

Lindgård, J., Andiç-Çakır, Ö., Fernandes, I., Rønning, T.F. & Thomas, M.D. 2012. Alkali–silica Reactions (ASR): Literature Review on Parameters Influencing Laboratory Performance Testing. *Cement and Concrete Research,* 42(2).

Lloyd, N. and Rangan, B. 2010. Geopolymer Concrete with Fly Ash. Paper presented at Second International Conference on Sustainable Construction Materials and Technologies.

Memon, F.A., Nuruddin, M.F., Khan, S., Shafiq, N. & Ayub, T. 2013. Effect of Sodium Hydroxide Concentration on Fresh Properties and Compressive Strength of Self-Compacting Geopolymer Concrete. *Journal of Engineering Science and Technology,* 8(1).

Motorwala, A., Shah, V., Kammula, R., Nannapaneni, P. & Raijiwala, D. 2008. ALKALI Activated FLY-ASH Based Geopolymer Concrete.

Naaman, A.E. & El-Tawil, S. 2008. Comparative Flexural Behavior of Four Fiber Reinforced Cementitious Composites. *Cement and concrete Composites*, 30(10).

Nath, P. & Sarker, P.K. 2012. Geoplymer Concrete for Ambient Curing Condition. http://asec2012.conference.net.au/papers/028.pdf

Nath, S. & Kumar, S. 2013. Influence of Iron Making Slags on Strength and Microstructure of Fly Ash Geopolymer. *Construction and Building Materials*, 38

Occidental Chemical Corporation. 2013. *Oxychem caustic soda handbook.* [Online]. Available:http://www.oxychile.cl/rps_oxychile_v56/OpenSite/Oxy%20Espa%C3%B1ol/Productos%20y%20Servicios/Soda%20C%C3%A1ustica%20L%C3%ADquida/20080124144950/HandbookCausticSoda_OFICIAL.pdf

Owens, G. 2009. *Fulton's concrete technology.* Midrand, South Africa: Cement & Concrete Institute

Pacheco-Torgal, F., Castro-Gomes, J. & Jalali, S. 2008. Alkali-Activated Binders: A Review: Part 1. Historical Background, Terminology, Reaction Mechanisms and Hydration Products. *Construction and Building Materials*,22(7).

Palomo, A., Grutzeck, M.W. & Blanco, M.T. 1999. Alkali-Activated Fly Ashes: A Cement for the Future. *Cement and Concrete Research*, 29(8).

Pereira, E.B., Fischer, G. & Barros, J.A. 2012. Direct Assessment of Tensile Stress-Crack Opening Behavior of Strain Hardening Cementitious Composites (SHCC). *Cement and Concrete Research*, 42(6).

PQ Europe. 2004. Sodium and Potassium Silicates: Versitile Componants for Your Applications. http://www.pqcorp.com/LinkClick.aspx?fileticket=dPoxh3Ed1j0%3D&tabid=166&mid=868

Provis, J.L. & Van Deventer, Jan Stephanus Jakob. 2009. *Geopolymers: Structure, processing, properties and industrial applications.* Woodhead Cambridge, UK

Puertas, F., Martínez-Ramírez, S., Alonso, S. & Vázquez, T. 2000. Alkali-Activated Fly ash/slag Cements: Strength Behaviour and Hydration Products. *Cement and Concrete Research*, 30(10).

Rangan, B.V., Hardjito, D., Wallah, S.E. and Sumajouw, D.M. 2005. Studies on Fly Ash-Based Geopolymer Concrete. Paper presented at Proceedings of the World Congress Geopolymer, Saint Quentin, France.

Rilem, T. 2002. 162-TDF (2002) Bending test–final Recommendation. *Materials and Structures*, 35

Saeed, A., Hammons, M.I. & Petermann, J.C. 2010. Alkali-Activated Geopolymers: A Literature Review.

Sagoe-Crentsil, K. & Weng, L. 2007. Dissolution Processes, Hydrolysis and Condensation Reactions during Geopolymer Synthesis: Part II. High Si/Al Ratio Systems. *Journal of Materials Science*, 42(9).

Sakulich, A.R. 2011. Reinforced Geopolymer Composites for Enhanced Material Greenness and Durability. *Sustainable Cities and Society,* 1(4).

Shaikh, F. 2013. Deflection Hardening Behaviour of Short Fibre Reinforced Fly Ash Based Geopolymer Composites. *Materials & Design,* 50

Silva, I., Castro-Gomes, J.P. & Albuquerque, A. 2012. Effect of Immersion in Water Partially Alkali-Activated Materials obtained of Tungsten Mine Waste Mud. *Construction and Building Materials,* 35

Sindhunata, , Van Deventer, J., Lukey, G. & Xu, H. 2006. Effect of Curing Temperature and Silicate Concentration on Fly-Ash-Based Geopolymerization. *Industrial & Engineering Chemistry Research,* 45(10).

Slag Cement Association. 2002. Slag Cement. http://www.slagcement.org/pdf/no1%20Slag%20Cement.pdf

South Africa National Standards. 2000. *SANS 10100. the structural use of concrete, part 1: Limit state design.* Pretoria, South Africa:

South African National Standard. 2006. ***SANS 5861-2:2006Concrete tests - consistence of freshly mixed concrete - slump test***. Pretoria: South African Bureau of Standards

South African National Standard. 2006. SANS 5863:2006 "Concrete Tests - Compressive Strength of Hardened Concrete".

Statista. 2014. ***United states and world cement production in 2010 and 2013*** . [Online]. Available: http://www.statista.com/statistics/219343/cement-production-worldwide/

Swanepoel, J. & Strydom, C. 2002. Utilisation of Fly Ash in a Geopolymeric Material. *Applied Geochemistry,* 17(8).

Temuujin, J., Van Riessen, A. & Williams, R. 2009. Influence of Calcium Compounds on the Mechanical Properties of Fly Ash Geopolymer Pastes. *Journal of hazardous materials,* 167(1).

Temuujin, J., Williams, R. & Van Riessen, A. 2009. Effect of Mechanical Activation of Fly Ash on the Properties of Geopolymer Cured at Ambient Temperature. *Journal of Materials Processing Technology,* 209(12).

Tjiptobroto, P. & Hansen, W. 1991. Mechanism for Tensile Strain Hardening in High Performance Cement-Based Fiber Reinforced Composites. *Cement and Concrete Composites,* 13(4).

Van Chanh, N., Trung, B.D. and Van Tuan, D. 2008. Recent Research Geopolymer Concrete. Paper presented at The 3rd ACF International Conference-ACF/VCA, Vietnam.

van Jaarsveld, J.G.S., van Deventer, J.S.J. & Lukey, G.C. 2003. The Characterisation of Source Materials in Fly Ash-Based Geopolymers. *Materials Letters,* 57(7).

Vandewalle, L. 2000. RILEM TC 162-TDF: Test and Design Methods for Steel Fibre Reinforced Concrete. *Materials and Structures,* 33(225).

Wallah, S. & Rangan, B. 2006. Low-Calcium Fly Ash-Based Geopolymer Concrete: Long-Term Properties. *Res.Report-GC2, Curtin University, Australia.pp,*

Wan, H., Shui, Z. & Lin, Z. 2004. Analysis of Geometric Characteristics of GGBS Particles and their Influences on Cement Properties. *Cement and Concrete Research*, 34(1).

Weng, L. & Sagoe-Crentsil, K. 2007. Dissolution Processes, Hydrolysis and Condensation Reactions during Geopolymer Synthesis: Part I—Low Si/Al Ratio Systems. *Journal of Materials Science*, 42(9).

Xu, H. & Van Deventer, J.S.J. 2000. The Geopolymerisation of Alumino-Silicate Minerals. *International Journal of Mineral Processing*, 59(3).

Yip, C.K., Lukey, G.C., Provis, J.L. & van Deventer, J.S. 2008. Effect of Calcium Silicate Sources on Geopolymerisation. *Cement and Concrete Research*, 38(4).

Yunsheng, Z., Wei, S. & Zongjin, L. 2006. Impact Behavior and Microstructural Characteristics of PVA Fiber Reinforced Fly Ash-Geopolymer Boards Prepared by Extrusion Technique. *Journal of Materials Science*, 41(10).

Zheng, Z. & Feldman, D. 1995. Synthetic Fibre-Reinforced Concrete. *Progress in Polymer Science*, 20(2).

Zollo, R.F. 1997. Fiber-Reinforced Concrete: An Overview After 30 Years of Development. *Cement and Concrete Composites*, 19(2).

Appendix A

Three point bending test results for the higher strength PFRGC

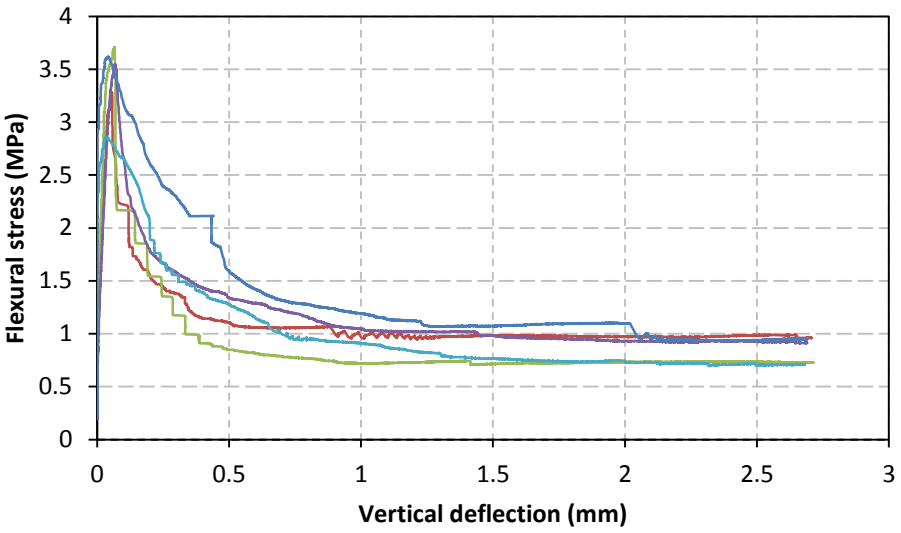

Figure A.1: Three point bending results for Mix 3b containing 3.64 kg/m^3 polypropylene fibres

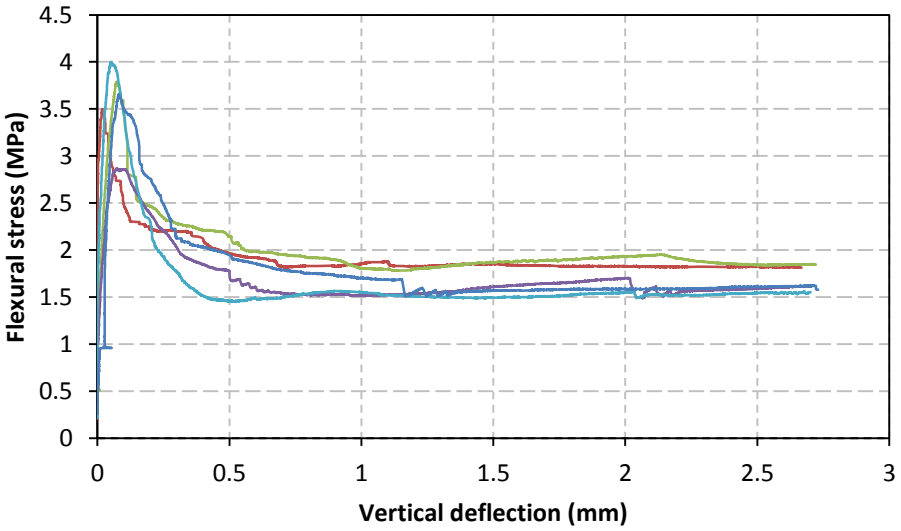

Figure A.2: Three point bending results for Mix 3b containing 7.28 kg/m^3 polypropylene fibres

Three point bending test results for the lower strength PFRGC

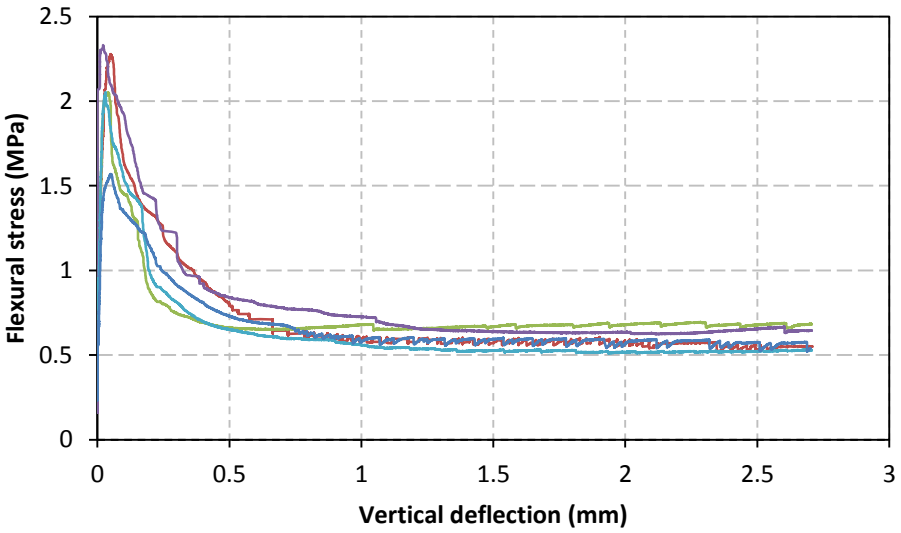

Figure A.3: Three point bending results for Mix 7b containing 3.64 kg/m^3 polypropylene fibres

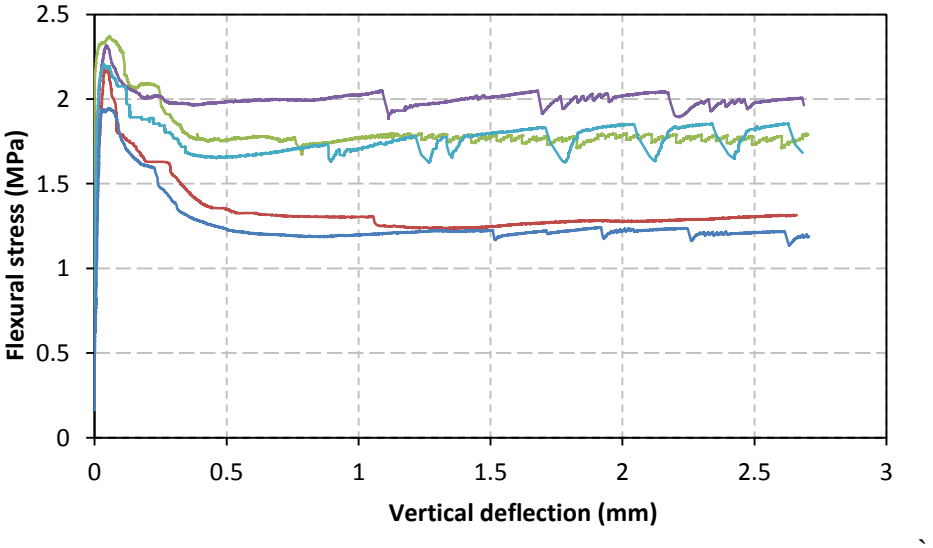

Figure A.4: Three point bending results for Mix 7b containing 7.28 kg/m^3 polypropylene fibres

Three point bending test results for the PFROC

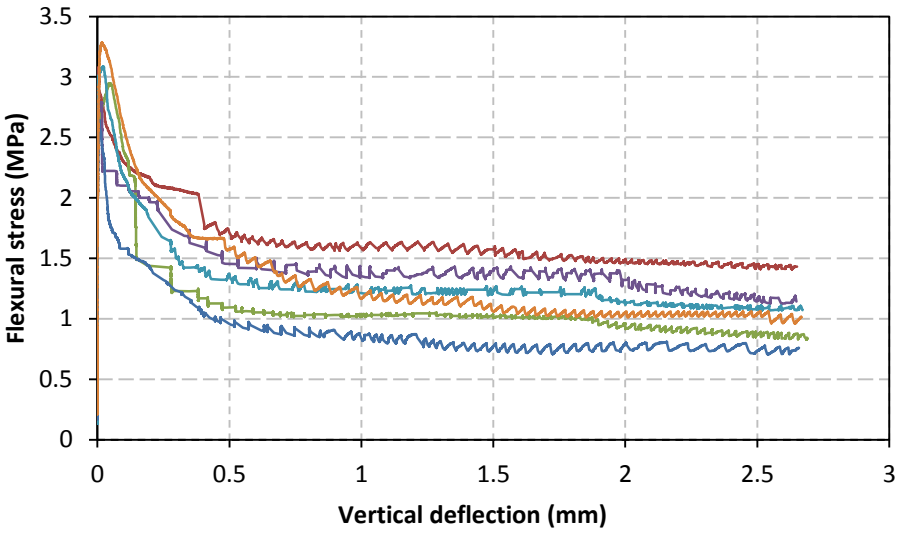

Figure A.5: Three point bending results for Mix 7-OPC containing 3.64 kg/m^3 polypropylene fibres

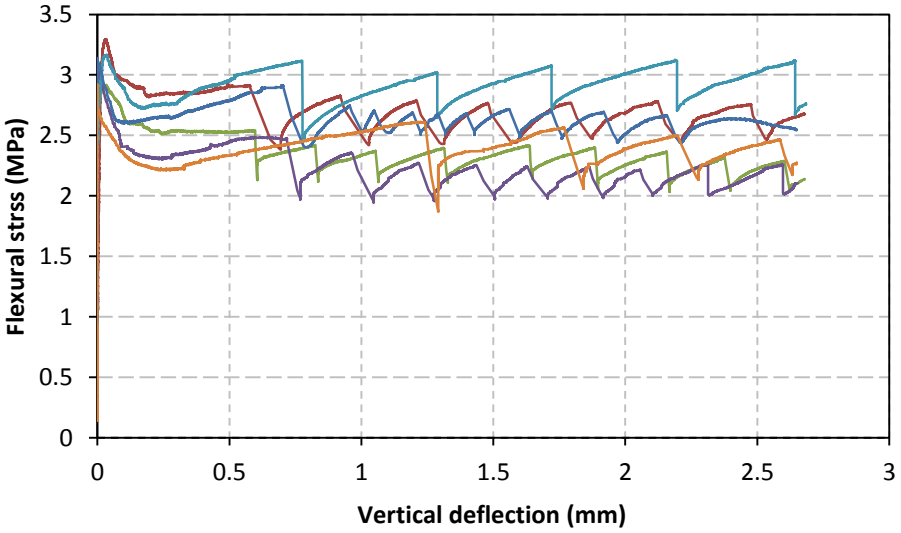

Figure A.6: Three point bending results for Mix 7-OPC containing 7.28 kg/m^3 polypropylene fibres

Three point bending test results for the higher strength SFRGC

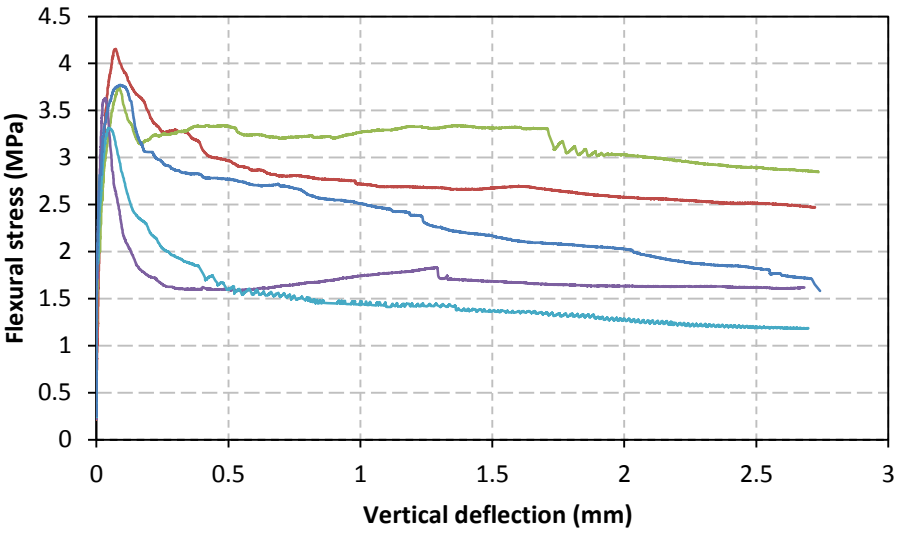

Figure A.7: Three point bending results for Mix 3b containing 31.2 kg/m^3 steel fibres

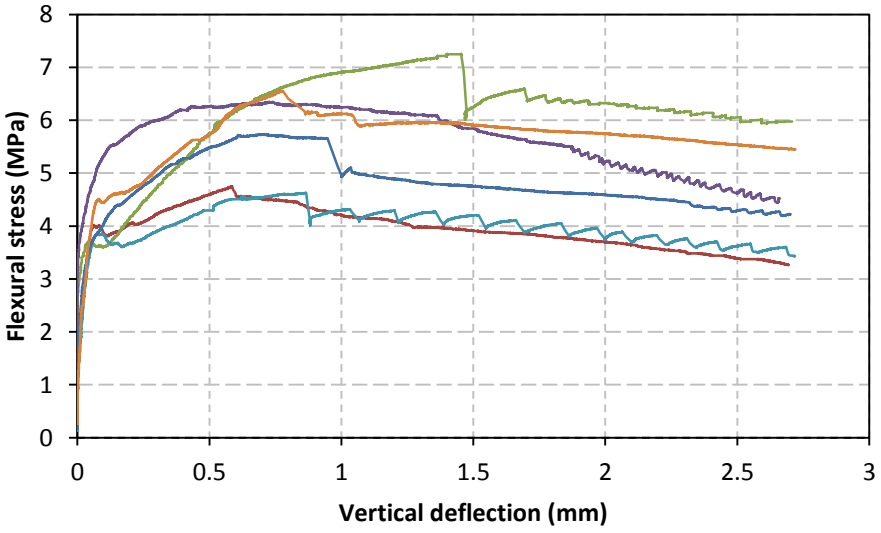

Figure A.8: Three point bending results for Mix 3b containing 62.4 kg/m^3 steel fibres

Three point bending test results for the lower strength SFRGC

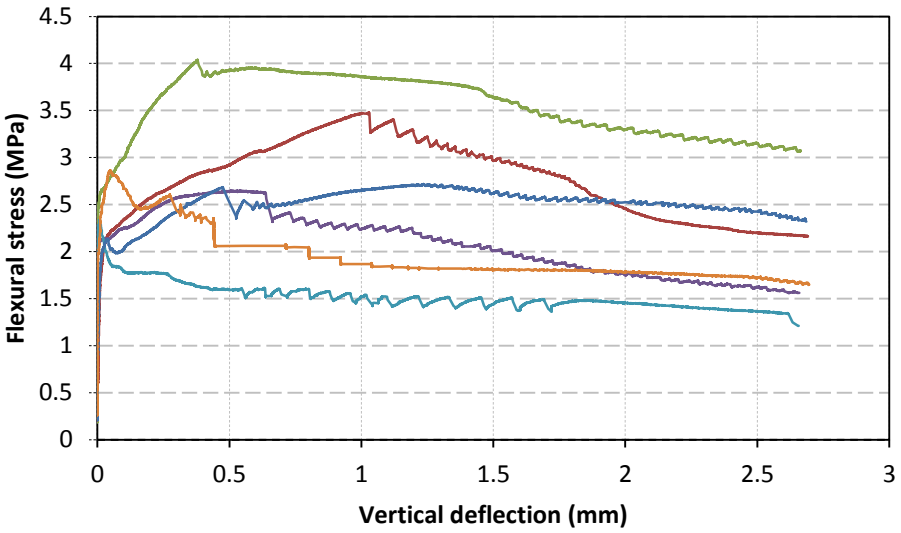

Figure A.9: Three point bending results for mix 7b containing 31.2 kg/m^3 steel fibres

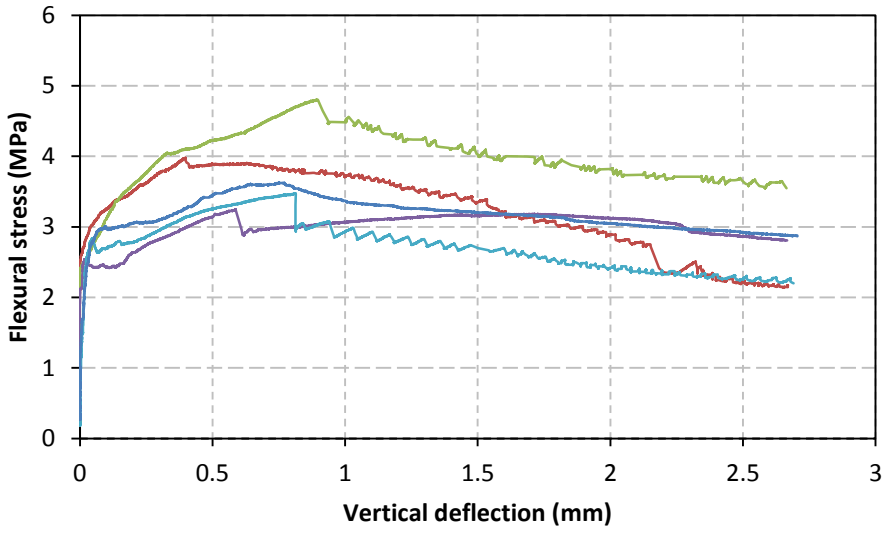

Figure A.10: Three point bending results for mix 7b containing 62.4 kg/m^3 steel fibres

Three point bending test results for the SFROC

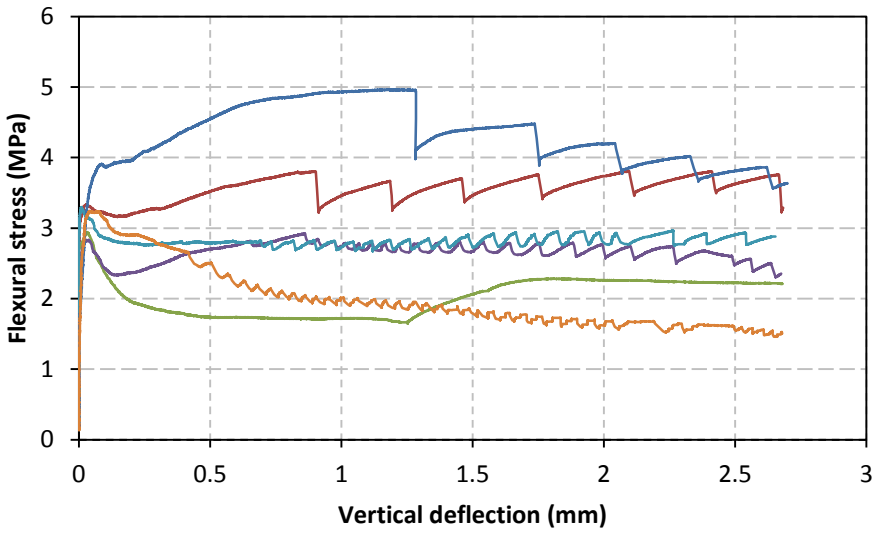

Figure A.11: Three point bending results for Mix 7-OPC containing 31.2 kg/m^3 steel fibres

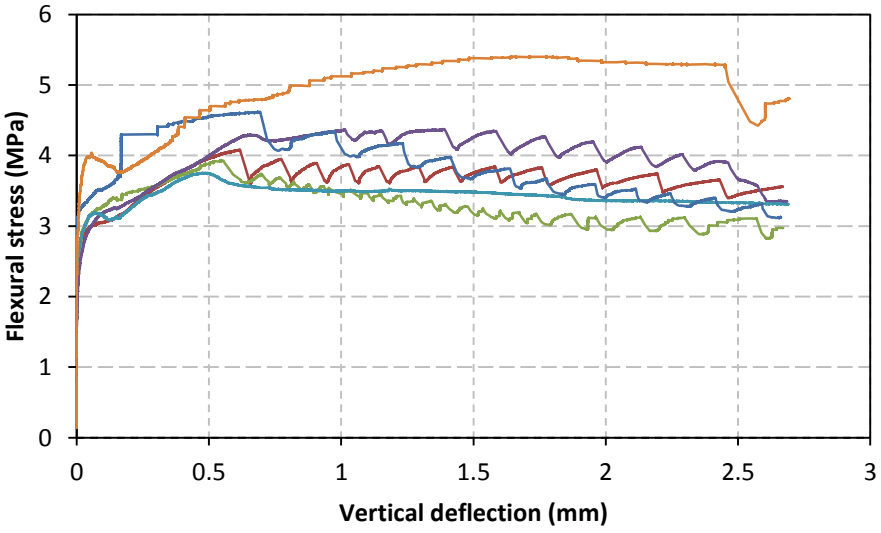

Figure A.12: Three point bending results for Mix 7-OPC containing 62.4 kg/m^3 steel fibres

Three point bending test results for the unreinforced concrete mixes

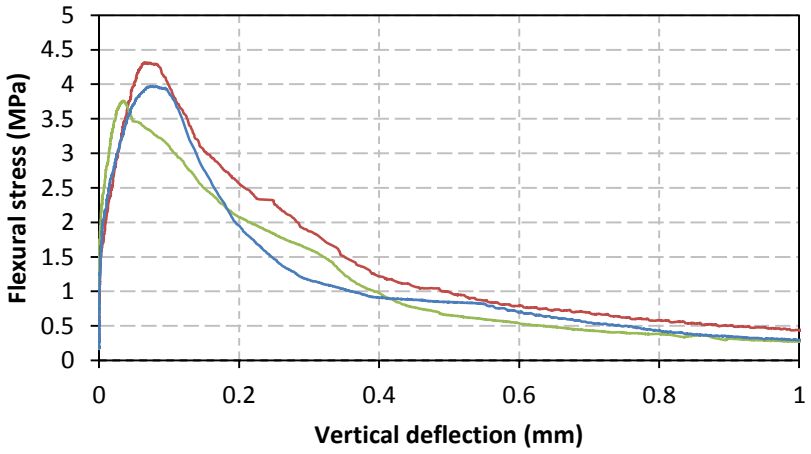

Figure A.13: Three point bending results for Mix 3b

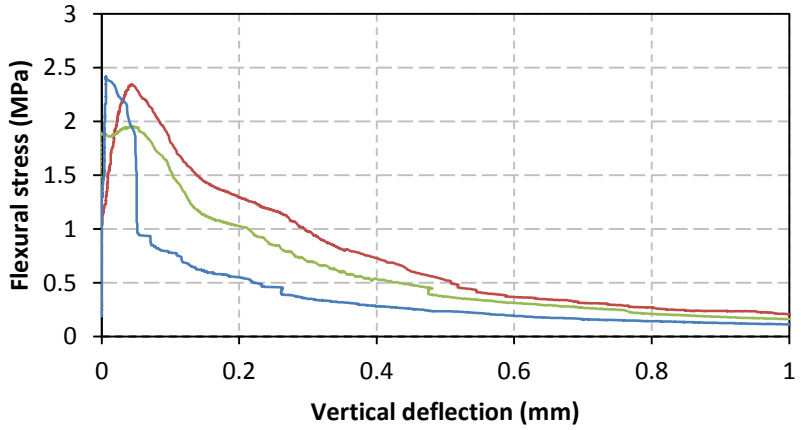

Figure A.14: Three point bending results for Mix 7b

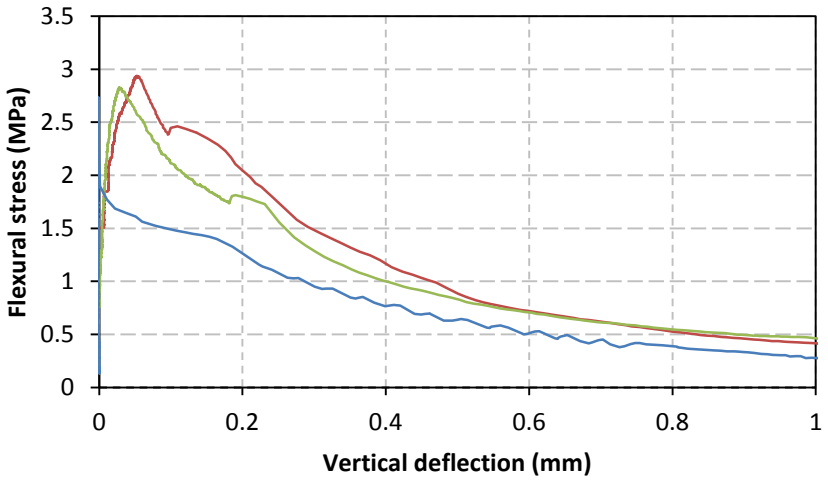

Figure A.15: Three point bending results for Mix 7-OPC

Round panel test results for the higher strength PFRGC

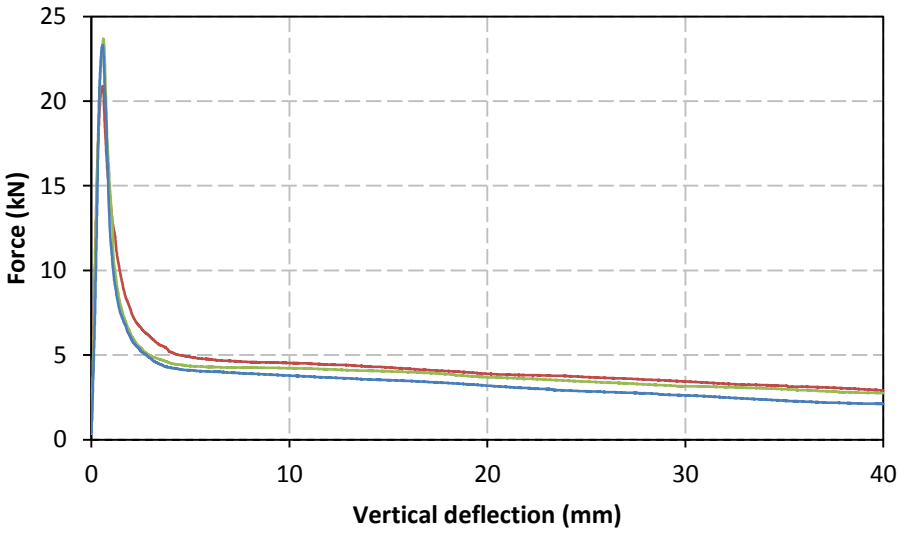

Figure A.16: Round panel test results for Mix 3b containing 3.64 kg/m^3 polypropylene fibres

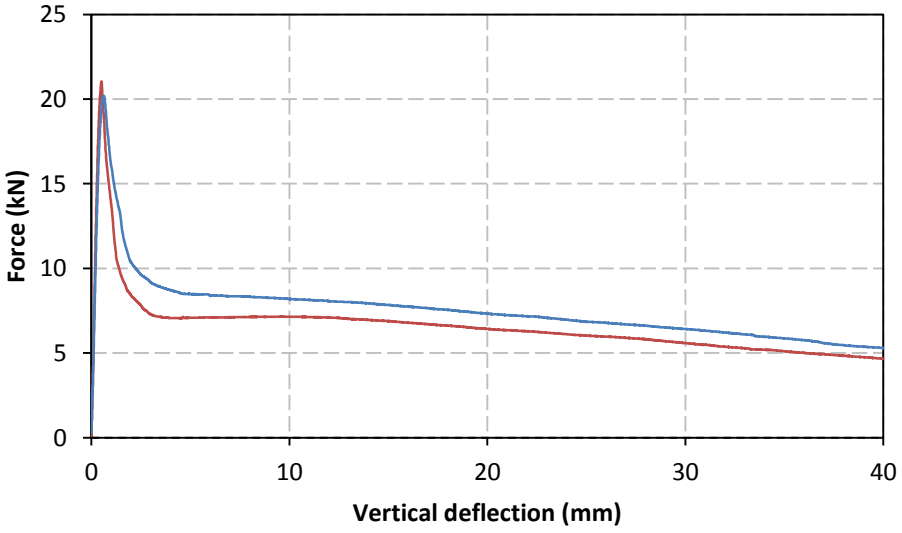

Figure A.17: Round panel test results for Mix 3b containing 7.28 kg/m^3 polypropylene fibres

Round panel test results for the lower strength PFRGC

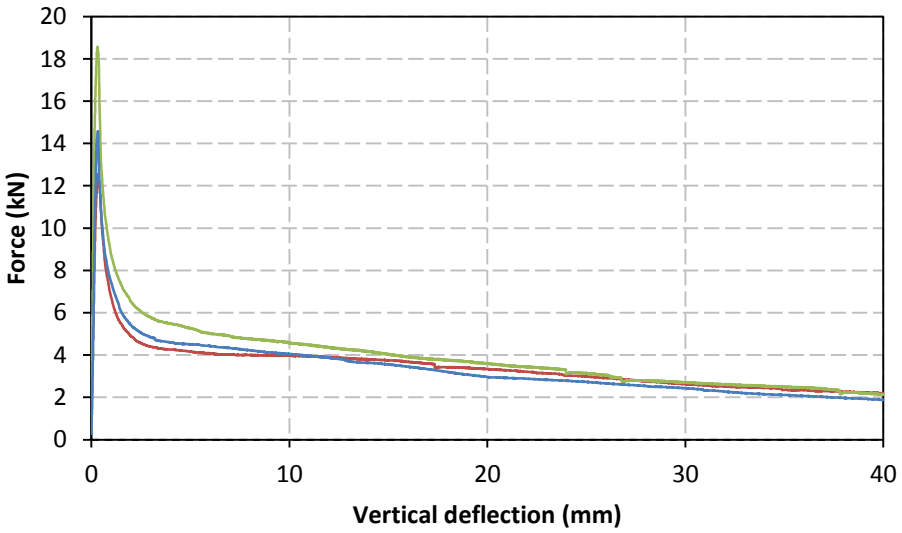

Figure A.18: Round panel test results for Mix 7b containing 3.64 kg/m^3 polypropylene fibres

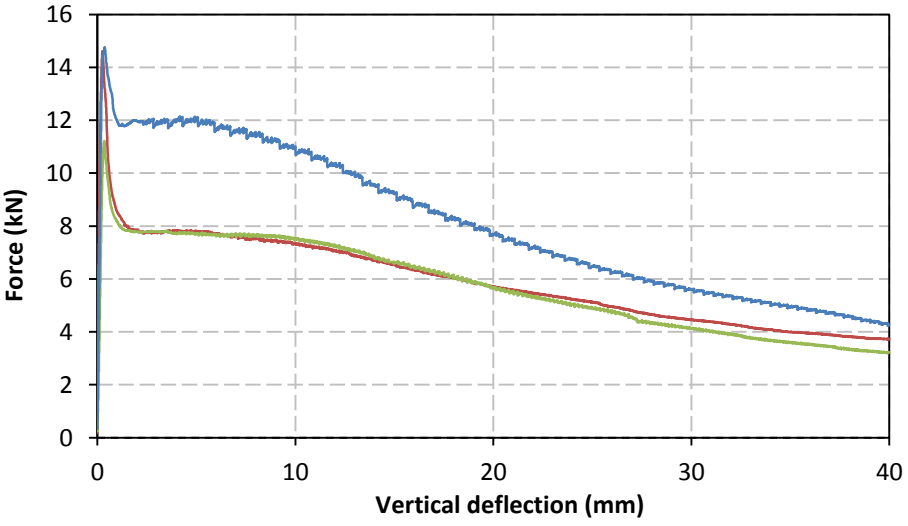

Figure A.19: Round panel test results for Mix 7b containing 7.28 kg/m^3 polypropylene fibres

Round panel test results for the PFROC

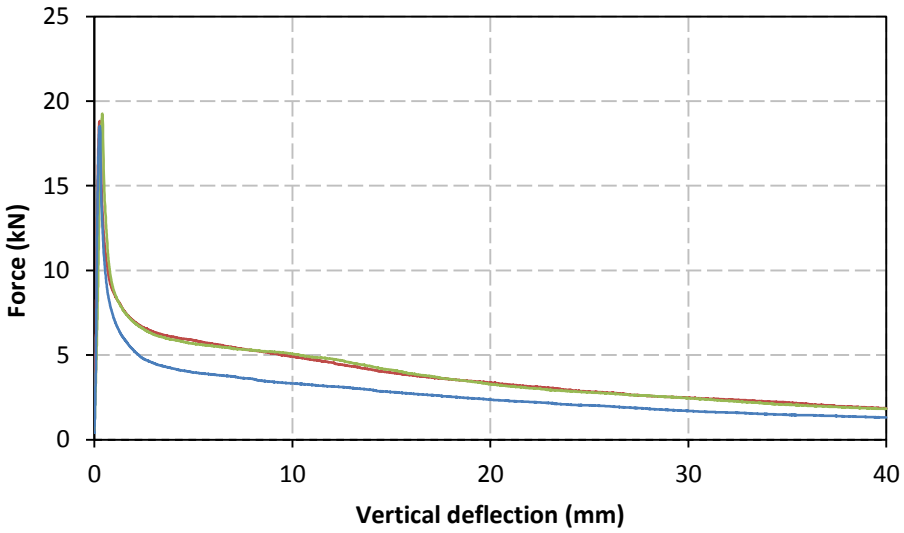

Figure A.20: Round panel test results for Mix 7-OPC containing 3.64 kg/m^3 polypropylene fibres

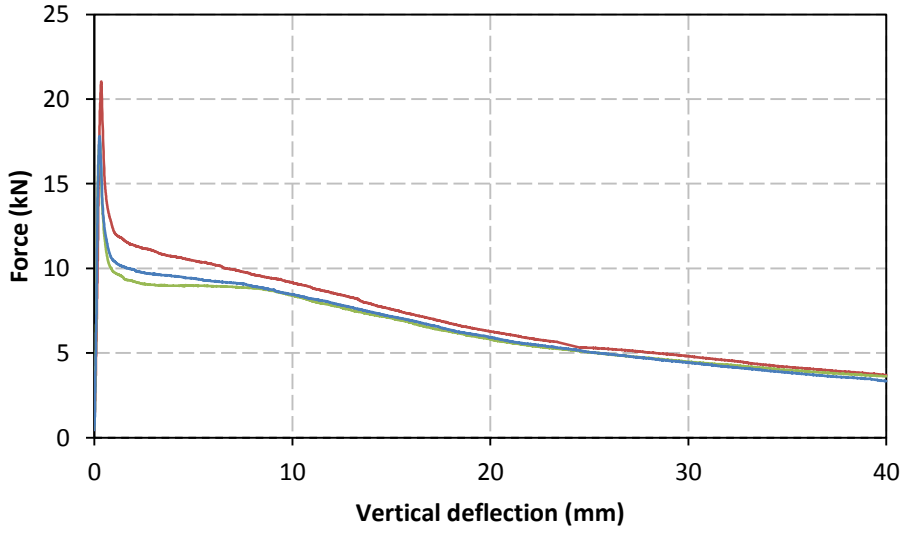

Figure A.21: Round panel test results for Mix 7-OPC containing 7.28 kg/m^3 polypropylene fibres

Round panel test results for the higher strength SFRGC

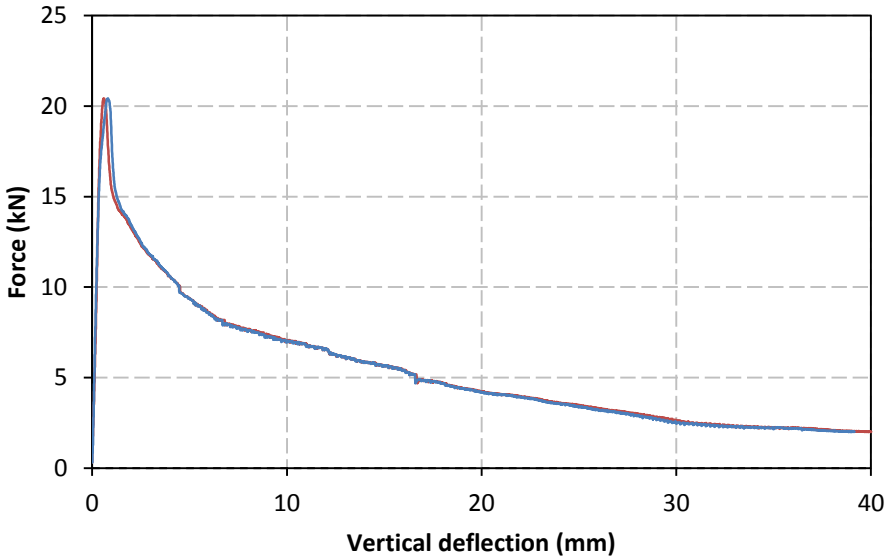

Figure A.22: Round panel test results for Mix 3b containing 31.2 kg/m^3 steel fibres

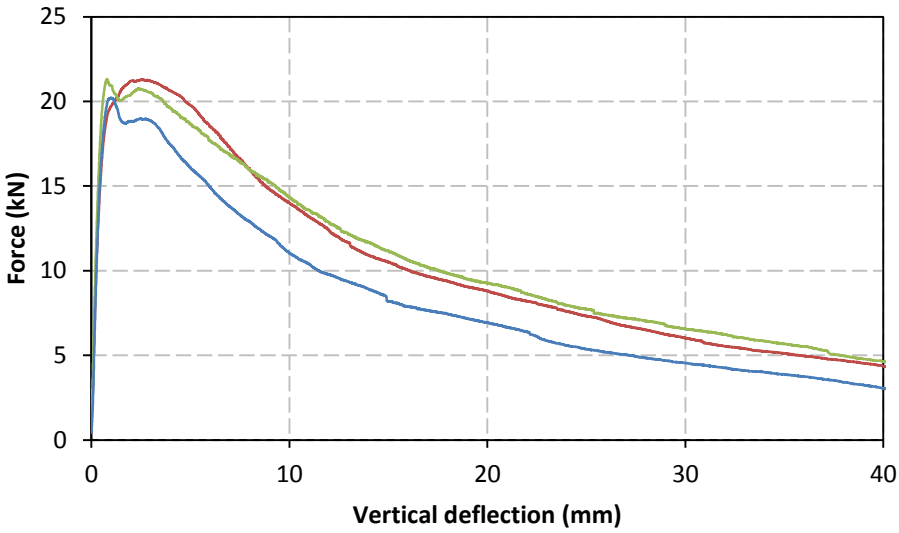

Figure A.23: Round panel test results for Mix 3b containing 62.4 kg/m^3 steel fibres

Round panel test results for the lower strength SFRGC

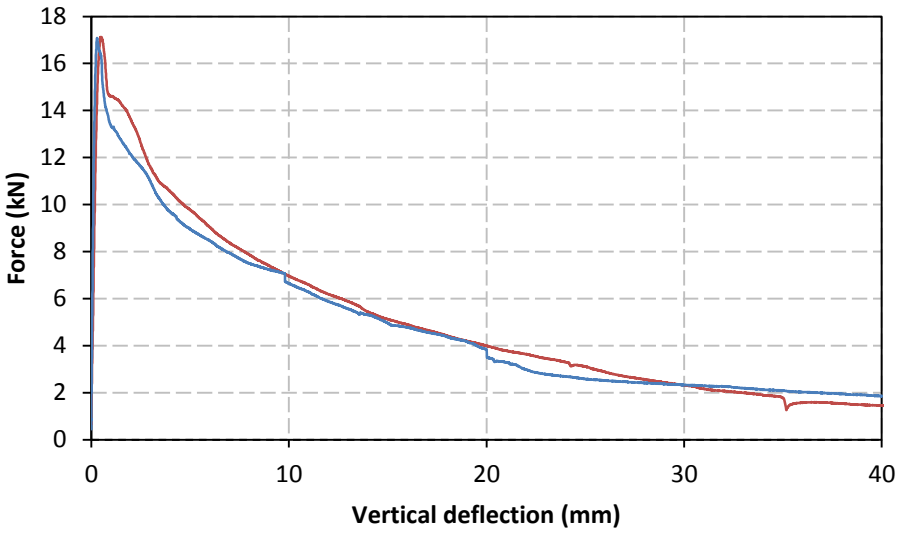

Figure A.24: Round panel test results for Mix 7b containing 31.2 kg/m^3 steel fibres

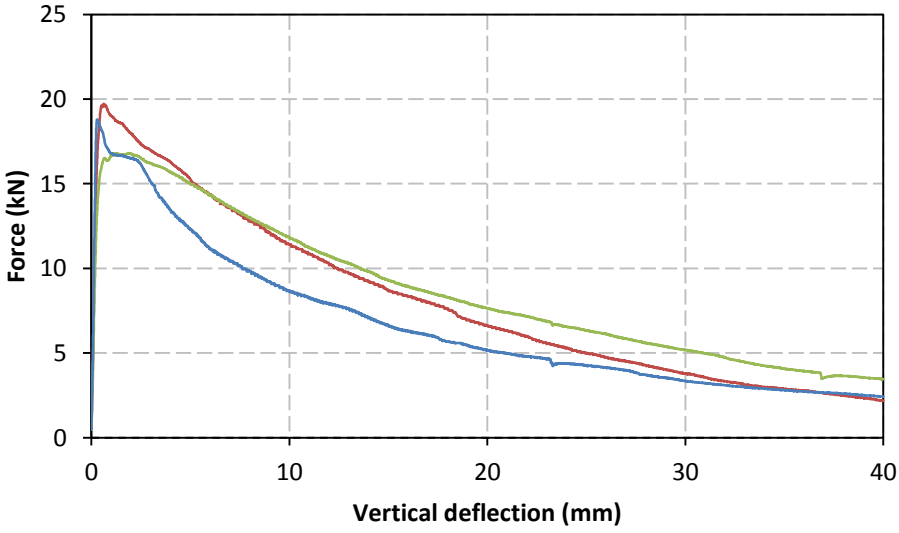

Figure A.25: Round panel test results for Mix 7b containing 62.4 kg/m^3 steel fibres

Round panel test results for the SFROC

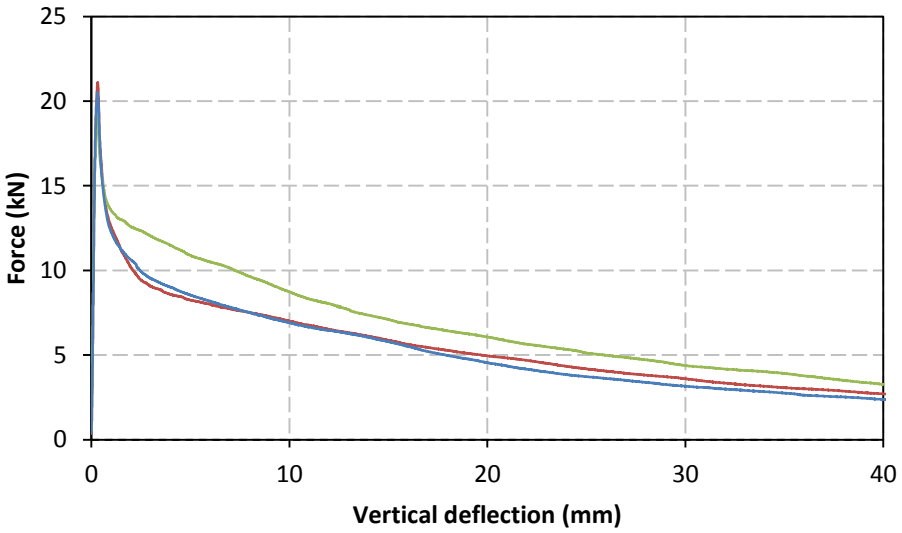

Figure A.26: Round panel test results for Mix 7-OPC containing 31.2 kg/m^3 steel fibres

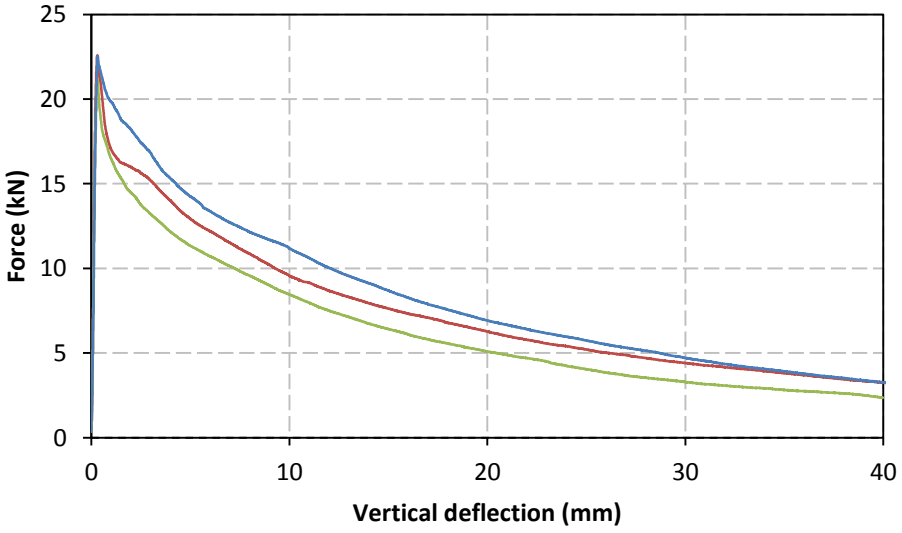

Figure A.27: Round panel test results for Mix 7-OPC containing 62.4 kg/m^3 steel fibres

Round panel test results of unreinforced concrete mixes

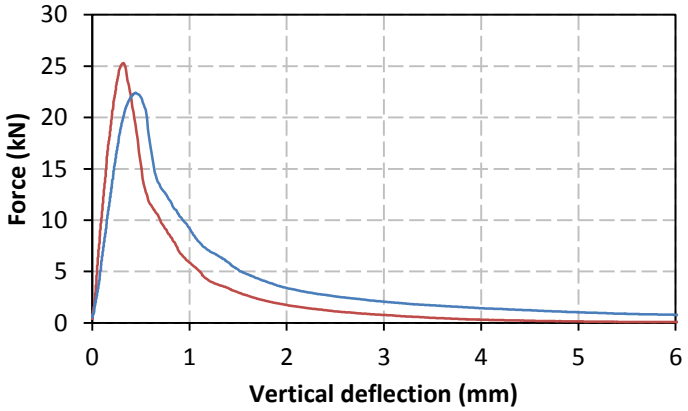

Figure A.28: Round panel test results for Mix 3b

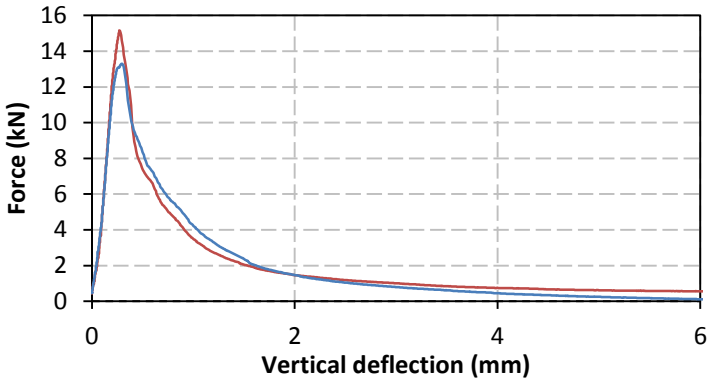

Figure A.29: Round panel test results Mix 7b

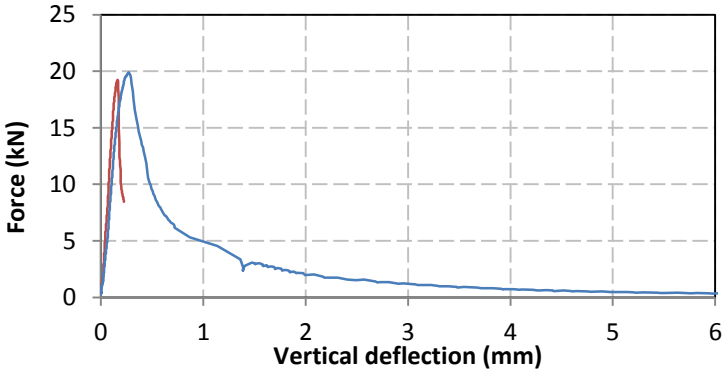

Figure A.30: Round panel test results for Mix 7-OPC

Appendix B

Table B.1: Mixes of Phase A

kg/2400kg	Total Mix	13.2mm Aggregate	Sand	GGBS	Fly ash	SS/SH	SS (Sodium silicate solution)	SH (Sodium Hydroxide solution)	SH MOLAR	Amount of water
1a	2400	1176	504	186	279	2.5	182	73	6	
2a	2400	1176	504	186	279	2	170	85	6	
3a	2400	1176	504	186	279	1.5	153	102	6	
4a	2400	1176	504	0	465	2.5	182	73	6	
5a	2400	1176	504	93	372	2.5	182	73	6	
6a	2400	1008	432	248	372	2.5	243	`97	6	
7a	2400	1092	468	217	325	2.5	213	85	6	
8a	2400	1008	672	186	279	2.5	182	73	6	
9a	2400	1008	432	284	427	2.5	178	71	6	
10a	2400	1008	432	265	397	2.5	213	85	6	
11a	2400	1176	504	186	279	2.5	182	73	3	
12a	2400	1176	504	186	279	2.5	182	73	8	
13a	2400	840	840	186	279	2.5	182	73	6	
14a	2400	924	756	186	279	2.5	182	73	6	

Table B.2: Mixes of Phase B

Mix	Total Mix	13.2mm Aggregate	Sand	GGBS	Fly ash	SS/SH	SS (Sodium silicate solution)	SH (Sodium Hydroxide solution)	SH MOLAR	Amount of water
1b	2321	858	520	259	394	1	108	92	8	90
2b	2315	858	520	259	394	1	98	82	8	104
3b	2306	858	520	259	394	1	81	69	8	125
4b	2291	858	520	259	394	1	54	46	8	162
5b	2301	858	520	148	485	1	108	92	8	90
6b	2295	858	520	148	485	1	98	82	8	104
7b	2286	858	520	148	485	1	81	69	8	125
8b	2297	858	520	126	504	1	108	92	8	90
9b	2291	858	520	126	504	1	98	82	8	104
10b	2282	858	520	126	504	1	81	69	8	125
11b	2316	776	597	259	394	1	108	92	8	90
12b	2310	776	597	259	394	1	98	82	8	104
13b	2301	776	597	259	394	1	81	69	8	125
14b	2317	858	572	239	364	1	98	82	8	104
15b	2298	858	572	137	448	1	98	82	8	104
16b	2295	858	572	116	465	1	98	82	8	104
17b	2318	858	624	219	333	1	98	82	8	104
18b	2301	858	624	125	410	1	98	82	8	104
19b	2306	609	754	259	394	1	108	92	8	90
20b	2300	609	754	259	394	1	98	82	8	104
21b	2291	609	754	259	394	1	81	69	8	125
22b	2326	941	442	259	394	1	108	92	8	90
23b	2320	941	442	259	394	1	98	82	8	104
24b	2311	941	442	259	394	1	81	69	8	125
25b	2302	858	520	259	394	1	54	92	8	125
26b	2314	858	520	259	394	2	101	57	8	125
27b	2313	858	520	259	394	2	110	47	8	125
28b	2303	858	520	259	394	1	81	65	6	125
29b	2312	858	520	259	394	1	81	75	12	125
30b	2317	858	520	259	394	1	81	80	16	125